ISSN 2227-6920

Research Bulletin SWorld

Modern scientific research and their practical application

Published by:

Kupriyenko Sergiy Vasilyovich *on* ***Project SWorld***

With the support of:

State research and development institute of the merchant marine of Ukraine

Odessa National Maritime University

Ukrainian National Academy of Railway Transport

Volume J21210

June 2012

SWorld /*Scientific World*/ - is a modern on-line project, acting in the name of science to achieve the high goal "international integration of research" (conferences, workshops, electronic journals, publishing support for academics)

Please use the following format to cite material from this book (*italics indicate the fields to change to your data*):

Author(s), 'Title of Paper," in Modern scientific research and their practical application, edited by Alexandr G. Shibaev, Sergiy V. Kuprienko, Alexandra D. Fedorova. Vol. J21210 (Kupriyenko Sergiy Vasilyovich, Odessa, 2012) *Article CID Number*.

This volume contains research papers of scientists in the field of PHYSICS AND MATHEMATICS.

Published by:

Kupriyenko Sergiy Vasilyovich
on ***Project SWorld***
P.O. Box 38, Odessa, 65001 Ukraine
Telephone: +380667901205
e-mail: orgcom@sworld.com.ua
site: www.sworld.com.ua

Paper Numbering: Papers are published as they are submitted and meet publication criteria. A unique, consistent, permanent citation identifier (CID) number is assigned to each article at the time of the first publication.

CONTENTS

PHYSICS AND MATHEMATICS

J21210-389	EXTERNAL STABLE DEFINITION OF FUZZY TEMPORAL GRAPH *	Bozhenyuk A.V.
J21210-792	EXTREMUM PROBLEM SOLUTION FOR NUMERIAL-ANALYTICAL APPROACH TO OPTIMAL CONTROL PROBLEM	Okhorzin V. A., Ryzhikov I. S.
J21210-476	FROM THE HISTORY OF THE DEVELOPMENT OF THE ORGANIZATIONAL FORMS OF PHYSICAL SCIENCE FROM ANTIQUITY TO THE MID-20TH CENTURY	Sabirova F.M.
J21210-846	ADVANCED PROOF THE RIEMANN HYPOTHESIS	Mazurkin PM
J21210-842	STABLE LAWS AND THE NUMBER OF ORDINARY	Mazurkin PM
J21210-843	STABLE LAWS AND THE NUMBER OF ORDINARY	Mazurkin PM
J21210-844	SERIES PRIMES IN BINARY	Mazurkin PM
J21210-925	THE ALTERNATIVE ANALYSIS: THEORY AND APPLICATIONS	Sukhotin A.M.
J21210-845	GROWTH PRIMES	Mazurkin PM
J21210-076	DIVISIBILITY OF RECURSIVE SEQUENCES ELEMENTS	Matyukhina A.G.
J21210-726	ANOTHER FORM OF THE RECORDS OF NEWTON'S EQUATION OF GRAVITATION.	G.M. Trunov
J21210-609	MOTION OF EDGE DISLOCATIONS IN HYDROSTATICALLY COMPRESSED METALS AND ALKALI-HALIDE CRYSTALS	Malashenko V.V., Malashenko T.I.
J21210-775	INSTITUTE OF GLOBAL PROBLEMS OF ENERGY EFFECTIVENESS AND ECOLOGY.	Borodzich EV
	CHEMISTRY	
J21210-716	RESEARCH IN STRUCTURE AND PROPERTIES OF OLEFINIC THERMOPLASTIC ELASTOMERS THROUGH THE METHOD OF DIELECTRIC SPECTROSCOPY	R.I.Ableev *, A.R.Valiev *, Z.A.Perestoronina **, S.K.Kurljand, A.S.Ramsh, I.V.Baranets **, R.N.Gimaev*
J21210-701	Ethylene Oligomerization on PdO/SO42--ZrO2	L.F. Sayfulina E.A Buluchevskii, A.V. Lavrenov
J21210-148	INFLUENCE OF IMPLANTATION OF CHROME AND TITAN IONS ON SUPERFICIAL PROPERTIES OF STEEL Cr18Ni10Ti	Maschenko S., Cherny A., Dogadajlo R., Goncharov V.

CID: J21210-389

UDK 681.327

Bozhenyuk A.V.

EXTERNAL STABLE DEFINITION OF FUZZY TEMPORAL GRAPH *

Taganrog Institute of Technology of Southern Federal University

In this paper the notion of fuzzy temporal graph is considered. Which one is a generalization of a fuzzy graph on the one hand, and a temporal graph on the other hand. The notion of external stable fuzzy set of fuzzy temporal graph is introduced.

Keywords: Fuzzy temporal graph, external stable fuzzy set.

The graphs theory draws the big attention of experts of various areas of knowledge. Traditionally graphs theory is used for representation of relations between elements of difficult structures of the various nature [1]. Thus the given relations between elements are constants and do not vary in time. Such graphs have been named by "static" [2]. In a case when relations between elements of some structure change in time, there is actual use by the graph model, in which communication between vertices of the count change in time, that is, temporal graph [3]. In a case when in temporal graph, communications between vertices are fuzzy, we come to concept fuzzy temporal graphs [4]. However using fuzzy temporal graphs as models of various systems has difficulties. These it is connected by that the majority of isomorphic transformations of graphs change their external representation, not changing their signature. In this connection, the questions connected with consideration invariants of fuzzy temporal graphs are actual. In the given work the concept of external stable fuzzy set of fuzzy temporal graph is introduced. It is invariant concerning isomorphic transformations considered fuzzy temporal graph. External stable fuzzy set allows to make structural analysis of fuzzy temporal graph.

The fuzzy temporal graph [5] is called the three $\widetilde{G}=(X,\{\widetilde{\Gamma}_t\},T)$, where X – set of graph vertices, $|X|=n$; $T=\{1,2,...,N\}$ – set of the natural numbers defining (discrete)

time; $\{\widetilde{\Gamma}_t\}$ – family of fuzzy equivalence, or fuzzy mappings of set of vertices X in itself during time moments $t \in T$. That is:

$$(\forall x \in X)(\forall t \in T)\ [\widetilde{\Gamma}_t(x) = \{< \mu_t(y) / y >\}],\ y \in X, \mu_t \in [0,1].$$

Graphically fuzzy temporal graph we can present in the form of the directed graph (Fig. 1.) on which edges the fuzzy set on set of time T is specified.

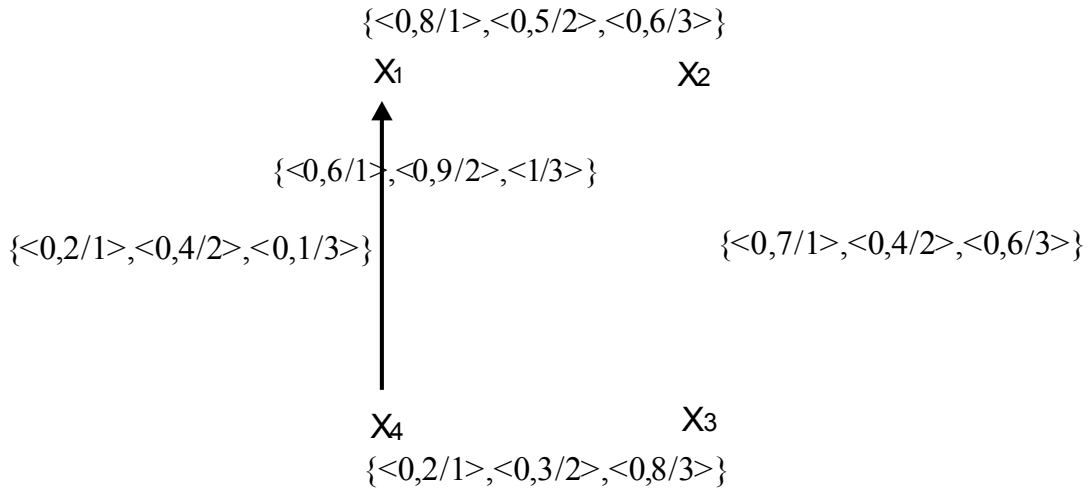

Fig.1 Example fuzzy temporal graph

Thus, fuzzy temporal graph is reduced to family T fuzzy sugraphs on the same set of vertices X.

Let's consider fuzzy sugraph $\widetilde{G}_t = (X, \widetilde{U}_t)$ of temporal fuzzy graph $\widetilde{G}$=(X,{$\widetilde{\Gamma}_t$ },T), where X – set of vertices, $\widetilde{U}_t = \{\mu_t(x_i, x_j) \mid (x_i, x_j) \in X^2\}$ - fuzzy set of edges at the moment time t with membership function $\mu_t : X^2 \to [0,1]$. Consider fuzzy sugraph $\widetilde{G}' = (X', \widetilde{U}')$, with $X' \subseteq X, \widetilde{U}' \subseteq \widetilde{U}_t$. Let X' - arbitrary subset of vertices set X. For each vertex $y \in X \setminus X'$ define the value

$$\gamma(y) = \max_{x \in X'} \{\mu_t(y, x)\}. \qquad (1)$$

The set X' we call fuzzy external stable set with the external stable degree $\beta(X') = \min_{y \in X \setminus X'} \gamma(y)$. Considering expression (1), we receive: $\beta(X') = \min_{y \in X \setminus X'} \max_{x \in X'} \{\mu_t(y, x)\}$.

Let's enter now concept of the minimum fuzzy external domination set of fuzzy temporal graph, who is expansion of set for fuzzy graphs. [6-8].

Subset $X' \subseteq X$ is called minimum fuzzy external domination set of sugraph $\widetilde{G}_t$ with the degree $\beta(X')$, if the condition $\beta(X'') < \beta(X')$ is carried out for any subset $X'' \subset X$.

Let $\tau_k = \{X_{K_1}, X_{K_2}, ..., X_{K_l}\}$ - family of all minimum fuzzy external domination steady *k* vertices sets with degrees of external stability $\beta^0_{X^1_k}, \beta^0_{X^2_k}, ..., \beta^0_{X^l_k}$ accordingly. Let's designate through $\beta^{\min}_k = \max\{\beta^0_{X^1_k}, \beta^0_{X^2_k}, ..., \beta^0_{X^l_k}\}$. If the family $\tau_k = \varnothing$, then define $\beta^{\min}_{X_k} = \beta^{\min}_{X_{k+1}}$. Value $\beta^{\min}_k$ means, that in the graph $\widetilde{G}$ there is a sugraph with *k* vertices with degree of external stability $\beta^{\min}_k$ and there is no other sugraph with *k* vertices, whose degree of internal stability would be more sizes $\beta^{\min}_k$.

Set $\widetilde{B}_t = \{<\beta^{\min}_{X_1}/1>, <\beta^{\min x}_{X_2}/2>, ..., <\beta^{\min}_{X_n}/n>\}$ is fuzzy set of external stable of fuzzy temporal sugraph $\widetilde{G}=(X,\{\widetilde{\Gamma}_t\},T)$ at the moment *t*. Set $\widetilde{T} = \underset{t=\overline{1,T}}{\&} \widetilde{B}_t$ we name fuzzy set of external stable of fuzzy temporal graph $\widetilde{G}=(X,\{\widetilde{\Gamma}_t\},T)$.

For the graph resulted above (fig. 1), fuzzy set of external stability is $\widetilde{T} = \{<0/1>.<0{,}5/2>, <0{,}6/3>, <1/4>\}$.

The given set means, in particular, that in the considered graph at any moment there is a subset of two vertices in which the remained two vertices are displayed with degree not less than 0,5; there is a subset of three vertices in which the remained vertex is displayed with degree 0,6.

* This work has been supported by the Russian Foundation for Basic Research project № 10-01-00029a.

References:

1. Christofides, N.: Graph Theory. An Algorithmic Approach. London: Academic press 1976.

2. Kostakos V. Temporal graphs. In Proc. of Physica A: Statistical Mechanics and its Applications, vol.388, Issue 6, Elsevier, 2008, p.1007-1023.

3. L.S.Bershtein, A.V.Bozhenyuk. The Using of Temporal Graphs as the Models of Complicity Systems // Izvestiya YFU. Technical Sciences. Taganrog: TTI YFU, 2010. №4 (105). – P.198-203.

4. L.S.Bershtein, A.V.Bozhenyuk, I.N.Rozenberg. Definition of Strong Connectivity of Fuzzy Temporal Graphs // OP&PM, 2011, vol.18, Issue 3, p.414-415.

5. L.S.Bershtein, S.L.Beliakov, A.V.Bozhenyuk. The Using of Fuzzy Temporal Graphs for Modeling in GIS // Izvestiya YFU. Technical Sciences. Taganrog: TTI YFU, 2012. №1 (126). – p.121-127.

6. L.S.Bershtein, A.V.Bozhenyuk. Determination of Fuzzy Internal Stable, External Stable Sets and Kernels of Fuzzy Oriented Graphs // Journal of Computer and Systems Sciences International. Vol.38, №1, 1999, p.153-157.

7. L.S.Bershtein and A.V.Bozhenuk. Maghout Method for Determination of Fuzzy Independent, Dominating Vertex Sets and Fuzzy Graph Kernels // Int. J. General Systems. Vol.30, №1, 2001. p.45-52.

8. Л.С.Берштейн, А.В.Боженюк. Fuzzy Graphs and Hypergraphs.. Moscow: Nauchny Mir, 2005, 256p.

CID: J21210-792

UDK 005; 519.7; 303.732

Okhorzin V. A., Ryzhikov I. S.

EXTREMUM PROBLEM SOLUTION FOR NUMERIAL-ANALYTICAL APPROACH TO OPTIMAL CONTROL PROBLEM

Siberian state Aerospace University

In this paper optimal control problem without any constraints for control function is considered. The initial task comes to the problem with costate variables, which are defined with the Hamiltonian function that can be found analytically. Then the main task comes to be reduced to real number global optimization problem. The objective function is a black box function, it is generally multimodal and complex, these facts tends us to use evolution algorithms as optimization ones.

Keywords: Optimal control, evolutionary strategies, differential evolution, particle swarm optimization, the maximum principle.

For some specific optimal control problems analytical solutions are exist and fully described in many manuscripts and papers, as well as numerical solutions are. The plenty of examples can be found in [1], [2]. The mathematical apparatus that is need to solve optimal control task is very complex so it cannot be accessible for engineers needs, because the apparatus is not similar to engineer's one. Optimal control problem in Pontryagin form allows to find a weak minimum, and the current approach is about the technique to find any of minima. In this paper, the control function structure is defined by the maximum principle, so knowing the system with costate variables, it is possible to find the control function and the system output solving the optimization problem with dimension that is equal to the dimension of the given system.

As it would be shown lower, the optimization task on the real numbers field is global, complex and the objective function is a black box. That is why the evolution based algorithms were used. For given examples, the evolutionary strategies method [7] and modification of it were considered, as also differential evolution method [6] and particle swarm optimization [3].

The main idea of optimal control problem numerical solution given in a paper [5]. Here the main idea of numerical-analytical approach is briefly given. For the system, defined with differential equation

$$\frac{dx}{dt} = f(x,u,t), \qquad 1)$$

where

$f(x,u,t): R^n \times R \times R^+ \to R^n$ is a continuous vector function of its arguments;

$x \in R^n$ is a vector of system state;

$u(t): R^+ \to R$ is a continuous control function;

$t \in R^+$ is a time.

We need to find a control law, that bring the system to state $x(T) = x^*$ from initial condition $x(0) = x^0$ that minimize the functional

$$I(x,u) = \int_0^T F(x,u)dt \to \min_u, \tag{2}$$

with finite time T and continuous function $F(x,u)$. According to Pontryagin's principle of maximum [2], [4], it is necessary to define the system with state variables and adjoint variables. The Hamiltonian function with adjoint variables $p \in R^n$

$$H(x,u,t) = -F(x,u) + p \cdot f(x,u,t), \tag{3}$$

determines Hamiltonian system

$$\frac{dx}{dt} = f(x,u,t),$$

$$\frac{dp}{dt} = -\frac{dH}{dx},$$

with boundary conditions $x(0) = x^0$ and $x(T) = x^*$. And, in general, unknown initial condition $p(0)$ that results on the system solution. Using the Hamiltonian stationary condition for the control function

$$\frac{dH}{du} = 0, \tag{4}$$

we would have the closed system.

The equation (4) determine the control law. To find a solution for optimal control task with system (1), criterion (2) and boundaries $x(0) = x^0$, $x(T) = x^*$ is to find initial condition $p(0)$ for adjoint variables.

Thus, optimal control problem is reduced to real number unconstrained optimization problem on the field R^n with $n = \dim(x)$.

Let $\tilde{x}(t), \tilde{p}(t), \tilde{u}(t)\big|_{\tilde{p}(0)=p^0}$ be the solution of Hamiltonian system for adjoint variables initial condition p^0. Now we can define the criterion for reduced problem

$$K(p^0) = \left\| x^* - \tilde{x}(T)\big|_{\tilde{p}(0)=p^0} \right\| \to \min_{p^0}, \tag{5}$$

where

$\|a\|, a \in R^n$ - is a norm function, for example, Euclidean norm function.

It is important to notice, that given approach based on improper minimum theory. Moreover, even if $K(p^0) = 0$, the optimal control problem solution may not bring the global minimum for (2).

The criterion for reduced problem is multimodal function for global optimization and, in general, with complex behavior.

The following equation describes the plant with inverted pendulum movement. The system equation was described in [1].

$$f(x,u,t) = \begin{pmatrix} x_1 \\ -x_1 + \sin(x_0) + u(t)\cdot\cos(x_0) \end{pmatrix}, \tag{6}$$

$$T = 5, x^0 = \begin{pmatrix} 1 \\ 2 \end{pmatrix}, x^* = \begin{pmatrix} 0 \\ 0 \end{pmatrix}, \tag{7}$$

$$F(x,u) = u^2 + x_0^2. \tag{8}$$

Without loss of generality, let the function

$$fitness(x): R^n \to (0,1],\ fitness(x) = \frac{1}{1+K(x)} \tag{9}$$

be the special function that is commonly used in evolution optimization theory. If $fitness(x) = 1 \Rightarrow K(x) = 0$. We can show the behavior of the function (9) for problem (6)-(8). Let initial condition domain to be a product of sets $p_0^0 \in [-50, 10]$ and $p_1^0 \in [0, 50]$, the surface on the given domain is illustrated on figure 1.

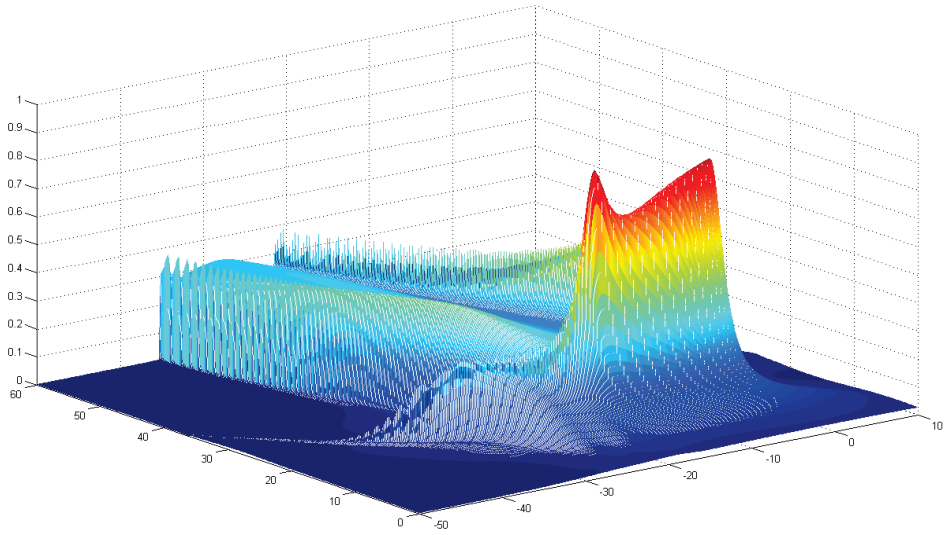

Figure 1. The fitness function plot.

The only maximum of function (9) reaches at point $p^0 \approx \begin{pmatrix} 8.95 \\ -22.15 \end{pmatrix}$, so that $fitness(p^0) \approx 1$, while there are large area with another local maximum that is less than 1. Moreover, that function is not an analytical, and the domain, which contains the extremum is unknown. That is why we use evolution optimization procedures.

We consider differential evolution algorithm [6] and particle swarm optimization [3] and modified evolutionary strategy method. The DE and PSO algorithm were taken as they are. The original ES optimization procedure can be found in [7]. Now we describe the modifications of given algorithm.

Let every individual be represented with tuple

$$H_i = \left\langle op^i, sp^i, fitness(op^i) \right\rangle, i = \overline{1, N_I},$$

where

$op_j^i \in R,\ j = \overline{1,k}$ is the set of objective parameters;

$sp_j^i \in R^+,\ j = \overline{1,k}$ is the set of strategic parameters;

N_I is population size.

The mutation of every offspring's gene takes place with chosen probability p_m. If we have the random value $z = \{0,1\}, P(z=1) = p_m$, which generates for every current objective gene and its strategic parameter:

$$op_i^{offspring} = op_i^{offspring} + z \cdot N(0, sp_i^{offspring});$$

$$sp_i^{offspring} = \left| sp_i^{offspring} + z \cdot N(0,1) \right|,$$

where

$N(m, \sigma^2)$ is normally distributed random value with mathematical expectation m and variance σ^2.

Also for N_1 randomly chosen individuals and for N_2 randomly chosen objective chromosomes we make N_3 iterations of local optimization with step h_l to determine the better solution. That is random coordinate-wise optimization. Local optimization goes on, while fitness function increases.

To compare different algorithms we set the maximum number of function evaluation to 8000. Every algorithm have its own parameters. For differential evolution we had differential weight $F_i^d = 0.2 \cdot i, i = \overline{1,10}$ and crossover probability $C_1^d = 0.5$ and $C_2^d = 0.8$. For evolutionary strategies there are 3 types of selection: proportional, rank and tournament; 3 types of recombination: discrete, intermediate and weighed intermediate; and 2 types of mutation: original and with probability $p_m = 0.5$. The parameters of local optimization $N_1 \in \{5, 10, 50\}$, $N_2 \in \{5, 10\}$ and $h_l \in \{1, 0.01\}$ with $N_3 = 1$. For particle swarm optimization parameters were set to $\varphi_i^{1,2} = 0.4 + 0.4 \cdot i, i = \overline{0,5}$. Moreover, algorithms were tested with different size of population and number of populations and for every distinct settings 10 runs of algorithm were made.

Let N_p be the number of solutions x, which have the $fitness(x) > 0.98$ for all the test for an algorithm with current settings and $\overline{f}$ be the mean fitness function value of best solution in every launch for every current algorithm settings.

After all the launches, the most effective settings were found. For differential equation algorithm: size of population is 20, number of populations is 400, $C^d = 0.5$, $F^d = 1.4$. For particle swarm optimization: size of population 50, number of

populations 170, $\varphi^1 = 0.4$, $\varphi^2 = 1.6$. And for hybrid modified evolutionary strategies method: 50 individuals, 50 populations, tournament selection with discrete crossover and modified mutation, mutation probability is $p_m = 0.5$. Parameters for local optimization are: $N_1 = 10$, $N_2 = 10$.

The results of testing are demonstrated in table 1.

Table 1

Algorithms statistic for problem (6)-(8)

	Statistics	
Algorithm	$\bar{f}$	N_p
Modified ES	0.9595	5
DE	0.9465	1
PSO	0.9449	3

For the best individual $p^0 = \begin{pmatrix} 8.9368 \\ -22.167 \end{pmatrix}$, the system state is shown on figure 2 and the control function is shown on figure 3.

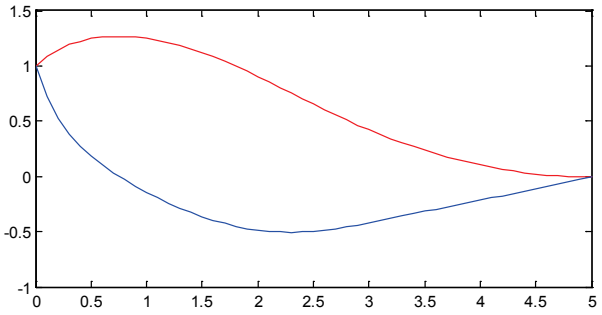

Figure 2. The system output coordinates.

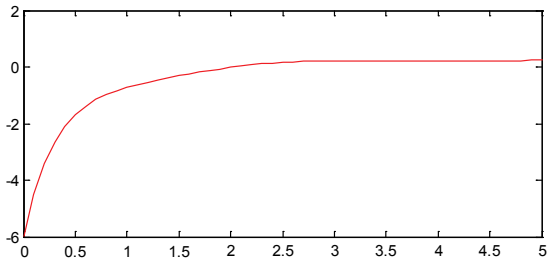

Figure 3. The control function

In this paper the optimization problem for numerical-analytical approach in the optimal control problem solution was described. The complexity of objective function tends us to use evolution algorithms as an optimization procedure. But not all of them are effective for current task definition. The hybrid modified evolutionary strategies method was the most effective in the current investigation with given problems. In future, the efficiency investigation will include more optimal control tasks and more searching techniques.

References:

1. Aleksandrov, V. (2005). Optimal motion control. Moscow: Fizmatlit
2. Alekseev, V.; Fomin, S. (2005). Optimal control. Moscow: Fizmatlit
3. Kennedy, J.; Eberhart, R. (1995). "Particle Swarm Optimization". Proceedings of IEEE International Conference on Neural Networks. IV. pp. 1942–1948
4. Okhorzin, V. (2009). Applied mathematics in Mathcad. St. Petersburg: Lan
5. Okhorzin, V. (2009). Numerical-analytical approach to optimal control problem solution. “Investigated in Russia”. 12, pp. 253-260.
6. Storn, R. (1996). "On the usage of differential evolution for function optimization". Biennial Conference of the North American Fuzzy Information Processing Society (NAFIPS). pp. 519–523.
7. Schwefel Hans-Paul. (1995). Evolution and Optimum Seeking. New York: Wiley & Sons.

CID: J21210-476

Sabirova F.M.

FROM THE HISTORY OF THE DEVELOPMENT OF THE ORGANIZATIONAL FORMS OF PHYSICAL SCIENCE FROM ANTIQUITY TO THE MID-20TH CENTURY

*Branch of Kazan (Volga) Federal University in Yelabug*a

The evolution of organizational forms of physical science is in-process exposed: from the ancient Lyceum, Academy, Alexandria Museum, medieval universities to scientific schools of end of 19th-mid 20th centuries. Disclosed to the role of each of the forms and in different historical periods.

Keywords: scientific school, academy, university, physical institute, laboratory.

An origin, formation and development of physics, crucially linked to the fact that in ancient times were the beginnings of collective forms of Science: Academy, lyceums, philosophical schools that provide continuity in the transfer of scientific knowledge. Well known were The School Of Pythagoras, the Academy of Plato, the Aristotle's Lyceum, the Alexandria Museum. The Alexandria Museum (or Mouseion) was an institution founded by Ptolemy I Soter. The Mouseion remained supported by the patronage of the royal family of the Ptolemies. It was the first public Research Institute, where the unique monuments of ancient science and culture were concentrated [1]. Museion was an association of scientists devoting to scientific researches: to astronomy, optics, mechanics, mathematics, and getting from a tsar paying for the activity. Here Euclid created the geometry, Archimedes occupied in a rich library.

In the epoch of middle ages the certain rudiments of collective forms of scientific researches can be looked after at first on Arabic East, afterwards in Western Europe. In the 9th-12th centuries there is a science bloom on Arabic East and schools are founded according to sample Alexandrian. The most famous was a sort of Academy, named after the House of wisdom (or "Academy of Ma'mun named its founder Khalifa Al Ma'moun). At the House of wisdom was well equipped observatory functioned at that, there was the state of translators and permanent researchers. As a result exactly in Arabic translations send to medieval Europe Heron’s «Mechanics», labours of Aristotle, Ptolemy, Archimedes.

European science initially focused in the universities. So, the center of research of mechanics was Merton College at Oxford University [2]. Here scientists in 20-30-ies of the 14 century engage in the decision of such problems of mechanics, as

distinction between a kinematics and dynamics, clarification of concept of speed, the distance in the case of uniformly accelerated motion. At the University of Paris began to develop a new inductive method of analysing scientific problems. Here J.Buridan, N.Orem and A.Saxon explore the problem of relativity of moving.

In universities the basic duty of professor was educating, and scientific activity was conducted exceptionally on the personal initiative at practical freedom of work.. A bloom of university educational and scientific life is on the end of 15th and early 16th centuries. But since the mid 16th century in universities of Europe had acquired Church-academic training and universities were not able to consolidate scientific forces, thus weakening the role of universities in the development of scientific knowledge.

On the stage of becoming of physics as science, covering the XVI-XVIII centuries, by an important moment, defining development and distribution of science, there is creation of scientific academies, especially in large numbers appeared in Italy. Thus, the Academy dei Lincei (literally the "Academy of the Lynx-Eyed"), founded in 1603, in Rome, has been studying and dissemination of scientific knowledge in the field of physics. Its coat of arms has served as the Lynx, which had been attributed to such a severe view that it penetrates through objects [3]. With 1611 the member of Academy was Galilei. Before 1630, the Academy flourished, published important scientific work, supported with open protection of Galilee. Claim of experimental direction in natural science is related to founded in 1657 in Florence of Academy of experiments. It also organized to promote science and should enhance physical knowledge through the collective of experimental activities of its members. At meetings of the academies were made and experiences reported their results, various topics in natural sciences. However, the activities of these academies was short-lived. Academy of experimentation lasted only 10 years and was closed under pressure from the Papal circles, that inflicted a large damage to Italian science.

According to sample Academies of experiments were created the Royal Society and of the Paris Academy of Sciences, the history of the grounds which begins long before their discovery with the circles of scientists. Since 1645, in London regularly

met circle-lovers of natural sciences, which discussed problems of physics, geometry, navigation, chemistry, etc. In connection with the civil war the members of the circle were nomads between Oxford and London. Its meetings were often semisecret, therefore R.Boyle named him the "Invisible College" [4]. The main aim of the Society consisted of development of new experimental method, and that is why the demonstration of various new phenomena and devices was one of the main lessons of weekly meetings. After the restoration of the monarchy by Robert Boyle society was recorded organizationally, and in 1660 got status of London Royal society. London Royal society was the association of private persons, bringing in membership dues on the charges of society on preparation and realization of experiments, edition of the printed matters. His organizational efforts contributed to the success of many sciences, including physical science.

In 1666, Louis XVI approved the Paris Academy of Sciences. It was assumed that it should address the practical challenges that are important to the State. Academics involved in research of flight of projectiles, building military fortifications, etc. As a nucleus of the future Academy of Sciences has been used circle established in 1625, through the efforts of the Franciscan monk M.Mersenne prime. Mersenn was called "people magazine", because through his correspondence with scientists all over Europe, becoming aware of new scientific discoveries that were discussed at the meetings of the circle. Mersenne dreamed about the opening of the academy of sciences, but did not live to see this. The first President was visiting from the Netherlands H.Huygens. Organizational activities contributed to the many successes of the Paris Academy of French science. This is it, since 1669, science must famous degree measurements, astronomical and physical observations in the equatorial countries, etc.

In XVII-XVIII centuries there is a splash of scientific activity of the European universities: on the base of universities scientific societies were founded and scientific magazines were published. They become the basis for the emergence of new organizational forms of physical science – physical laboratories and research institutes. So at the Berlin university Magnus physical laboratory was created.. On its

base and the circle of scholars, gruppirovavšihsâ around, Magnus, in 1845, occurred the Berlin physical society, and was a scientific journal "Advances in Physics". Scientific researches are conducted in Oxford and Cambridge. In 1831, in England, a British Association for the advancement of science, which funded the research on various branches of natural science. n 1871, the descendants of Henry Cavendish in the University of Cambridge Department of experimental physics was established and began construction of the building of the laboratory known as Cavendish. It was opened in 1874, and first Professor of faculty and the first head of the laboratory became J.C.Maxwell. Since then, the Cavendish laboratory became the Centre of the world of physical science.

Physical laboratories and research institutes were the backdrop for the emergence of scientific schools in the physics, becoming basis of forming of collective scientific work.. The scientific revolution in the late 19th – early 20th centuries led to the further "collectivization" of science. By the beginning of the 20th century, single-ended, and professors almost scientific studies were conducted by three categories of employees: University professors, members of the scientific organizations of industry and Government researchers. Development of modern physical science requires large financial investment, therefore the role of public and intergovernmental organs grew on co-ordination of scientific researches, the division of scientific labor happened in an international scale, that resulted in international co-operation in physical researches, appearance of large international physical institutes, research centers and coordinating organizations.

On development of quantum presentations and becoming of quantum mechanics substantial influence was rendered by scientific schools in physics, such as international scientific schools of J.J.Thomson and P.N.Lebedev, school of nuclear physics E.Rutherford, theoretical School of M.Born's at the University of Göttingen, Copenhagen Theoretical School of T.Bohr. A great role in the development of not only of home physics was rendered: physical school A.F.Ioffe, optical school of S.I.Vavilov, theoretical schools of L.D.Landau and I.E. Thamm, school of nuclear

physics of I.V.Kurchatov, Kazan scientific School of magnetic radiospektroskopy and many others.

Thus, development of physics from times of her origin and becoming in natural way it is related to development of its organizational forms.

Literature:

1. Frolov E. D. Musejon Antique in his development of private law institution to a State Agency //E.D. Frolov. Paradoxes of history – paradoxes of antiquity. SPb., 2004. – P. 314-334.

2. Gajdenko V.P., Smirnov G.A. Western science in the middle ages: General principles and teachings of the movement. – M.: Nauka, 1989.-P. 288.

3. Modina, E.B., Frankfurt U.I. From the history of scientific thought of the seventeenth century//At the sources of classical Science: Collection of articles /M.: Nauka, 1968 – P. 333.

4. Kopelevič Y.X. Origin of scientific academies: mid-17th to mid-18th centuries. -L.: Nauka, 1974.. – p. 52.

CID: J21210-846

Mazurkin PM

ADVANCED PROOF THE RIEMANN HYPOTHESIS

Mari State Technical University, Yoshkar-Ola

In the proof of the correctness of the Riemann hypothesis held strong Godel's incompleteness theorem. In keeping with the ideas of Polya and Hadamard's mathematical inventions, we decided to go beyond the modern achievements of the Gauss law of prime numbers and Riemann transformations in the complex numbers, knowing that at equipotent prime natural numbers will be sufficient mathematical transformations in real numbers.

In simple numbers on the top left corner of the incidence matrix blocks are of the frame. When they move, a jump of the prime rate. Capacity of a number of prime

numbers can be controlled by a frame, and they will be more reliable digits. In the column $i = 1$ *there is only one non-trivial zero on* $j = (0,\infty)$. *By the implicit Gaussian "normal" distribution* $z_{1j} = 1 - \exp(-10{,}11900(P_j - 2)^2)$, *where* P_j *- a number of prime numbers with the order-rank* j. *On the critical line of the formula for prime numbers*

$$z_{2j} = 1/2 - 0{,}.707107\cos(\pi P_j / 2 - 0{,}78540) = \frac{1}{2} - 0{,}707107\cos(\frac{\pi}{2}P_j - \frac{\pi}{4}).$$

By "the famous Riemann hypothesis is that the real part of the root is always exactly equal to 1/2" is obtained - the vibration frequency of a series of prime numbers is equal $\pi/2$, *and the shift of the wave -* $\pi/4$.

Montgomery and Dyson gave the average frequency of occurrences of zeros. But it turns out, it is different and functionally related to the number of spaces $\pi = 3{,}14159....$ *In 1972, Montgomery showed oscillatory nature of the arrangement of zeros on the critical line. We saw that they (and 1) really varies.*

Keywords: prime numbers, the full range, critical line, the equation

Introduction. While working on the proof of the correctness of the Riemann hypothesis held *strong Godel's incompleteness theorem*: "The logical completeness (or incompleteness) of any system of axioms cannot be proved within this system. For its proof or refutation of the required additional axioms (strengthening of the system)".

The incompleteness of the known ***law of distribution of prime numbers*** is as follows:

1) in order $n = 1,2,3,...$ not considered zero (truncated natural numbers);

2) a traditional series of prime numbers $a(n) = 2,3,5,7,...$ does not include zero and one [1];

3) the assumption that "the ratio x to $\pi(x)$ the transition from a given degree of ten to follow all the time increases by about 2,3" is clearly incorrect [1];

4) a statement that $\pi(x) \sim |x/\ln x|$, proposed in 1896 by Gauss, takes the prime numbers from the decimal number system in a number system with base $e = 2{,}71828...$;

5) the power of prime numbers $\pi(x)$ in a series of natural numbers x from the orders taken in decimal arithmetic, and the ratio $x/\ln x$ - in base of natural logarithms.

In keeping with the ideas of mathematicians Poya and Hadamar about mathematical inventions, we decided to go beyond the modern achievements of the Gauss law of prime numbers and Riemann transformations in the complex numbers, realizing that at equipotent prime natural numbers will be sufficient mathematical transformations in real numbers [2].

Full range, methods and data. Prime number - this is a natural number $N = \{0,1,2,3,4,5,6,...\}$ with a natural divider 1 (division by himself – is redundantly).

Of prime numbers $P = \{0,1,2,3,5,7,...\}$ "ladder of Gauss-Riemann" separated "step" increase with the parameter of ***prime numbers*** $p_j = P_{j+1} - P_j$, where $j = 0,1,2,3,4,...$ - is the rank order. Rejection of the system with base $e = 2,71828...$ led to the translation of the binary system. Understand that mathematics, fascinated by the factorization of prime numbers, forget about the benefits of the decomposition of numbers.

Table 1 shows the conversion of 500 prime numbers from decimal to binary. The decomposition of primes is known by the simple rules on the discharge rank $i = 0,1,2,3,4,....$ Then, a binary (real) numbers z were revealed distinctive features of the distribution of prime numbers and their growth on critical lines of the Riemann and envelope of the left border lines 1.

Factor analysis $P = \{0,1,2,3,5,7,...,3559\}$ gave the number 1/2.

Table 1. **Parameters of the total number of 500 prime numbers in binary**

Options			Prime number in binary															Increase in the binary system							
The order of the rank j	Prime number P_j	Growth p_j	Envelope		Discharge-the rank of the number i_j^P of binary													Envelope		Discharge-the rank i_j^p						
			Border P'_j	discharge $i_{j\max}^P$	12	11	10	9	8	7	6	5	4	3	2	1	0	border p'_j	discharge $i_{j\max}^p$	6	5	4	3	2	1	0
					Part of the prime number $P_{ij} = 2\wedge(i_j^P - 1)$												2^{-1}			Part of the increase						2^{-1}
					2048	1024	512	256	128	64	32	16	8	4	2	1				32	16	8	4	2	1	
0	0	1	1	1												1	½	1	1						1	½
1	1	1	1	1		Trivial zeros										**1**	½	1	1	Trivial zeros					1	½
2	2	1	2	2											**1**	0	½	1	1						1	½
3	3	2	2	2										1	**1**	½		2	2					1	**0**	½
4	5	2	4	3									1	**0**	***1***	½		2	2					**1**	0	½
5	7	4	4	3									**1**	***1***	**1**	½		4	3				**1**	0	**0**	½
6	11	2	8	4								**1**	0	1	***1***	½		2	2					**1**	0	½
7	13	4	8	4								1	**1**	***0***	**1**	½		4	3				**1**	0	**0**	½
8	17	2	16	5							1	0	0	**0**	***1***	½		2	2					**1**	0	½
9	19	4	16	5							1	0	0	***1***	**1**	½		4	3				**1**	0	**0**	½

10	23	6	16	5								1	0	1	**1**	***1***	½	4	3				1	**1**	0	½
11	29	2	16	5								1	1	**1**	***0***	**1**	½	2	2					1	**0**	½
12	31	6	16	5								1	**1**	1	**1**	***1***	½	4	3				1	**1**	0	½
13	37	4	32	6							1	**0**	0	**1**	***0***	**1**	½	4	3				**1**	0	**0**	½
14	41	2	32	6							**1**	0	**1**	0	0	***1***	½	2	2					**1**	0	½
15	43	4	32	6							1	**0**	1	0	***1***	**1**	½	4	3				**1**	0	**0**	½
16	47	6	32	6							1	0	**1**	1	**1**	***1***	½	4	3				1	**1**	0	½
17	53	6	32	6							1	1	0	**1**	***0***	**1**	½	4	3				**1**	1	**0**	½
18	59	2	32	6							1	1	1	0	**1**	***1***	½	2	2					**1**	**0**	½
19	61	6	32	6							1	1	1	1	***0***	**1**	½	4	3				1	**1**	**0**	½
20	67	4	64	7						1	0	0	0	0	1	***1***	½	4	3				**1**	0	0	½
32	127	4	64	7						1	1	1	1	1	1	1	½	4	3				1	0	0	½
33	131	6	128	8					1	0	0	0	0	0	1	1	½	4	3				1	1	0	½
55	251	6	128	8					1	1	1	1	1	0	1	1	½	4	3				1	1	0	½
56	257	6	256	9				1	0	0	0	0	0	0	0	1	½	4	3				1	1	0	½
98	509	12	256	9				1	1	1	1	1	1	1	0	1	½	8	4			1	1	0	0	½
99	521	2	512	10			1	0	0	0	0	0	1	0	0	1	½	2	2					1	0	½
173	1021	10	512	10			1	1	1	1	1	1	1	1	0	1	½	8	4			1	0	1	0	½
174	1031	2	1024	11		1	0	0	0	0	0	0	0	1	1	1	½	2	2					1	0	½
310	2039	14	1024	11		1	1	1	1	1	1	1	0	1	1	1	½	8	4			1	1	1	0	½
311	2053	10	2048	12	1	0	0	0	0	0	0	0	0	1	0	1	½	8	4			1	0	1	0	½
499	3557	2	2048	12	1	1	0	1	1	1	1	0	0	1	0	1	½	2	2					1	0	½
500	3559	12	2048	12	1	1	0	1	1	1	1	0	0	1	1	1	½	8	4			1	1	0	0	½

Note. Discontinuities table shows the beginning and end of blocks 0 and 1 in a series of 500 prime numbers.

Table 1 shows the symmetrical geometric patterns, but their analysis we did not. It is seen that any prime number before itself has a ratio of 1/2.

But it is a sum of terms is not included. Complex mathematical expressions, the parameters of the series has the form:

$$i_j = (1, m),\ j = (0, n),\ m = 6,\ n = 500, \tag{1}$$

$$P_{j+1} = P_j + p_j,\ p_j = P_{j+1} - P_j, \tag{2}$$

$$P_j = P'_j + P''_j,\ P'_j = 2^{i_{j\max}-1},\ P''_j = \sum_{i_j=1}^{i_{j\max}-1} \xi_{ij} 2^{i_j-1},\ \xi_{ij} = 0 \vee 1, \tag{3}$$

$$p_j = p'_j + p''_j,\ p'_j = 2^{i_{j\max}-1},\ p''_j = \sum_{i_j=1}^{i_{j\max}-1} \xi_{ij} 2^{i_j-1},\ \xi_{ij} = 0 \vee 1. \tag{4}$$

In table 1 we have two types of zeros - the trivial (empty cells) and unconventional (0). The first prime numbers to the left of the broken line 1. A non-trivial zeros lie inside the two columns 1. More complicated with the growth - the

bending around all j1 is the wave, and the line itself is always concerned the critical line $i_j^p = 2$.

Mathematical "landscape". In the film «De Code» (19.07; 26.07 and 02.08.2011) showed a three-dimensional picture of the Riemann zeta function. All pay attention to the nontrivial zeros on the critical line. They are already counted several trillion.

Alignment of the binary system is infinitely high "mountain" transforms into ledges of identical height, equal to unity. Figure 1 shows the landscape of the 24 first prime numbers.

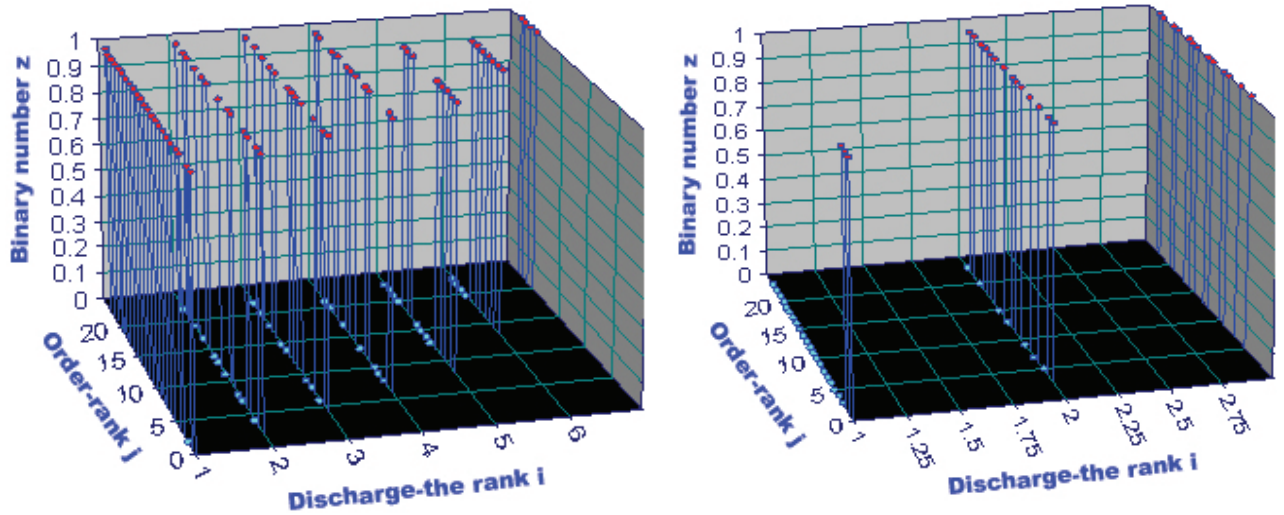

Prime numbers at the beginning of the distribution The growth of prime numbers at the beginning

Fig. 1. Mathematical "landscape" binary distribution of the 24 first prime numbers

In figure 1, there is a "ceiling" of 1, except the "floor" of the nontrivial zeros. Between them there is an unknown factorial relationship. Then the hard surface of the Riemann zeta function, due to the submission of complex numbers is transformed into "two-layer cake."

Benchmarks. They are on the upper left corner blocks of prime numbers. It was during the transition to them occurs a jump increase in prime. Therefore, power series of prime numbers is quite possible to manage with the help of a benchmarks, they will be safer decimal digits.

Table 2. **Asymptotic benchmarks a number of 500 primes**

i	1	2	3	4	5	6	7	8	9	10	11	12
j	0	2	4	6	8	13	20	33	56	99	174	311
P_{ij}	0	2	5	11	17	37	67	131	257	521	1031	2053
N_R	1	2	4	8	16	32	64	128	256	512	1024	2048

From table 1, we write the nodal values N_R (table 2) and other parameters of benchmarks. Power measurement range of prime numbers on benchmark is much more economical $\pi(x)$.

P_{ij} - N_R	-1	0	1	3	1	5	3	3	1	9	7	5

Influence of prime numbers per grade. Table 1 shows, at $i = 0$ there is $z_0 = 1/2$.

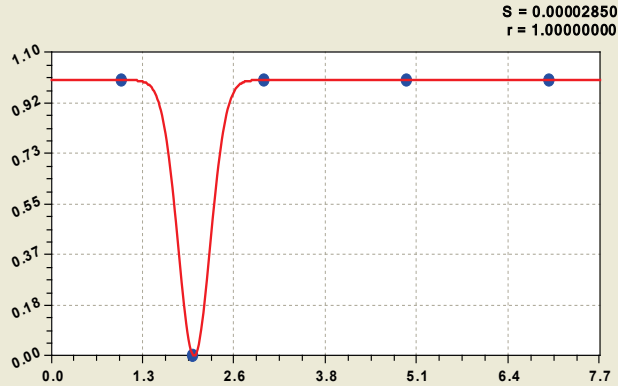

Fig. 2. Schedule of the formula (5) the distribution of the binary:
S - dispersion; r - correlation coefficient

And in the column $i = 1$ (fig. 2) there is only one nontrivial zero throughout $j = (0, n)$, i.e. before $j = (0, \infty)$.

By implicitly [3, 4] given us the law of Gauss "normal" distribution have

$$z_{1j} = 1 - \exp(-10{,}11900(P_j - 2)^2). \qquad (5)$$

Then the prime number 2 is a critical and noncritical series begins with 3.

On the critical line is the formula

$$z_{2j} = 1/2 - 0{,}.707107\cos(\pi P_j / 2 - 0{,}78540) = \frac{1}{2} - 0{,}707107\cos(\frac{\pi}{2}P_j - \frac{\pi}{4}). \qquad (6)$$

Completed (fig. 3) evidence of "the famous Riemann hypothesis about that the real part of the root is always exactly equal to 1/2".

The frequency of oscillation is equal $\pi/2$, and the shift - $\pi/4$.

There were two fundamental physical constants: in formula (5) - Napier number $e = 2{,}71828...$ (the number of times) in equation (6) - Archimedes number $\pi = 3{,}14159...$ (the number of spaces).

What does it mean 0,707107 - we do not know.

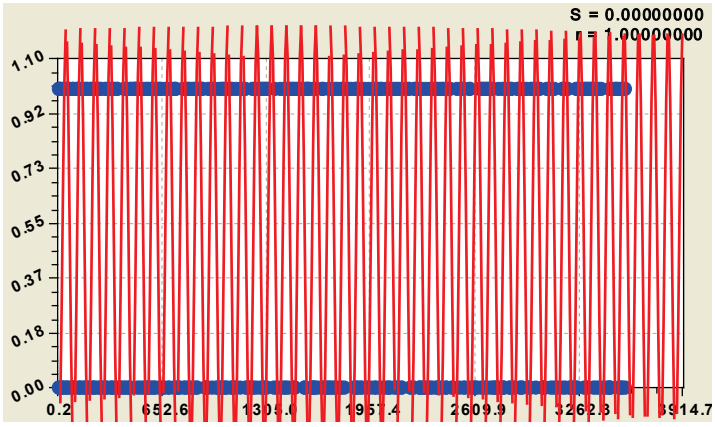

Fig. 3. Schedule of the formula (6) the distribution of the binary

Then obtained (fig. 4) model

$$z_{3j} = \frac{1}{2} - 0{,}707107 \cos\left(\frac{\pi}{4} P_j - \frac{\pi}{2}\right). \qquad (7)$$

Montgomery and Dyson applied statistical physical methods of the analysis of distributions with respect to a number of primes and determined the average frequency of occurrences of zeros.

But it turns out, the average frequency over the binary conversion of prime numbers is obtained by functionally related to the number of spaces $\pi = 3{,}14159...$.

From the remains of up to 0,25 for the fourth level was obtained (fig. 4) model

$$z_{4j} = \frac{1}{2} - 0{,}648348 \cos\left(\frac{\pi}{8} P_j - \frac{\pi}{2}\right). \qquad (8)$$

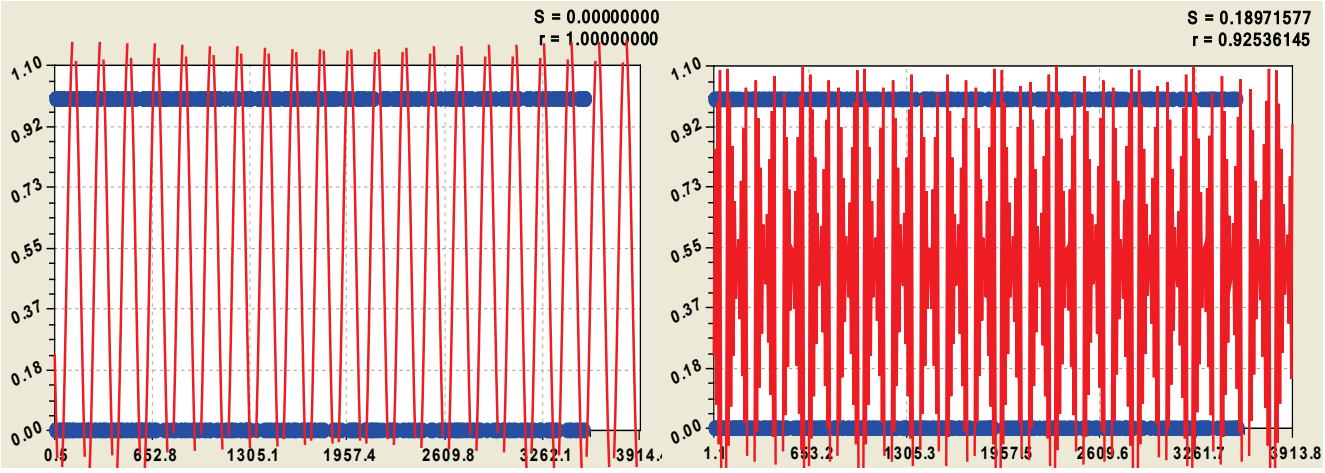

The statistical model (7) for the third rank — The statistical model (8) at the fourth digit

Fig. 4. Graphs of the distribution of the binary components of prime numbers

For the fifth and sixth digits (fig. 5) were obtained regularities:

$$z_{5j} = \frac{1}{2} - 0{,}643132 \cos\left(\frac{\pi}{16} P_j - \frac{\pi}{2}\right); \qquad (9)$$

$$z_{6j} = \frac{1}{2} - 0{,}638209\cos\left(\frac{\pi}{32}P_j - \frac{\pi}{2}\right). \qquad (10)$$

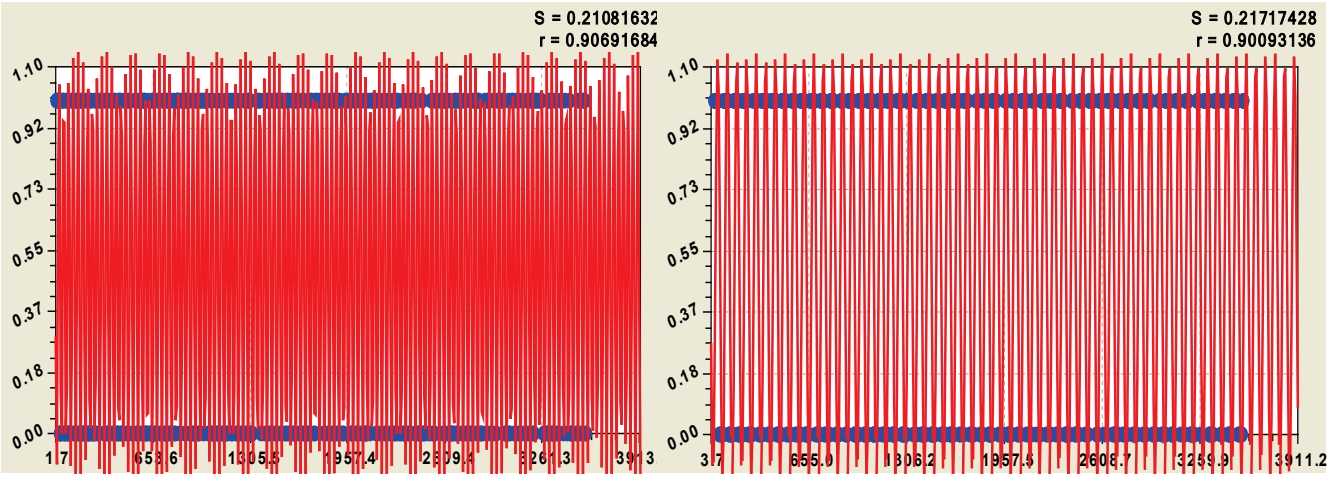

The statistical model (9) at the fifth discharge The statistical model (10) at the sixth discharge

Fig. 5. Graphs of the distribution of the binary components of prime numbers

It is noticeable that with increasing level binary system balances (absolute error) increases. This can be seen in the graphs to reduce the correlation coefficient.

In 1972 Montgomery proved nature of the distribution of the zeros on the critical line. From formulas (6) and other shows that they (and 1) is indeed fluctuate. We explain the desire of prime numbers, as well as convert them to binary 0 and 1, diverge from each other because of the power produced in the progression $P'_j = 2^{i_{j\max}-1}$. A nontrivial zeros of scatter in the plane $(i,\ j)$ in laws (3) for summand P''_j at $\xi_{ij} = 0 \vee 1$.

For the seventh and eighth categories (fig. 6) formulas of a similar design are received:

$$z_{7j} = \frac{1}{2} - 0{,}633145\cos\left(\frac{\pi}{64}P_j - \frac{\pi}{2}\right); \quad (11) \qquad z_{8j} = \frac{1}{2} - 0{,}636929\cos\left(\frac{\pi}{128}P_j - \frac{\pi}{2}\right). \quad (12)$$

For the ninth and tenth digits (fig. 7) have produced similar pattern:

$$z_{9j} = \frac{1}{2} - 0{,}638599\cos\left(\frac{\pi}{256}P_j - \frac{\pi}{2}\right); \quad (13) \qquad z_{10j} = \frac{1}{2} - 0{,}636726\cos\left(\frac{\pi}{512}P_j - \frac{\pi}{2}\right). \quad (14)$$

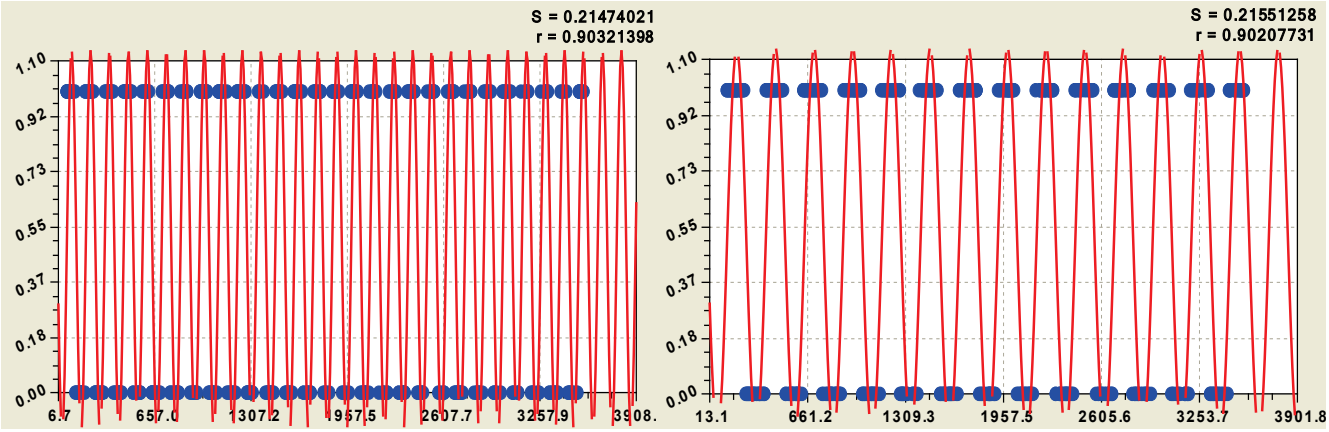

The statistical model (11) for the seventh digit The statistical model (12) for the eighth digit

Fig. 6. Graphs of the distribution of the binary components of prime numbers

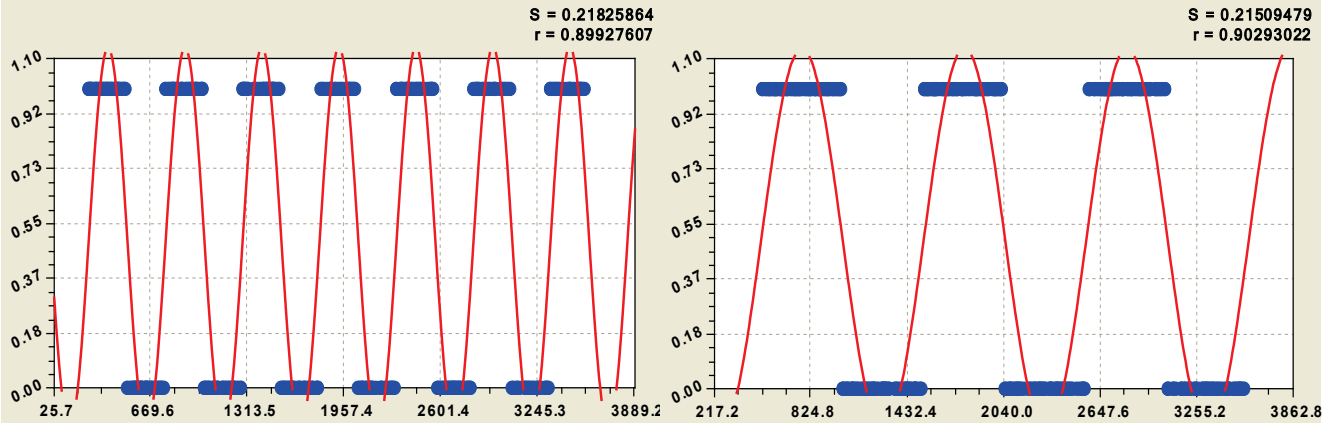

The statistical model (13) at the ninth discharge The statistical model (14) at the tenth category

Fig. 7. Graphs of the distribution of the binary components of prime numbers

For the 11-th digit (fig. 8) similarly has been received the formula (with the $z_{12j} = 1$)

$$z_{11j} = \frac{1}{2} - 0{,}633526\cos\left(\frac{\pi}{1024} P_j - \frac{\pi}{2}\right). \qquad (15)$$

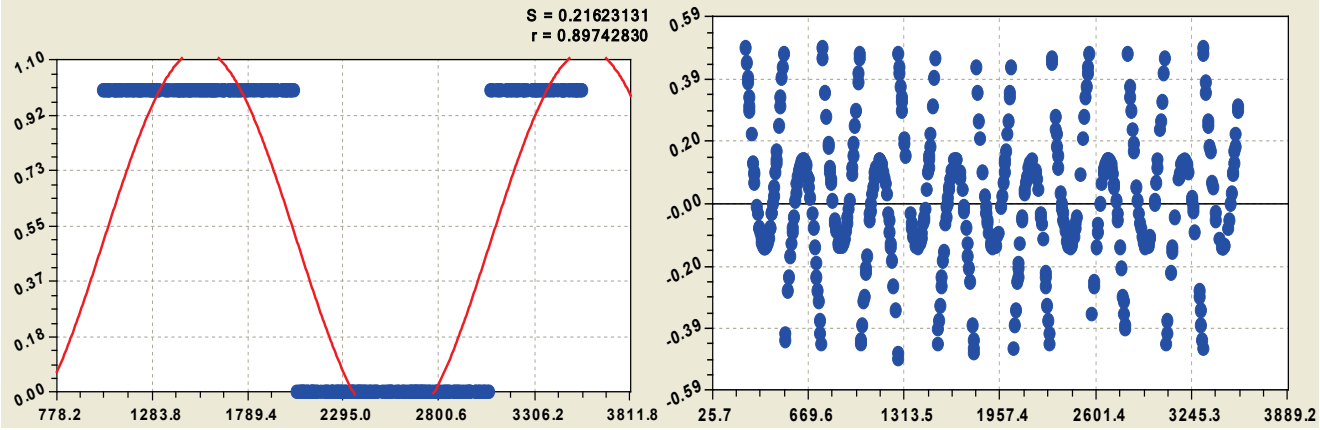

The statistical model (15) in the 11-th category Residues after formula (13) the ninth grade

Fig. 8. Graphs of the distribution of the binary components of prime numbers

There are among mathematicians claim: in the distribution of prime numbers there is no geometry. The pattern on the binary matrix in table 1 and for residues in figure 8 disprove this statement. However, what and how to identify them, we do not yet know.

Effect of growth in charges. Bernhard Riemann in 1859, according to the analysis of the zeta function asserted that the zeros are on the same line. Now believe it as critical line crosses the mathematical landscape of the zeta function.

From the data of table 1 shows that for the new parameter of a number - increase of the number of primes - there is a single line. This - the vertical $i_j^p = 2$. We show that the rest of the vertical, of the components of the primes slowly approaching the critical line on the condition $j \to \infty$.Thus once again confirming the proof of the Hardy about the fact that in a number of there are an infinite number of non-trivial zeros, part of which can not lie on the critical line.

For 1 and 2 categories (fig. 9) on unbroken trivial zeros of the verticals are:

$z_{1j} = 1348{,}7836 \exp(-7{,}20702 p_j)$ - the law of the Laplace (in physics - Mandelbrot); (16)

$$z_{2j} = 1/2 - 1/2 \cos(\pi p_j / 2). \qquad (17)$$

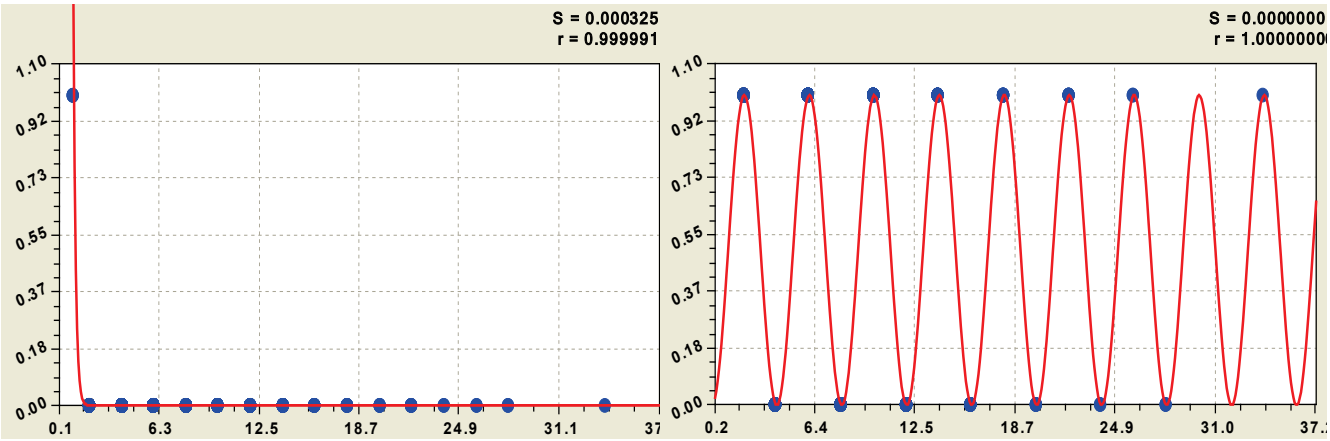

Statistical model (16) at the first category Functional model (17) on a critical line

Fig. 9. Schedules of distribution of binary number at components of a gain of simple numbers

The critical line $i_j^p = 2$ has received the unequivocal formula, and without wave shift.

In our example, from 500 in increments of prime numbers $z_{6j}=1$. For 3, 4, and 5 bits are excluded from the vertical cell with trivial zeros.

The general equation for these lines receives a variable frequency of the oscillation. For 3 or 4 digits (fig. 10) were obtained by the formula:

$$z_{3j}=\frac{1}{2}-0{,}707107\cos\left(\frac{\pi}{4}p_j-\frac{\pi}{2}\right),\ \text{совпадает с формулой (7);} \qquad (18)$$

$$z_{4j}=0{,}45433-0{,}62621\cos\left(\pi p_j/(155{,}4496-128{,}0887\,p_j^{\,0{,}038904})+0{,}99258\right). \qquad (19)$$

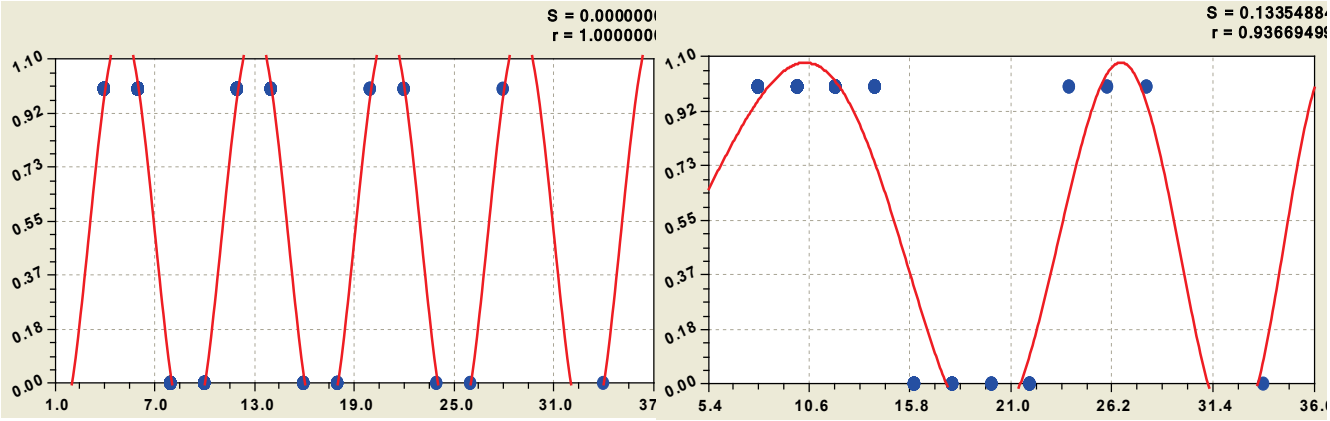

The statistical model (18) for the third digit growth — The statistical model (19) for the fourth digit

Fig. 10. Graphs of the distribution of the binary number of the components of the growth of the number of primes

Even greater deviation from the critical line (fig. 11) is on the fifth category:

$$z_{5j}=0{,}50303-0{,}50302\cos\left(\pi p_j/(708{,}9266-17{,}94895\,p_j^{\,1{,}02956})+2{,}82289\right). \qquad (20)$$

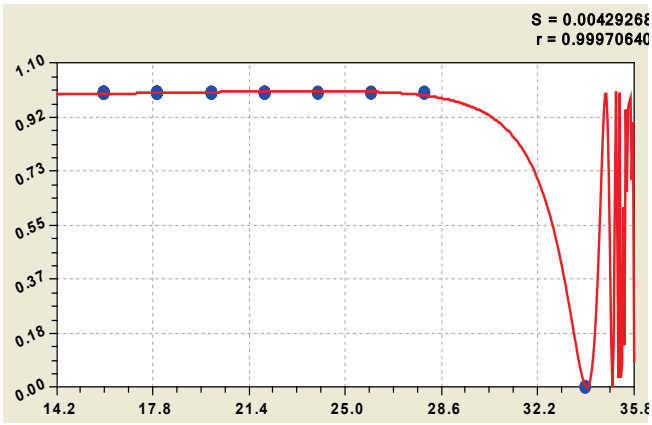

Fig. 11. Graph (20) the distribution of the binary number

The beginning of a critical line. Formula (17) is observed at the minimum short of the critical line containing two points (fig. 12).

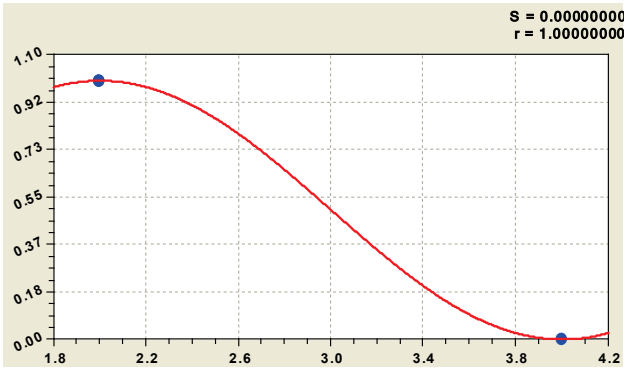

Fig. 12. Schedule of two binary numbers of increments

Conclusions. The famous Riemann hypothesis is proved. For this was accomplished the transformation of a number of prime numbers from decimal notation to binary. We obtain four new

criteria. There were geometric patterns. Became visible "on the floor" non-trivial zeros and appeared units "on the ceiling" of the distribution of 0 and 1 instead of abrupt "hills" of zeta-function.

Literature

1. Don Zagier. The first 50 million prime numbers. URL: http://www.ega-math.narod.ru/Liv/Zagier.htm.

2. Number. URL: http://ru.wikipedia.org/wiki/%D0%A7%D0%B8%D1%81%D0%BB%D0%BE.

3. Mazurkin P.M. Biotechnical principle and sustainable laws of distribution // Successes of modern natural sciences. 2009. № 9, 93-97. URL: www.rae.ru/use/?section=content&op= show article&article_id=7784060.

4. Mazurkin PM The statistical model of the periodic system of chemical elements D.I. Mendeleev. Yoshkar-Ola: MarSTU, 2006. 152.

CID: J21210-842

Mazurkin P.M.

STABLE LAWS AND THE NUMBER OF ORDINARY

Mari State Technical University, Yoshkar-Ola

Power total number of primes from the discharge of the decimal system is identified by the law of exponential growth with 14 fundamental physical constants. Model obtained on the parameters of the physical constants, proved less of the error and it gives more accurate predictions of the relative power of the set of prime numbers.

The maximum absolute error of power (the number of primes), the traditional number is three times higher than suggested by us complete a number of prime numbers. Therefore, the traditional number 2, 3, 5, 7, ... is only a special case.

The transformation $\ln 10 = 2{,}302585...$ *it was a rough rounded, leading to false identification of physico-mathematical regularities of different series of prime numbers.*

Model derived from physical constants, proved more accurate than the relative accuracy, and it gives more accurate predictions of the relative power of the set of prime numbers with increasing discharge the decimal number system.

Keywords: primes, total number, physical constants, the relationship

Introduction. Prime number - is a natural number $N = \{0,1,2,3,4,5,6,...\}$ that has two positive divisors: one and itself.

There are several variants of distribution or **a series of prime numbers (SPN):**

1) finite number of critical primes $P = \{0,1,2\}$;

2) non-critical prime numbers $P = \{3,5,7,11,13,17,...\}$;

3) the traditional [1] number of primes $a(n) = \{2,3,5,7,11.13.17,...\}$ with order (serial number) $n = \{1,2,3,...\}$, which was considered by many scientists and by Riemann;

4) part series of prime numbers [2] $P = \{1,2,3,5,7,11,13,17,...\}$;

5) the total number of prime numbers $P = \{0,1,2,3,5,7,11,13,17,...\}$ that are equivalent row N.

The literature focuses on SPN_3, and we did not find sufficient publications on the analysis of SPN_4 and other ranks have been proposed by us. In this reader a series of five articles examined SPN_1, SPN_2 SPN_5 and compared with evidence SPN_3.

Methodology. The main type of natural numbers are in $(0;\infty)$. If we miss this kind of integers due to rejection of negative numbers. For convenience, we will use mathematical analysis, recording the results of calculations in the form of rational numbers just to prove the Riemann hypothesis. Quantitative analysis is a leap to mind the actual (real) numbers, according to the scheme $P \subset N \subset R \not\subset C$ without taking into account the complex numbers, but with irrational numbers such as $e = 2{,}71...$ and $\pi = 3{,}14...$ (18 characters after the decimal point in the software environment CurveExpert) and other fundamental constants.

In the analysis of stable laws (table 1) have been applied [3] to the distribution of prime numbers.

Biotechnical law and its fragments. Under the scheme "from the simple to the complex structure" in table 1 are all stable laws are used to construct formulas biotech laws. Generalizing formula is biotech law [3]. Most often, the sum of two biotech laws constitutes a deterministic allocation model.

Table 1. **Mathematical constructs in the form of stable laws to build a statistical model**

Fragments without previous history of the phenomenon or process	Fragments from the prehistory of the phenomenon or process
$y = ax$ - law of linear growth or decline (with a negative sign in front of the right side of this formula)	$y = a$ - the law does not impact adopted by the variable on the indicator, which has a prehistory of up period (interval) measurements
$y = ax^b$ - **exponential growth law** (law of exponential death) $y = ax^{-b}$ is not stable because of the appearance of infinity at zero explanatory variable	$y = a\exp(\pm cx)$ - Law of Laplace in mathematics (Zipf in biology, Pareto in economics, Mandelbrot in physics) exponential growth or loss respect to which the Laplace created a method of operator calculus
$y = ax^b \exp(-cx)$ - biotech law (law of life skills) in a simplified form	$y = a\exp(\pm cx^d)$ - **law of exponential growth or death** (P.M. Mazurkin)
$y = ax^b \exp(-cx^d)$ - **biotech law**, proposed by professor P.M. Mazurkin	

Note. In bold the full design of stable laws.

Formula, together with a finite set SPN runs in a software environment CurveExpert for parameter identification of a stable law and wave patterns. Search for the model parameters is called the ***structural-parametric identification***. For the processes of behavior of living and/or inert substances (according to V.I. Vernadsky) parameters a,b,c,d biotech law and its fragments may approach to the fundamental physical constants, and it has been shown in the distribution of chemical elements [4].

Power series of prime numbers. According to [1] SPN_3 and our calculations on SPN_5 in table 2 shows the cardinal numbers and their relationships SPN_5/SPN_3.

Table 2. **The relative cardinal number the increase in the capacity (quantity) of prime numbers**

Discharge i_{10}	The power of numbers $N = \{0,1,2,3,...\}$ x	Traditional SPN_3 [1]		Full SPN_5		SPN_5/SPN_3, %	
		Power $\pi(x)$	$x/\pi(x)$	Power $\pi(x)$	$x/\pi(x)$	$\pi(x)$	$x/\pi(x)$
1	10	4	2.5	6	1.6667	**150,00**	66,67
2	100	25	4.0	27	3.7037	108,00	92,59
3	1 000	168	6.0	170	5.8824	101,19	98.04
4	10 000	1 229	8.1	1 231	8.1235	100,16	100,29

5	100 000	9 592	10.4	9 594	10.4232	100,02	100,22
6	1 000 000	78 498	12.7	78 500	12.7389	100,00	**100,31**
7	10 000 000	664 579	15.0	664 581	15.0471	100,00	100,31
8	100 000 000	5 761 455	17.4	5 761 457	17.3567	100,00	99,75
9	1 000 000 000	50 847 534	19.7	50 847 536	19.6666	100,00	99,83
10	10 000 000 000	455 052 512	22.0	455 052 514	21.9755	100,00	99,89

In the first digit decimal numbers the difference between a full and traditional rows of simple number is equal to 150 %. The relative cardinal number is the maximum 100,31 at $i_{10} = 6$ and minimum 66.67 at $i_{10} = 1$. What SPN better? In advance, we say that SPN_5.

Traditional SPN. With the increase in decimal place of natural numbers the increase in the relative cardinal number of the set of prime numbers with a capacity of more than 455 million occurs (fig. 1) by a deterministic model of the law of exponential growth

$$x / \pi(x) = 0{,}00066575 \exp(8{,}10285 i_{10}^{\,0{,}10893}). \qquad (1)$$

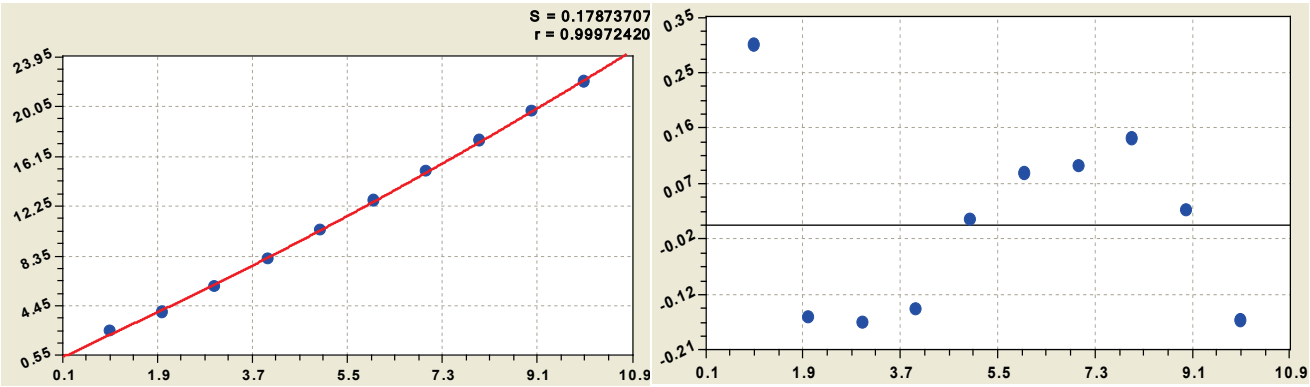

Fig. 1. The schedule of the law of exponential growth (1) the relative power and remains after it: S - dispersion; r - correlation coefficient

On the balances was obtained (fig. 2) of the wavelet function (described in the second article)

$$\varepsilon = 88{,}26937 \exp(-5{,}36239 i_{10}^{\,0{,}098706}) \cos(\pi i_{10} / (0{,}59537 + 1{,}47125 i_{10}^{\,0{,}27860}) - 0{,}67755). \qquad (2)$$

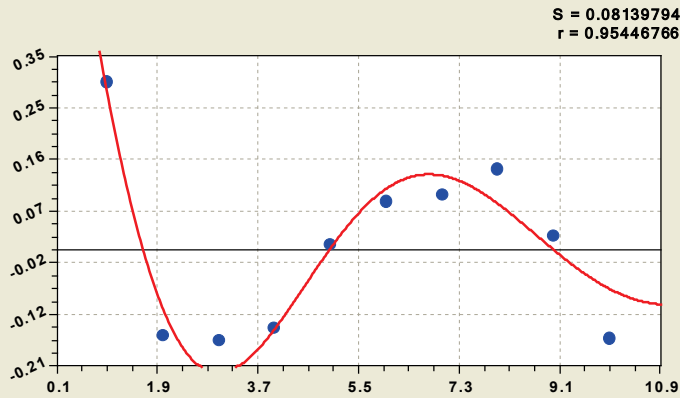

Fig. 2. Balance diagram for the model (2)

The law of exponential death before the cosine function shows half of the amplitude of the oscillatory perturbations of power SPN_3. Because of the high value of the remainder for $i_{10} = 1$, we have that zero discharge is theoretically possible number of prime numbers must be 88.

Combining formulas (1) and (2) gives the model with the wave function (fig. 3)

$$x / \pi(x) = 0{,}00074272 \exp(8{,}15289 i_{10}^{\,0{,}10111}) +$$

$$+ 956{,}514 \exp(-5{,}28998 i_{10}^{\,0{,}21896}) \cos(\pi i_{10} / (-0{,}14154 + 15{,}52749 i_{10}^{\,-0{,}33681}) + 1{,}38397) . \qquad (3)$$

Top of the wave has moved up to 957 prime numbers with zero discharge of the decimal system. In addition, under the function of the cosine of half-cycle fluctuations has changed: the beginning shifted to the first digit of the negative numbers. Half-life increases sharply, and the intensity parameter of death -0.33681 shows anomalous behavior of the model (3).

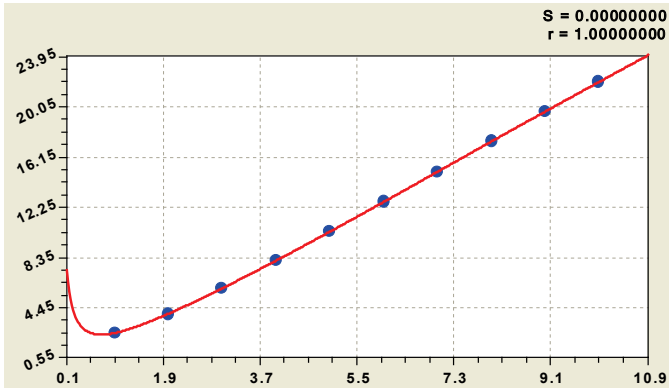

Fig. 3. The relative power of the traditional series

From the graph in figure 3 we can see that the shape of the curve repeats part of the curve of the Riemann zeta-function, located in the positive area of complex numbers.

Full range. This SPN_5 received a deterministic pattern (fig. 4) the type of

$$x / \pi(x) = 1{,}50030 \cdot 10^{-24} \exp(55{,}46724 i_{10}^{\,0{,}019036}) . \qquad .(4)$$

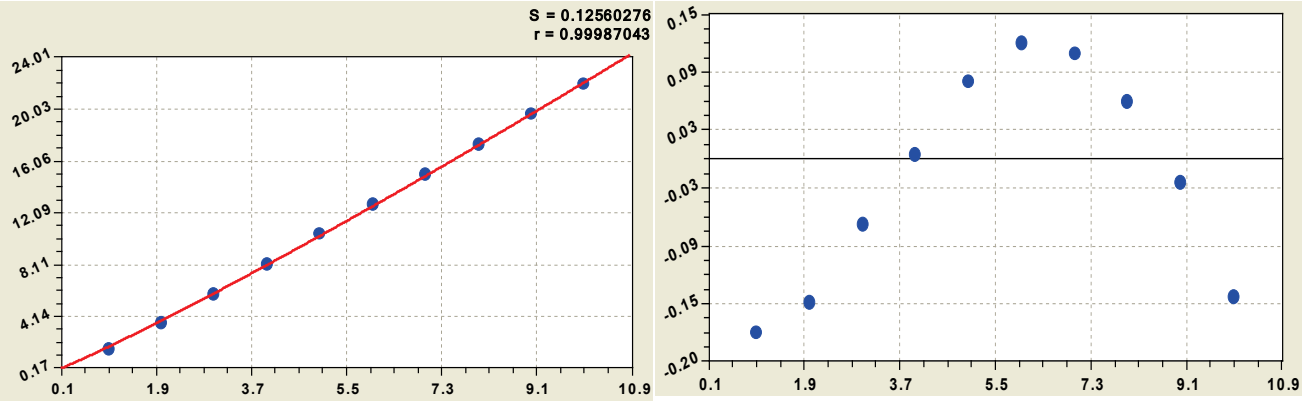

Fig. 4. Schedule of the law of exponential growth (4) and residues from him

Residues have a relatively smooth swing and determined (fig. 5) by the formula:

$$\varepsilon = -0{,}20751\exp(-0{,}16759 i_{10}{}^{0{,}48624})\cos(\pi i_{10}/(8{,}19322 - 0{,}31718 i_{10}{}^{0{,}99304}) - 0{,}22080). \qquad (5)$$

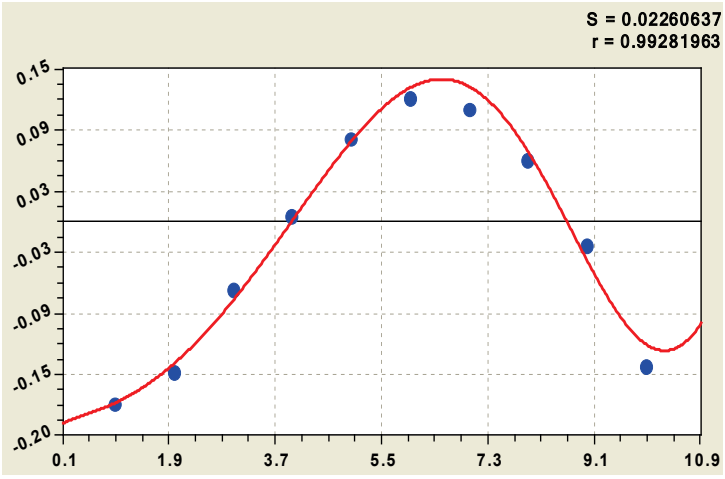

Рис. 5. График остатков по модели (5)

In a number of natural numbers ***0***, ***1***, ***2***, **3**, 4, **5**, 6, **7**, 8, 9, there are six prime numbers, three of which (0, 1, 2) critical (negative sign before the formula vibration), and three numbers (3, 5, 7) - a non-critical. At zero there is no prime numbers, so the law of exponential growth begins with a small actual (real) numbers $1{,}50030 \cdot 10^{-24}$, and -0.20751.

In formula (5), half of the amplitude of the perturbations of the power SPN_5 has the numerical value of all 0,20751. The initial half-life 8,19322 damped oscillations approaching 8.

We express the frequency response $8{,}19322 - 0{,}31718 i_{10}{}^{0{,}99304}$ of the oscillatory disturbance is half-wave decline, i.e. with increasing discharge i_{10} is the growth rate fluctuations on the scale of natural numbers $N = \{0,1,2,3,...\}$, and it - the effect of the tremor.

The general equation (fig. 6) is characterized by binomial formula

$$x/\pi(x) = 1{,}49766 \cdot 10^{-24}\exp(55{,}46556 i_{10}{}^{0{,}019025}) -$$

$$-0{,}18905\exp(-0{,}0032736 i_{10}{}^{1{,}00713})\cos(\pi i_{10}/(7{,}40869 - 0{,}23358 i_{10}{}^{0{,}61848}) - 0{,}028862). \qquad (6)$$

Remains of the formula (6) are so small that, as seen in the upper right corner in figure 6, the variance of the residual is zero and the correlation coefficient is unity.

Comparison of the remains of the formulas (3) and (6) shown in figure 7.

The maximum absolute error of power (the number of primes), the traditional number is three times higher compared to the total number of primes.

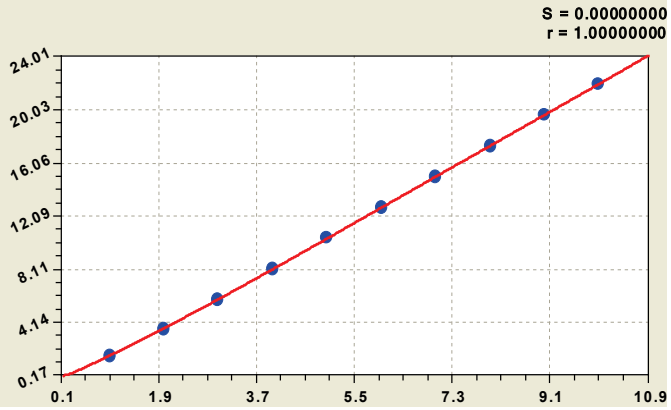

Fig. 3. The relative power of the complete series

Then it turns out that the traditional number is only a special case.

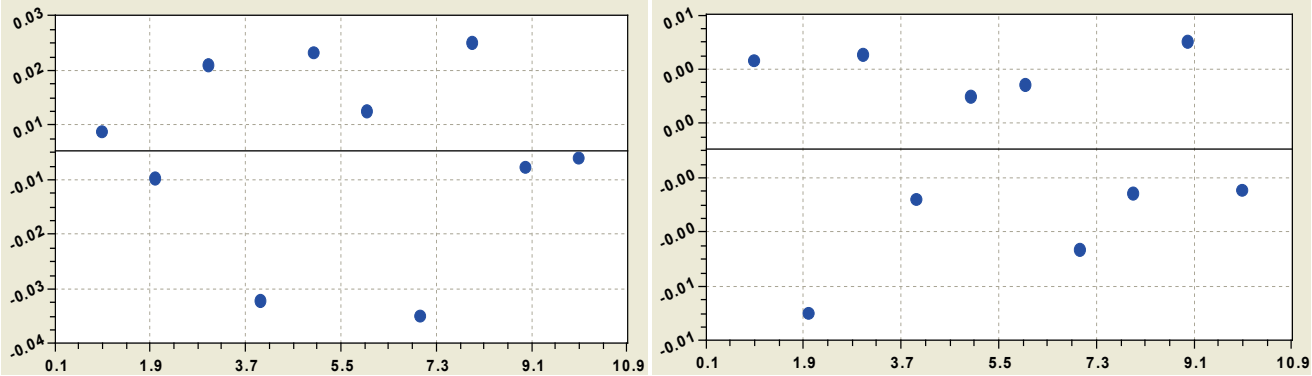

Residues resulting from the model (3) Residues resulting from the model (6)

Fig. 7. Graphs of the absolute error the laws of growth of capacity of prime numbers

Do not change the scale of reference of natural primes. This recommendation for the future in the study of prime numbers comes from the fact that, from Riemann used the natural logarithm and are looking for an empirical formula [1]. To quote from an article by Don Zagier:

"Apparently (see table 2.), that the ratio of x to π(x) the transition from a given degree of ten to follow all the time increases to about 2.3. Mathematics is recognizable among the 2.3 log 10 (of course, to base e). The result suggested that the $\pi(x) \sim |x / \ln x|$, where the sign ~ means that the ratio of their expressions are connected with x tends to 1. This asymptotic equation, first proved in 1896, is now the law of ***distribution of prime numbers***. Gauss, the greatest of mathematicians, discovered this law in the age of fifteen, studying tables of primes contained in the gift to him a year before the table of logarithms".

We were not too lazy to check the statement "the ratio of x to π (x) in the transition from the present level of ten to follow all the time increases by about 2.3" and the results of the calculations resulted in table 3. Here, the number 2.30 in SPN_3 not (if there is, the approximation error to 2.30 at 100(2.5 - 2.3) / 2.3 = 8.70%, which is very much), but there is an aspiration to 1. At the same time the full range of gives at the beginning of the interval of digits in a larger multiplicity 2,22 (error of 3.47 %).

Table 3

The multiplicity of cardinal number

Discharge	Private SPN_3 [1]		Full SPN_5	
i_{10}	$x/\pi(x)$	multiplicity	$x/\pi(x)$	multiplicity
1	2.5	-	1.6667	-
2	4.0	1.60	3.7037	2.22
3	6.0	1.50	5.8824	1.59
4	8.1	1.35	8.1235	1.38
5	10.4	1.28	10.4232	1.28
6	12.7	1.22	12.7389	1.22
7	15.0	1.18	15.0471	1.18
8	17.4	1.16	17.3567	1.15
9	19.7	1.13	19.6666	1.13
10	22.0	1.12	21.9755	1.12

Equal to the power of two sets SPN_3 and SPN_5 can be considered, starting with the digits $i_{10} \geq 9$ in decimal notation.

With the growth of x a true statement is the convergence to 1. For this purpose we identify the law of death (in a general form of table 1) according to the statistical data of table 3.

For the full range of the obtained formula

$$card(x_i / \pi(x_i) / (x_{i-1} / \pi(x_{i-1})) = 1{,}09980 + 1788{,}3968 \exp(-6{,}20754 i_{10}^{\,0{,}24956}) . \qquad (7)$$

Equation (7) shows that the ratio of cardinal numbers will not come near to the unit and can only reach the values of the 1,0998.

From the article [1] reads: «After more than a careful and complete calculation, Legendre in 1808 found that particularly good approximation is obtained if we subtract from ln x is not 1, but 1.08366, i.e. $\pi(x) \sim |x/(\ln x - 1{,}08366)|$». In the formula (7) the constant 1.09980 is little different.

Thus, number of prime numbers, the power has been studied in a number system with base $e = 2.718281828$ .... . It is known that this system has the greatest density of information recording and refers to the nonintegral positional systems. But non-integers do not belong to the natural numbers N, let alone to a series of prime numbers $a(n) = \{2,3,5,7,11.13.17,...\}$.

Thus, the transformation $\ln 10 = 2{,}302585...$ it was a rough rounded, leading to false identification of physico-mathematical regularities of different series of prime numbers.

With "easy" hands Gauss in mathematics, vigorously developed ***the theory of approximation***, which made it possible to linearize the scale of the abscissa and ordinate in terms of $\ln x$ and $\ln y$. Thus is the fundamental transformation of the statistical data presented at the beginning of the decimal system, in logarithmic. As a result, the ***closed form of design patterns*** that are not only difficult to understand, but they have lost and the visibility of graphics and even more so - the physical representation. Therefore, we continue to recommend in its publications to readers ***an open system of mathematical constructs*** according to the laws of table 1.

Fundamental constants. Formulas from table 1 gives the identification of fundamental physical constants to the parameters a,b,c,d. Processes themselves are unknown.

Carefully consider the formula (4), and compare the values of parameters of the mathematical model with the fundamental constants. Recall that Don Zagier [1] analyzed (see Table 2.) a very large number of natural numbers $\widetilde{N} = \{0,1,2,3,...,10^{10}\}$ with a finite number $a(n) = \{2,3,5,7,11.13.17,...\}$ of prime numbers and gave them a set of up $\pi(x) \to 455\ 052\ 512$.

We put forward a hypothesis (table. 4): with an increase in the relative power of the total number of prime numbers, the parameters of the model (4) will tend to the fundamental constant [5].

Table 4

Comparison of parameters of the model (4) of power SPN_5 with the fundamental physical constants

Parameter of the first term of the statistical model (6)			The fundamental physical constant		The multiplicity to a parameter of the model (4)
Type	Name	Value	Name	Value	
the number of time		18 characters*	Number of Napier	$e = 2{,}71828...$	≈ 1
Trend (tendency) of prime numbers	Initiation of a series of prime numbers	$1{,}50030 \cdot 10^{-24}$	Bohr magneton	$\mu_B = 9{,}27402 \cdot 10^{-24}$	$6{,}1814 \to 10\varphi^{-1}$
	Active growth	55,46724	Electron mass (amu) $\times 10^{-4}$	$m_e = 5{,}485799$	55,58486

	of power				$= m_e \sigma_=$ 1,0021105
	The growth rate of power	0,019036	Radiation: a second constant	$c_2 = 0{,}0143877$	0,75582 $\to \pi/4$
The number of harmony		18 characters*	Golden section $\varphi = 1{,}61803...$	$\varphi^{-1} = 0{,}61803...$	≈ 1
Parameters of the Earth	Atmosphere	exactly	Standard atmosphere	$\sigma_a = 101325$	1
	Gravitation	The acceleration of gravity (standard)		$g_n = 9{,}80665$	1
Atom	Proton	Magnetic moment / nuclear magneton		$\mu_p / \mu_N = 2{,}7928474$	≈ 1
		Mass of the proton (amu)		$m_p = 1{,}00727647$	≈ 1
	Neutron	Magnetic moment of the neutron		$\mu_n = 0{,}96623707$	≈ 1
		Mass of the neutron (near.)		$m_n = 1{,}0086649$	≈ 1
	Electron	Magnetic moment of / Bohr magneton		$\mu_e / \mu_B = 1{,}00115965$	≈ 1
		Anomaly magnetic moment		$g_e = 2{,}0023193$	≈ 1
Number of space		18 characters*	Number Of Archimedes $\pi/4 \approx 0{,}78540$	$\pi = 3{,}14159...$	≈ 1

Note. * In the mathematical environment CurveExpert the possibility of representing irrational numbers.

To a first approximation we replace the law (4) to the physical equivalent to the formula

$$x/\pi(x) = \frac{\sqrt{5}+1}{2 \cdot 10} \frac{\mu_p}{\mu_N} \mu_B e^{(m_e \sigma_a \frac{g_n}{10} \frac{m_p}{m_n}) i_{10}^{\frac{4}{\pi} c_2 (\frac{\mu_e}{\mu_B} g_e - 1)^8}}, \qquad (8)$$

legend of the model parameters (8) are given in table 4 (10 - radix).

The law with the fundamental constants. After substituting the fundamental physical constants in table 4 we write the model (8) as a law of exponential growth

$$x/\pi(x)_f = 4{,}1908462 \cdot 10^{-24} \exp(54{,}435096 i_{10}^{\,0{,}0190103}). \qquad (9)$$

Next check the adequacy of the models (4) and (9). Known formulas allowing to calculate the number of primes faster. In this way, it was calculated that up to 10^{23} is 1 925 320 391 606 803 968 923 primes.

Then we get to the data [1] the new value $x/\pi(x) = 51{,}9394$ (table 5).

Table 5

The adequacy of the law of exponential growth

Discharge i_{10}	$\frac{x}{\pi(x)}$	Model (4)			Model (9)		
		$x/\pi(x)$	ε	Δ,%	$x/\pi(x)_f$	ε	Δ,%
1	1.6667	1.8420	-0.1753	**-10.52**	1.8330	-0.1663	**-9.98**
2	3.7037	3.8481	-0.1444	-3.90	3.7735	-0.0698	-1.88
3	5.8824	5.9481	-0.0657	-1.12	5.7822	0.1002	1.70

4	8.1235	8.1181	0.0054	0.07	7.8429	0.2806	3.45
5	10.4232	10.3452	0.0780	0.75	9.9462	0.4770	4.58
6	12.7389	12.6211	0.1178	0.92	12.0861	0.6528	5.12
7	15.0471	14.9398	0.1073	0.71	14.2584	0.7887	5.24
8	17.3567	17.2969	0.0598	0.34	16.4598	0.8969	5.17
9	19.6666	19.6890	-0.0224	-0.11	18.6876	0.9790	4.98
10	21.9755	22.1132	-0.1377	-0.63	20.9399	**1.0356**	4.71
23	51.9394	55.8321	**-3.8927**	-7.49	51.8993	0.0401	0.08

ε - absolute error ; Δ - relative error , %.

Model (9), obtained from the physical constants in table 4, was even more precise on the relative error, and it gives more accurate predictions of the relative power of the set of prime numbers.

The error for the array $i_{10} = 23$ is equal to only 0,08 %.

By the remnants of (9) is obtained (fig. 8) the equations of the perturbation.

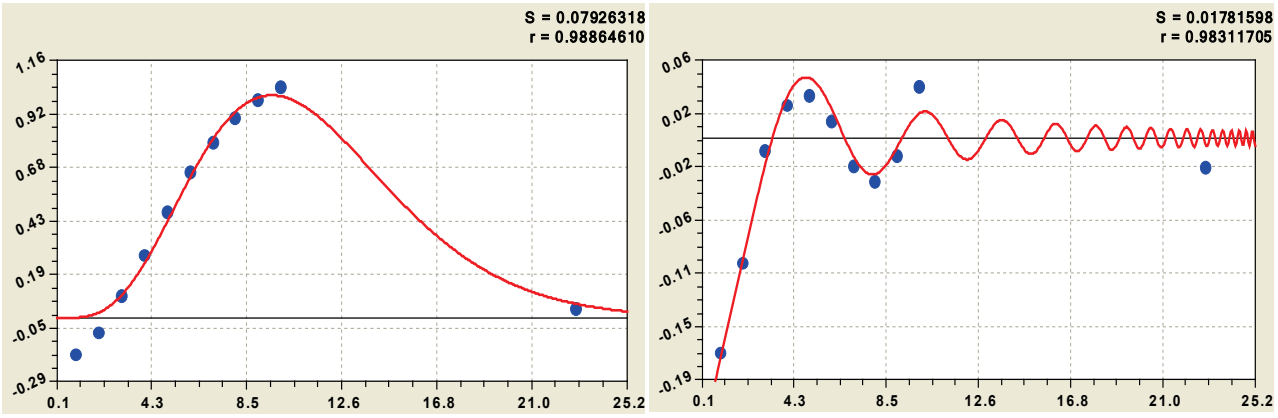

disturbance SPN_5 on biotech law the wave of the damped oscillatory perturbations

Fig. 8. Diagrams of the perturbation capacity of prime numbers depending on the order of the decimal system

Biotechnical law as a supplement to (9) shows that after the discharge $i_{10} = 23$ in the relative power is going on a decline. Damped oscillation shows that with increasing power of primes wave $x/\pi(x)$ tends to zero. When $i_{10} >> 23$ the perturbation is almost excluded.

Conclusions. Power total number of primes from the discharge of the decimal system is identified by the law of exponential growth to the fundamental physical constants. With the growth of the power of the prime numbers increases the adequacy of equation (8) with the physical constants, which can lead in the future to the general equation four interactions.

Literature

1. Don Zagier. The first 50 million prime numbers. URL: http://www.ega-math.narod.ru/Liv/Zagier.htm.

2. Number. URL: http://ru.wikipedia.org/wiki/%D0%A7%D0%B8%D1% 81% D0%BB%D0%BE.

3. Mazurkin P.M. Biotechnical principle and sustainable laws of distribution // Successes of modern natural sciences. 2009. № 9, 93-97. URL: www.rae.ru/use/? section=content&op= show article&article_id=7784060.

4. Mazurkin PM The statistical model of the periodic system of chemical elements D.I. Mendeleev. Yoshkar-Ola: MarSTU, 2006. 152.

5. Fundamental physical constants. URL;
http://www.akin.ru/spravka/s_fund.htm.

CID: J21210-843

Mazurkin P.M

STABLE LAWS AND THE NUMBER OF ORDINARY

Mari State Technical University, Yoshkar-Ola

We adhere to the concepts of Descartes, the need to apply algebraic equations directly as a final decision. The concept of wavelet signal allows to abstract from an unknown number of primes of a physical quantity.

Any number of primes can be decomposed into a finite set of asymmetric wavelets with variable amplitude and frequency. For example, taken a number of A000040.

The first term of the total number of model A000040 according to the law of exponential growth is the contribution of the absolute error 97,53 %.

The first member of the general model of a number of A000040 on the law of exponential growth is the contribution of the absolute error 97,53 %. The remaining 35 wavelets amount to a total of 2.47 %. But their influence on the number of primes $a(n) = \{2,3,5,,...,271\}$ *very significant.*

It is proved that any type of fnite-dimensional number of primes can be decomposed into a fnite-dimensional set of asymmetric wavelets with variable amplitude and frequency of oscillatory perturbations

Keywords: prime numbers, the family of wavelets, fractal levels

Introduction. It is necessary to identify a stable law of distribution of prime numbers, by analogy with the methodology, we have shown the growth of the relative atomic mass of 109 chemical elements according to atomic number in the Periodic Table D.I. Mendeleev [1]. For example, take a series of prime numbers 11 $a(n) = \{2,3,5,7,11.13.17,...\}$ at 22 $n = \{1,2,3,...\}$ and 33 $1 \le n \le 58$ for an array A000040. The article shows the physical and mathematical approach to the analysis.

Wavelet (splash) - a mathematical function. The word «wavelet» means "small wave". Wavelets - a family of functions, "the waves coming one after another." According to [2] the term "wavelet" refers to some soliton-like function.

The abscissa axis can be not only time but also any other value. Wavelet has a clear amplitude-frequency characteristic of prime numbers in order (conditional time). If $n = \{1,2,3,...\}$ - the abscissa, then the y-axis will share $a(n) = \{2,3,5,7,11.13.17,...\}$.

In [3] graphics, similar to the wavelet, called a smooth oscillating function. Therefore, a smooth function of the type $a(n) = f(n)$ require continuous wavelet transform in real numbers. It is known that wavelets with continuous analysis are subject to Heisenberg's uncertainty principle and, consequently, the basis of the wavelet is also not initially determined with respect to the x-axis plots. These sites appear in the identification process.

The properties of the wavelet. The main features of the wavelet the following:

1) amplitude-frequency localization of the axes of rectangular coordinates (x , y);

2) self-similarity (fractal) of the wavelet as quantitative mapping process;

3) removal of the uncertainty principle for the sequence of appearance of wavelets;

4) independence of the wavelet function from the object of mathematical analysis;

5) invariance of the wavelet shift the origin of coordinates on the x-axis;

6) integral of the wavelet, i.e. the footprint of the schedule, shall be equal to or close to zero.

On these grounds the wavelet analysis is often compared to a "mathematical microscope", revealing internal structure of heterogeneous objects, phenomena and processes.

Asymmetrical wavelet. We adhere to the concepts of Descartes, the need to apply algebraic equations directly as final solutions without the use themselves primitives (differential and / or integral equations).

Asymmetrical wavelet function of the form completely satisfies the six conditions

$$y = \sum_{i=1}^{m} y_i \ , \ y_i = a_{1i} x^{a_{2i}} \exp(-a_{3i} x^{a_{4i}}) \cos(\pi x / (a_{5i} + a_{6i} x^{a_{7i}} \exp(-a_{8i} x^{a_{9i}}) - a_{10i}) , \qquad (1)$$

where y - the index (dependent factor), i - the number of component (1), m - the number of components, x - the explanatory variable (influencing factor), $a_1 ... a_{10}$ - parameters (1), taking the numerical values in the process of structural-parametric identification of model (1).

In most cases, to identify patterns apply wavelet type

$$y = \sum_{i=1}^{m} y_i \ , \ y_i = a_{1i} x^{a_{2i}} \exp(-a_{3i} x^{a_{4i}}) \cos(\pi x / (a_{5i} + a_{6i} x^{a_{7i}}) - a_{8i}) . \qquad (1a)$$

A number of prime numbers as a series of signals. Physical and mathematical approach involves understanding a number of prime numbers as a reflection of a composite process of reality.

Signal - a material carrier of information. And the information we have understood as a ***measure of interaction***. The signal can be generated, but the reception is not mandatory. For example, the number of primes known for thousands of years, but its essence is a set of signals has not yet been disclosed. The signal can be any physical process, but it features a number of prime numbers is not yet clear. It turns out that changing the set of unknown signals has long been known through a series of prime numbers. So take a ***number of prime numbers*** for the fractal set of ***analog signals*** that vary continuously in a certain time in order. n

Then each term of equation (1a) can be written as a kind of harmonic wavelet

$$y = A_{0.5} \cos(\pi x / p_{0.5} - a_8) , \ A_{0.5} = a_1 x^{a_2} \exp(-a_3 x^{a_4}) , \ p_{0.5} = a_5 + a_6 x^{a_7} , \qquad (2)$$

where $A_{0.5}$ - the amplitude (half) of the wavelet (axis y), $p_{0.5}$ - half-period fluctuations (axis x).

By (2) with two fundamental constants e and π (irrational numbers), formed inside the quantized wavelet signal in the proportion of 0.5 (real number) or 1/2 (rational number), and quantization step 1/2 fits under the Riemann hypothesis.

Further record 0.5 in indexes it is lowered.

The concept of wavelet signal allows to abstract from an unknown number of primes of a physical quantity. We are confident that, as the signals in biology, identified patterns of primes as sums of wavelets - will be an important event. As in living cells: a signal - this is an event of regulatory importance for the functioning of cells. There is an analogy with the signals in a series of prime numbers, which must first be identified as wavelets.

Table A000040. Table 1 shows baseline data for wavelet analysis. Schedule A000040, or "the ladder of the Gauss-Riemann" are listed in the Internet. Computational experiments have shown that for $n > 500$ need a supercomputer petaflop class.

Table 1. **Finite-dimensional range of primes A000040:**

n - the order of a prime number; **a (n)** - prime

n	a(n)	n	a(n)	n	a(n)	n	a(n)	n	a(n)	n	a(n)
1	2	11	31	21	73	31	127	41	179	51	233
2	3	12	37	22	79	32	131	42	181	52	239
3	5	13	41	23	83	33	137	43	191	53	241
4	7	14	43	24	89	34	139	44	193	54	251
5	11	15	47	25	97	35	149	45	197	55	257
6	13	16	53	26	101	36	151	46	199	56	263
7	17	17	59	27	103	37	157	47	211	57	269
8	19	18	61	28	107	38	163	48	223	58	271
9	23	19	67	29	109	39	167	49	227		
10	29	20	71	30	113	40	173	50	229		

The first wavelet. Trend (fig. 1) after 90000 steps is calculated in the software environment CurveExpert-1.38 was the law of exponential growth by the formula

$$a(n) = 6.57251 \cdot 10^{-83} \exp(189{,}7135 n^{0{,}0065804}) . (3)$$

The residue of the first order of prime numbers is equal to 0.38096. But simple numbers begin with $n = 1$, and the ordinate is equal $a(n) = 2$. In a number zero values are absent. The remainder of the deterministic model (3) in the form of the law of exponential growth was obtained by the wavelet of the form (1a) in the formula (fig. 2)

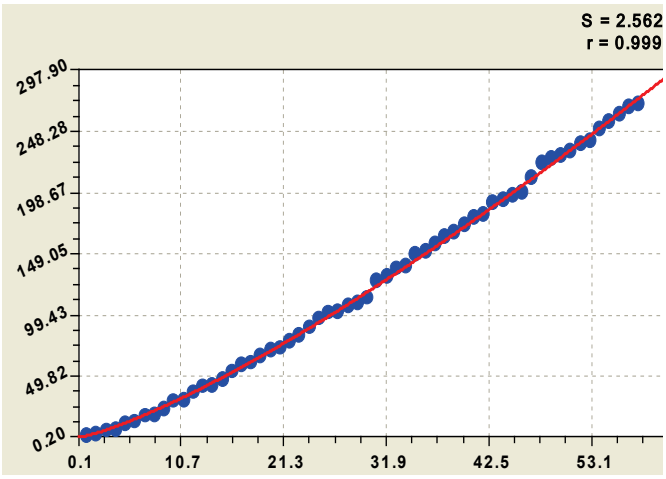

Fig. 1. Graph the trend (3) of the set A000040 of prime numbers:

S - Dispersion; r - correlation coefficient

$$a_2(n) = A_1 \cos(\pi n / p_1 + 1{,}41491), \quad (4)$$

$$A_1 = 16{,}40912 n^{-1{,}81310} \exp(+0{,}40441 n^{0{,}63429}), \; p_1 = 92{,}03817 - 68{,}33022 n^{0{,}050053} .$$

The graph in figure 2 is similar to graph the Riemann zeta function. The difference is that instead of the complex domain (4) is located in the positive quadrant of real numbers.

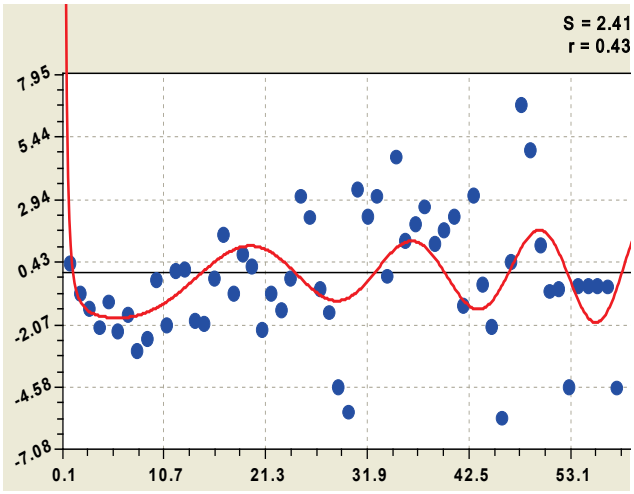

Fig. 2. Schedule of the first wave oscillatory perturbations

The amplitude of the formula (4) changes in the anomalous biotech law, when the signs of the second and third parameters of bio-law change. In contrast to the zeta function of half-cycle fluctuations in (4) is reduced, and is not constant, the oscillation frequency increases with the growth of a prime number. In $n = 0$ the period of oscillation is $2 \times 92{,}03817 \approx 184$. It's more of the series $1 \le n \le 58$.

The second wave of disturbance (fig. 3) gets the function of asymmetric wavelet

$$a_3(n) = A_2 \cos(\pi n / p_2 - 1{,}33556), \quad (5)$$

$A_2 = -0{,}00011633n^{4{,}01562}\exp(-0{,}49274n^{0{,}62216})$, $p_2 = 4{,}78606 - 0{,}00034507n^{1{,}88011}$.

Amplitude has a negative sign, i.e. perturbation series of prime numbers is a crisis. In model (4) is the shift of the wave is equal to 1,41941 order to the right of $n = 0$, and in the (5) shift is equal to 1,33556. Solitary wave ends after $n = 58$. A left boundary to the left of zero order. Significant interval of the soliton starts around with $n = 8$ or $a(n) = 19$.

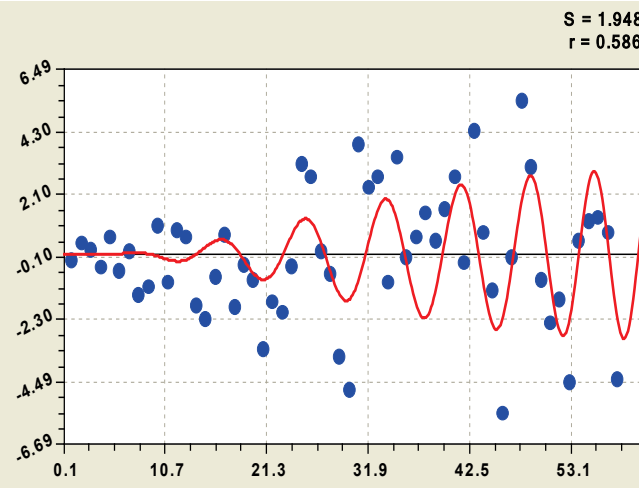

Fig. 3. The graph of the second wave of the oscillatory perturbations

Combining wavelets. Features CurveExpert (19 parameters) are small, so can "shake" together for more dense packing of wavelets, only three components (fig. 4) and obtain a general model of the form

$$a(n) = a_1(n) + a_2(n) + a_3(n), \qquad (7)$$

$a_1(n) = 5.82517 \cdot 10^{-83}\exp(189{,}83601n^{0{,}0065753})$, $a_2(n) = A_1\cos(\pi n / p_1 + 1{,}41453)$,

$A_1 = 19{,}39898n^{-1{,}73234}\exp(+0{,}23129n^{0{,}76261})$, $p_1 = 93{,}75309 - 70{,}10898n^{0{,}048713}$,

$a_3(n) = A_2\cos(\pi n / p_2 - 1{,}44553)$, $A_2 = -0{,}00011171n^{4{,}00261}\exp(-0{,}49079n^{0{,}61786})$,

$p_2 = 4{,}74039 - 0{,}00027372n^{1{,}92343}$.

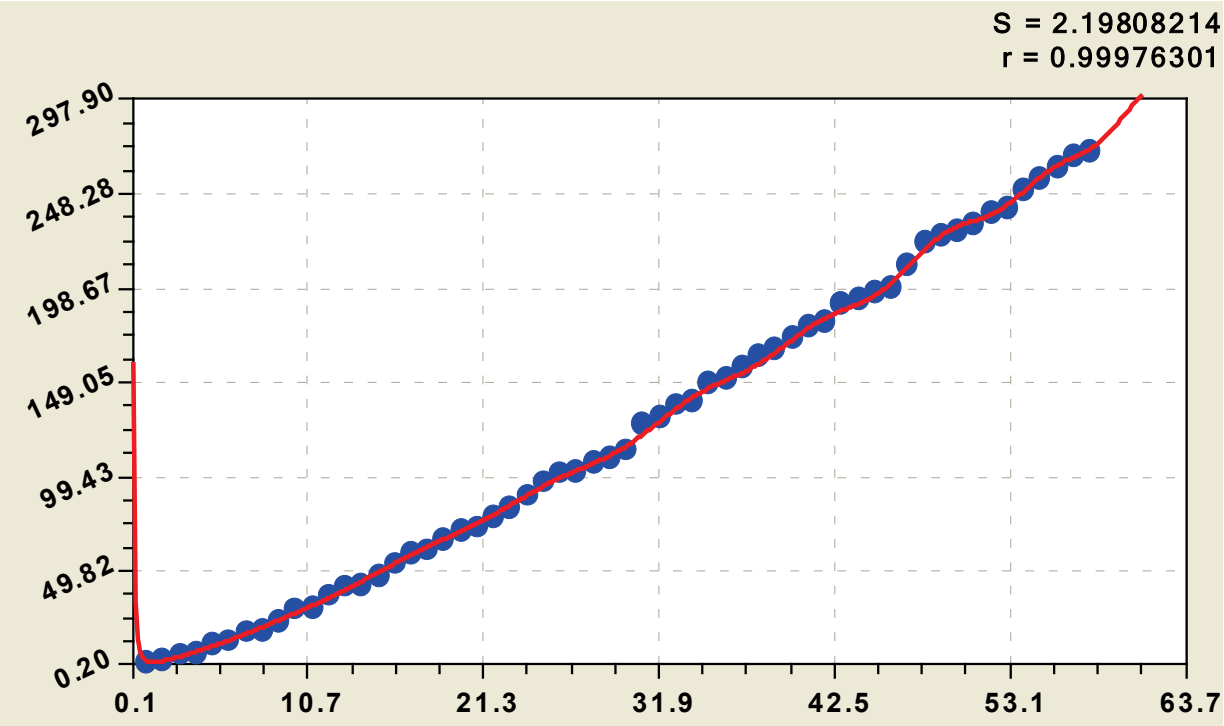

Fig. 4. Chart sum of three wavelets growth of the number of primes

Two waves gives rise to a correlation coefficient with 0.999546 in trend (fig. 1) to 0.999763 in the model (7). But such small increments give the opportunity to the decomposition of a series of prime numbers on wavelets $a(n) = f(n)$.

Compact recording wavelets. The parameters of the model can be written in the form of a matrix (table. 2). The trend is a solitary wave with a half-period, which considerably exceeds the interval of the order of prime number.

Need a special software environment to "shake" together the full sum of wavelets.

Fractal groups of wavelets. All were identified 36 wavelets on seven groups of the components of the general model. In this anomalous wave of the second component was repeated on the 36th member of the set. The grouping is made on the jumps decrease in balances of the module, as shown in table 3. Graphs of groups of wavelets are shown in figures 5-8.

Table 2. **Parameters of the general equation of growth of number of primes of set A000040**

Number i	Wavelet $y_i = a_{1i}x^{a_{2i}} \exp(-a_{3i}x^{a_{4i}})\cos(\pi x/(a_{5i} + a_{6i}x^{a_{7i}}) - a_{8i})$			Correlation coefficient
	amplitude (half) the fluctuations	half-period	shift	

	a_{1i}	a_{2i}	a_{3i}	a_{4i}	a_{5i}	a_{6i}	a_{7i}	a_{8i}	r
1	5,82517e-83	0	-189,83601	0,0065753	0	0	0	0	
2	19,39898	-1,73234	-0,23129	0,76261	93,75309	-70,10898	0,048713	-1,41453	0,9998
3	-0,00011171	4,00261	0,49079	0,61786	4,74039	-0,00027372	1,92343	1,44553	
4	1,24610e-43	31,64837	0,060802	1,53064	16,36546	-0,19364	1,03795	-4,00668	0,499
5	5,56081e-23	17,97705	0,0043979	2,23659	16,94340	-3,48197	0,36080	-4,50713	0,497
6	0,021536	1,41090	0,00077267	1,97238	54,23757	-3,77334	0,53026	-1,91737	0,536
7	1,04309e-86	50,52931	3,54300	1	16,80229	-0,70449	1	-1,82130	0,375
8	1,70137e-15	14,37566	0,47611	1,00424	1,40716	0,033313	0,34232	2,31806	0,488
9	-4,06038e-35	66,89465	7,47700	0,99717	4,45330	-0,20420	1,01131	-2,82198	0,318
10	-2,02068e-12	14,10056	3,53171	0,52917	1,84833	-0,14689	0,32830	-3,55583	0,680
11	8,92820e-80	54,00030	0,014702	1,84395	4,37877	-0,00081240	1,75655	-3,02207	0,332
12	1,18070e-5	4,78940	0,19683	1	2,07024	-0,00027510	1,34578	-1,12678	0,293
13	-3,38101e-8	5,76583	0,0012728	2,20188	2,18782	-0,43852	0,22272	-0,69168	0,8776
14	-521,1866	4,37952	7,50836	0,38100	1,45463	-0,16507	0,091410	2,86731	0,477
15	2,54885e-6	4,01934	0,088735	1	2,40526	0,016938	1	2,36226	0,423
16	1,09156e-22	19,19700	0,61836	0,96619	6,08203	0,00035135	1,66701	-4,41882	0,365
17	-0,0059078	1,18206	0,0085163	1,40727	2,41174	0,00019104	1,62562	2,35497	0,317
18	-0,083202	0,18659	0,064990	0,45064	8,27728	-0,15579	0,99938	-2,96093	0,377
19	-1,68978e-36	26,46217	0,16725	1,24814	1,83808	0,0011193	1,19831	0,092090	0,7794
20	-2,36039e-13	16,30454	1,36566	0,91503	2,73707	-0,071939	0,92727	-2,97519	0,693
21	2,93607e-10	10,25109	0,54899	1	11,61479	-0,25836	1	0,23163	0,407
22	-1,89540e-6	8,85309	0,90538	0,99540	2,13247	-0,048777	0,99977	0,31235	0,518
23	-6,94085e-18	13,23390	0,29628	0,99986	0,83762	0,0028770	0,99853	0,80734	0,579
24	1,43427e-38	35,77440	0,79521	1,13034	1,84401	-0,013419	0,98188	-5,53047	0,539
25	1,06010e-22	15,41216	0,13593	1,15576	3,16118	0,00027502	1,63773	4,84800	0,510
26	-0,0036569	2,47324	0,31615	1	11,32210	-0,45103	1	-2,21077	0,355
27	7,58224e-7	3,62252	0,083916	1,02103	6,43220	-0,016110	0,99970	-1,10336	0,157
28	-1,52119e-5	2,09124	0	1	3,13542	-0,011853	0,99928	-0,85981	0,7050
29	0,012398	1,01396	0,25956	0,75747	2,03834	-0,00052756	1,52643	1,56442	0,476
30	4,34226e-5	2,04230	0,033661	1,00138	10,68980	0,021455	1,01024	0,47087	0,513
31	-0,093145	3,23242	1,04851	0,99848	1,07959	-0,0013151	1,17492	4,12146	0,523
32	1,93548e-13	14,59147	0,91161	1,00513	1,25837	0,0043789	1,05760	5,23704	0,429
33	4,05962e-7	3,42328	0,054790	0,99867	3,32185	-0,0047885	1,04828	-3,09568	0,580
34	-1,18100e-12	10,26508	0,42189	0,97466	1,18580	-0,00091799	1,33998	-0,93562	0,466
35	-0,0010015	1,16087	0,062654	0,99977	46,92809	0,072304	0,61386	-0,53443	0,394

36	-0,0049178	-0,43329	-0,035896	1,01859	8,80314	-0,020204	1,00481	-3,33438	0,401

Table 3. **Fractal reduction of balances (by module) after the components of the statistical model (1a)**

1 group		2 group		3 group		4 group		5 group		6 group		7 group	
i	$.\lvert\varepsilon_{\max}\rvert$	i	$.\lvert\varepsilon_{\max}\rvert$	i	$.\lvert\varepsilon_{\max}\rvert$	i	$.\lvert\varepsilon_{\max}\rvert$	i	$.\lvert\varepsilon_{\max}\rvert$	i	$.\lvert\varepsilon_{\max}\rvert$	i	$.\lvert\varepsilon_{\max}\rvert$
0	271	4	4.591	10	1.764	16	0.473	22	0.167	28	0.059	34	0.021
1	6.696	5	2.995	11	1.764	17	0.508	23	0.158	29	0.050	35	0.018
2	5.592	6	2.365	12	1.522	18	0.503	24	0.148	30	0.050	36	0.017
3	4.575	7	2.365	13	0.643	19	0.361	25	0.086	31	0.031		
		8	2.461	14	0.548	20	0.231	26	0.086	32	0.031		
		9	2.461	15	0.472	21	0.209	27	0.081	33	0.021		

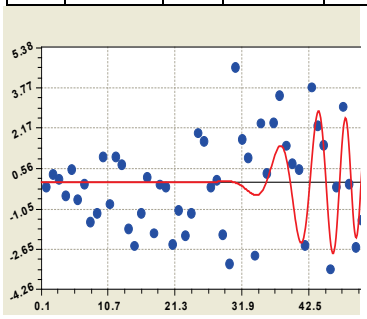

Wavelet № 4

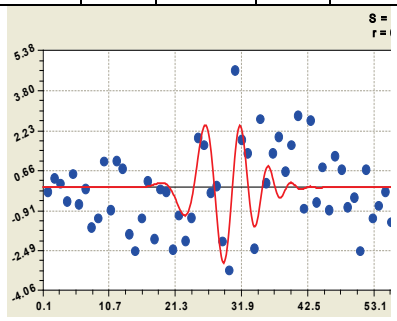

Wavelet № 5

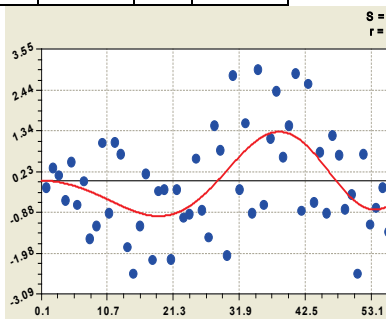

Wavelet № 6

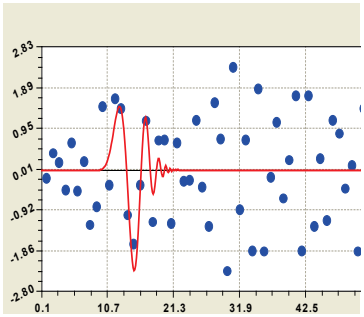

Wavelet № 7

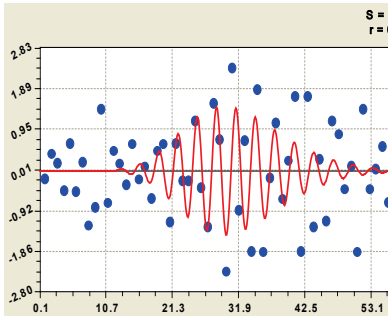

Wavelet № 8

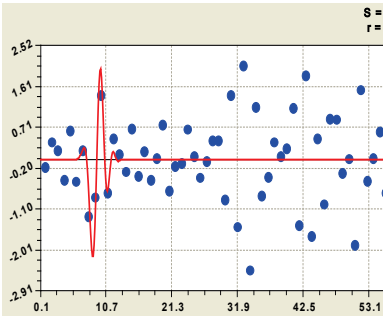

Wavelet № 9

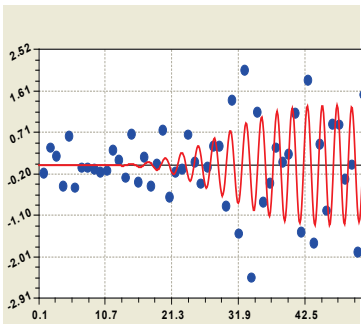

Wavelet № 10

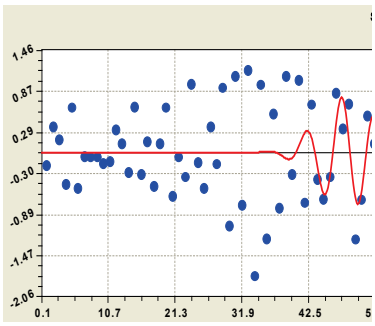

Wavelet № 11

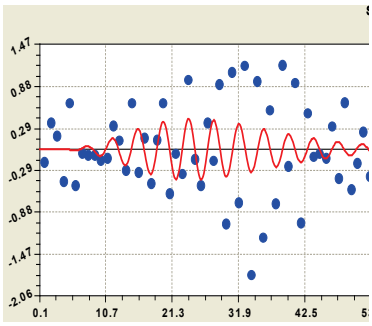

Wavelet № 12

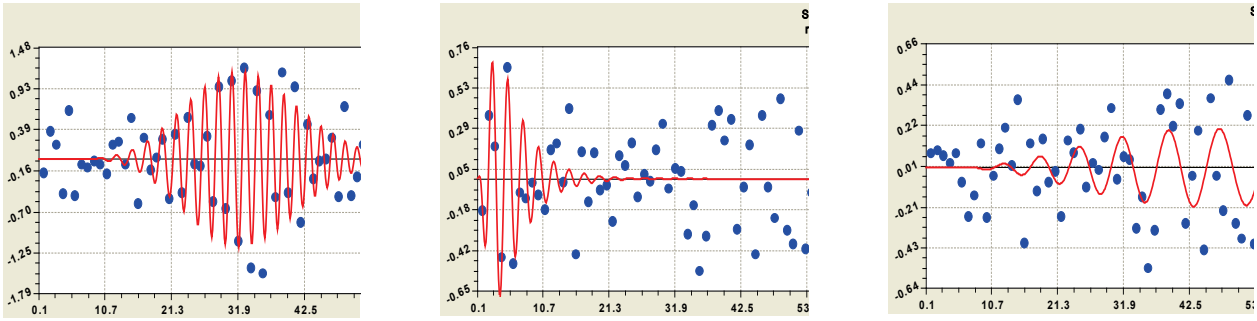

Wavelet № 13 Wavelet № 14 Wavelet № 15

Fig.5. Graphics wavelets of the second and third groups (table. 3)
the distribution of the primes A000040

Wavelet number 14 is closer to the left side of the number of primes, but the computer gave the sequence, which is consistently identified by the software environment CurveExpert. A series of signals from the expansion of a number of prime numbers does not coincide with the number of wavelet. But this series should be specified only after the procedure package of all 36 components of the general model of the type (1a), but this requires a software package that allows you to simultaneously take into account the tens of wavelets with several hundreds of model parameters.

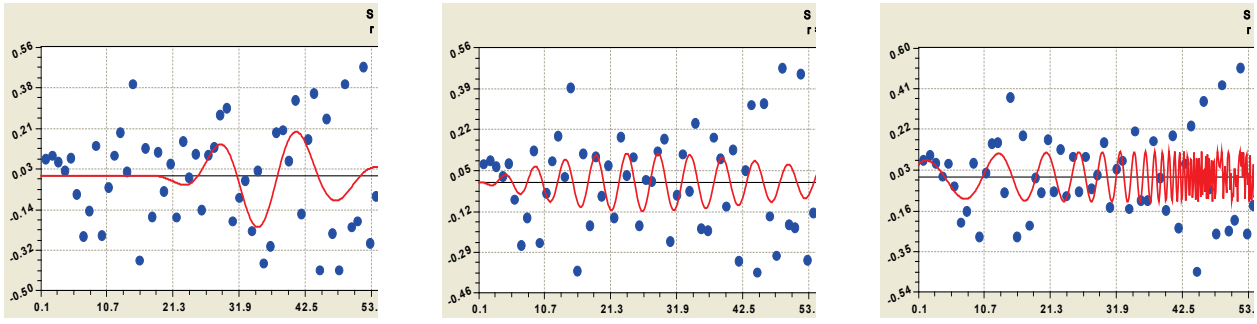

Wavelet № 16 Wavelet № 17 Wavelet № 18

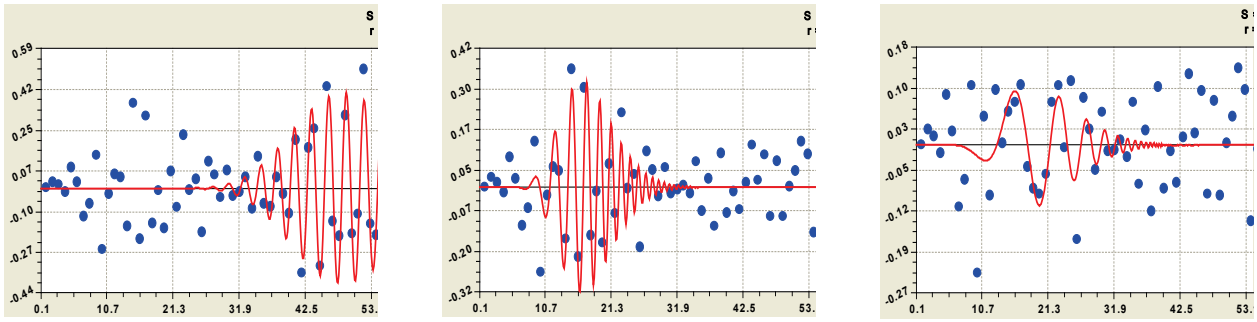

Wavelet № 19 Wavelet № 20 Wavelet № 21

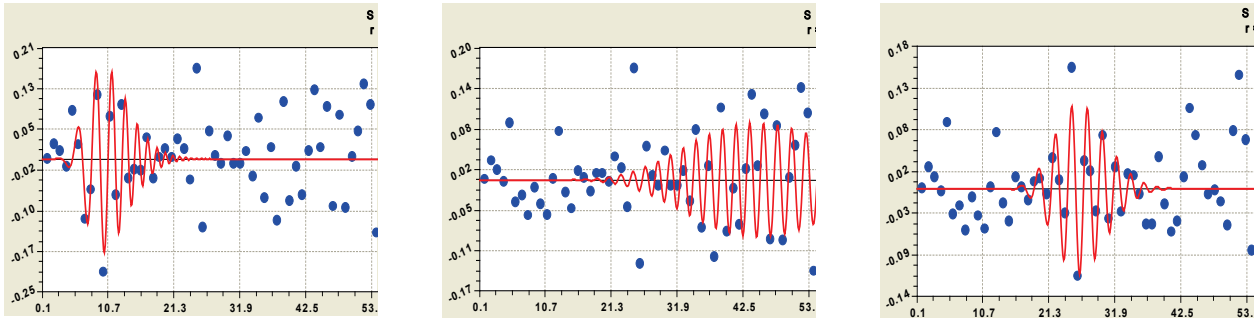

Wavelet № 22 Wavelet № 23 Wavelet № 24

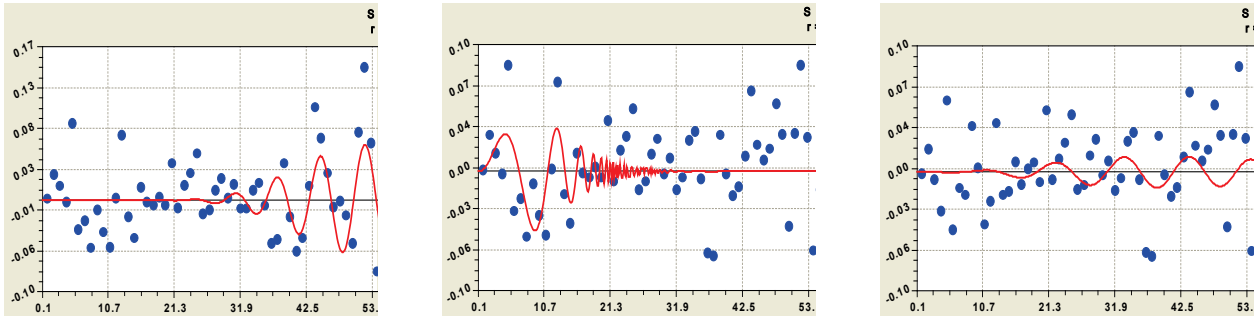

Wavelet № 25 Wavelet № 26 Wavelet № 27

Fig. 6. Graphs of wavelets fourth and fifth groups of the distribution of prime numbers A000040

Analysis of the fractal sum of wavelets. Different signals in the form of a self-similar, i.e. fractal through a common model of the type (1a). It is known, that fractals like the through the law of Mandelbrot $y = a_1 \exp(-a_2 x)$. For the fractal model of the sum of wavelets indicator has a maximum absolute error (residue) $|\varepsilon_{\max}|$. According to table 3 of the received

$$|\varepsilon_{\max}| = 271\exp(-6{,}95984i) + 2{,}66495\cdot 10^{9} i^{2{,}99207} \exp(-19{,}84166 i^{0{,}15133} +$$

$$+ 473460{,}03 i^{2{,}18365} \exp(-13{,}64245 i^{0{,}13941}) \cos(\pi i/(0{,}72506 + 0{,}056028 i^{1{,}22448}) + 0{,}69650)$$

(8)

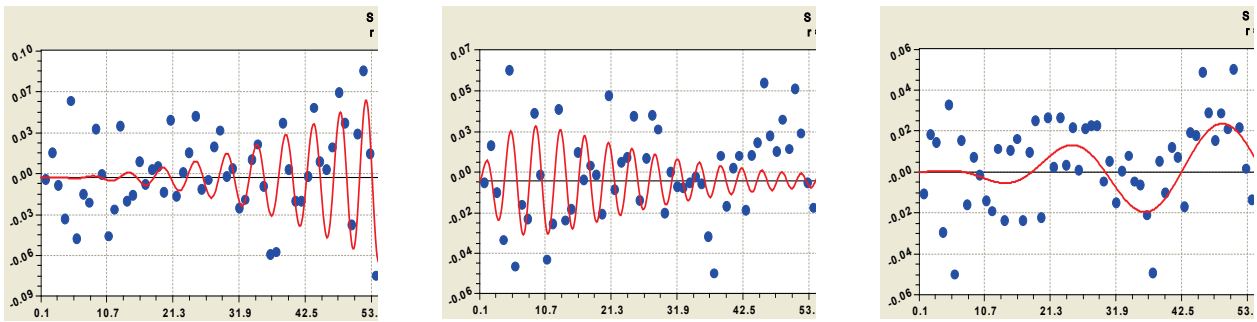

Wavelet № 28 Wavelet № 29 Wavelet № 30

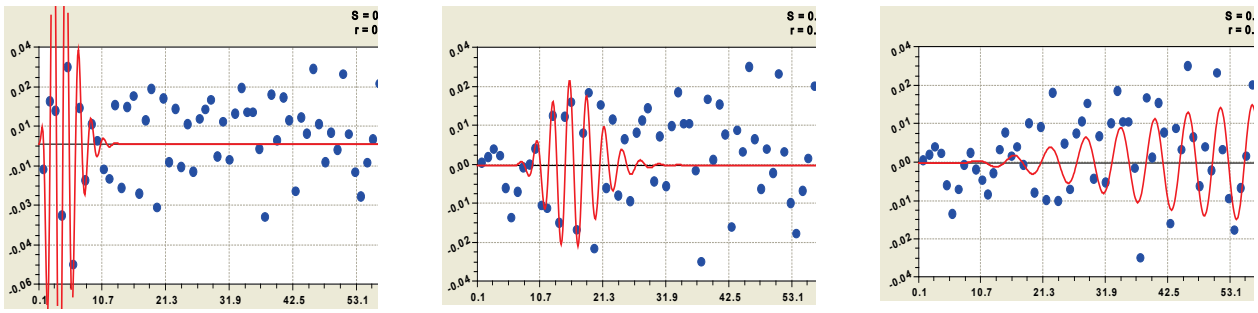

Wavelet № 31 Wavelet № 32 Wavelet № 33

Fig. 7. Graphics wavelets of the sixth group of distribution of prime numbers A000040

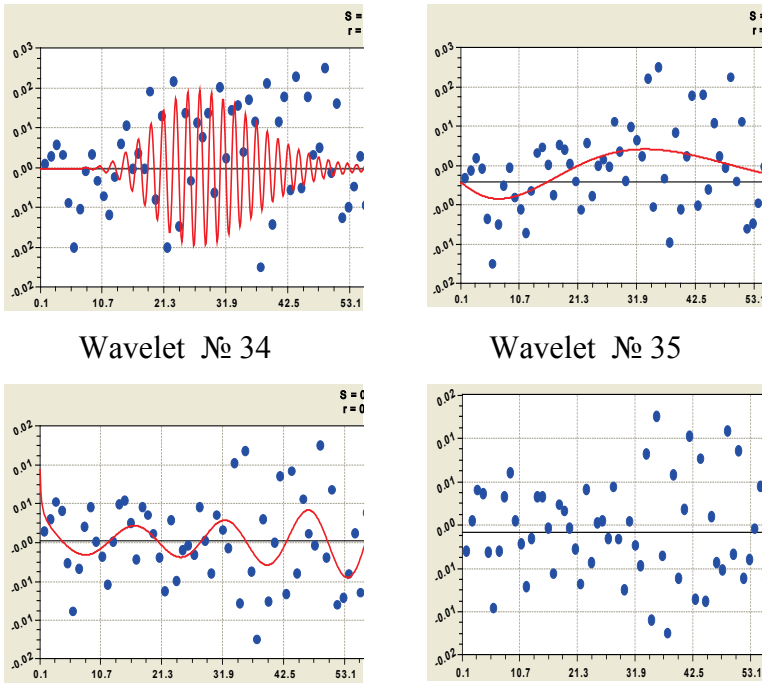

Wavelet № 34 Wavelet № 35

Wavelet № 36 The leftovers after the № 36

Fig. 8. Graphics wavelets seventh group

The main three members of the formula (7) give the contribution to the reduction of residues 100(271-4,575)/271 = 98,32 %.. In this case the first term under the law of exponential growth is the contribution of the absolute error of 100(271-6.696) /271 = 97,53 %. The remaining 35 wavelets give just 2.47%. However, their impact on a number $a(n) = \{2,3,5,,...,271\}$ of very significant.

Conclusion. Any type of a number of primes can be decomposed into a finite-dimensional set of asymmetric wavelets with variable amplitude and frequency of vibration disturbance.

Literature

1. Mazurkin P.M. The statistical model of the periodic system of chemical elements D.I. Mendeleev. Yoshkar-Ola: MarSTU, 2006, 152.

2. Astafieva N.M. Wavelet-analysis: fundamentals of theory and examples of the application // The successes of the physical sciences. 1996. Volume 166, № 11 (november), 1145-1170.

3. Don Zagier. The first 50 million prime numbers. URL: http://www.ega-math.narod.ru/Liv/Zagier.htm.

CID: J21210-844

Mazurkin P.M.

SERIES PRIMES IN BINARY

Mari State Technical University, Yoshkar-Ola

To prove the famous Riemann hypothesis, that the real part of the root is always exactly equal to 1/2, a series of 500 and the other prime numbers has been converted from decimal to binary number system. At the same time was a clear non-trivial zeros.

Any prime number can be represented as quantized into binary digital signal. Quantization step to not dilute a number of prime numbers is 1. Number of levels (binary digits) depends on the power of the quantized number of primes. As a result, we get two types of zeros - the trivial and nontrivial.

Capacity of a finite number of primes must be taken based on the completeness of block incidence matrix. Average statistical indicator is a binary number, and influencing variable - itself a prime number.

The binary representation allows to visualize and geometric patterns in the full range of prime numbers.

Keywords: simple numbers, conversion, geometry, criteria

Introduction. The decimal number system in areal density inferior to many other systems of notation, but in convenience and in the force of habit in the frequency of use of man at the time of 02.07.2011 superior to other number system (from the Internet).

The binary number system for a number of primes should be the effective positioning system. It has only two whole numbers: 0 and 1 [1].

Quantization of a simple number. Any prime number can be represented as the quantum of the binary system of the sampled signal. In the quantization of the entire range of the signal is divided into levels, the amount of which shall be represented in the numbers of a given digit capacity [2].The distance between these levels is called the quantization step, and it is equal to 1 is not for the diluted number of primes. The number of levels (bits of the binary notation) depends on the power of the quantized number of primes.

500 prime numbers. We take a number of primes $a(n) = \{2,3,5,...,3571\}$ at $n = \{1,2,3,...,500\}$. Table 1 shows the fragments of quantization on the boundary crossings (frames) between the discharges i_2 of the binary system. Given on the left i_{10} of the decimal system.

Table 1. **A number of prime numbers in decimal and binary number systems**

Power series $\pi(x)$	Digit number i_{10}	Order of the prime number n	Prime number $a(n)$	The category of the number i_2 of binary numbering system (quantization level)											
				12	11	10	9	8	7	6	5	4	3	2	1
				The value of the part $a_{i_2}(n) = 2^{i_2-1}$ of the prime number on the level											
				2048	1024	512	256	128	64	32	16	8	4	2	1
4	1	1	2											1	0
	1	2	3											1	1
	1	3	5										1	0	1
	1	4	7										1	1	1
25	2	5	11									1	0	1	1
	2	6	13									1	1	0	1
	2	7	17								1	0	0	0	1
	2	8	19								1	0	0	1	1
	2	9	23								1	0	1	1	1
	2	10	29								1	1	1	0	1
	2	11	31								1	1	1	1	1
	2	12	37							1	0	0	1	0	1
	2	13	41							1	0	1	0	0	1
	2	14	43							1	0	1	0	1	1
	2	15	47							1	0	1	1	1	1
	2	16	53							1	1	0	1	0	1
	2	17	59							1	1	1	0	1	1
	2	18	61							1	1	1	1	0	1
	2	19	67						1	0	0	0	0	1	1
	2	20	71						1	0	0	0	1	1	1

168	3	30	113						1	1	1	0	0	0	1
	3	31	127						1	1	1	1	1	1	1
	3	32	131					1	0	0	0	0	0	1	1
	3	33	137					1	0	0	0	1	0	0	1

168	3	53	241					1	1	1	1	0	0	0	1
	3	54	251					1	1	1	1	1	0	1	1
	3	55	257				1	0	0	0	0	0	0	0	1
	3	56	263				1	0	0	0	0	0	1	1	1

168	3	96	503				1	1	1	1	1	0	1	1	1
	3	97	509				1	1	1	1	1	1	1	0	1
	3	98	521			1	0	0	0	0	0	1	0	0	1
	3	99	523			1	0	0	0	0	0	1	0	1	1

1229	4	171	1019			1	1	1	1	1	1	1	0	1	1
	4	172	1021			1	1	1	1	1	1	1	1	0	1
	4	173	1031		1	0	0	0	0	0	0	0	1	1	1
	4	174	1033		1	0	0	0	0	0	0	1	0	0	1

1229	4	308	2029		1	1	1	1	1	1	0	1	1	0	1
	4	309	2039		1	1	1	1	1	1	1	0	1	1	1
	4	310	2053	1	0	0	0	0	0	0	0	0	1	0	1
	4	311	2063	1	0	0	0	0	0	0	0	1	1	1	1

1229	4	496	3541	1	1	0	1	1	1	0	1	0	1	0	1
	4	497	3547	1	1	0	1	1	1	0	1	1	0	1	1
	4	498	3557	1	1	0	1	1	1	1	0	0	1	0	1
	4	499	3559	1	1	0	1	1	1	1	0	0	1	1	1
	4	500	3571	1	1	0	1	1	1	1	1	0	0	1	1

Has long been known that the numbers that grow naturally, for example, such as powers of two, would, of course, absurd to look for an instance, surpassing all known. For simple numbers is making enormous efforts to do just that. Primes were factorization, i.e. expansion in numbers and multipliers with large powers of two. It is this passion and are not allowed mathematicians to use the binary system for the analysis no multipliers of the prime number, and quantized in binary terms.

Prime properties. The hierarchy we consider several basic properties.

1. Any simple contains the number of bits $i_2 = 1,2,...$ of the binary system and components

$$a_{i_2}(n) = 2^{i_2-1}. \quad (1)$$

2. Any prime number is the sum of the components of the given matrix incidence

$$a(n) = \sum_{i_2=1}^{\infty} \xi(i_2, n) a_{i_2}(n) = \sum_{i_2=1}^{\infty} \xi(i_2, n) 2^{i_2-1}, \quad (2)$$

where $\xi(i_2, n)$ - is the incidence matrix, and always $\xi(i_2, n) = 0 \vee 1$. For an infinite-dimensional of a number of primes have levels of quantization or area of digits in the binary system $i_2 = (1, \infty)$.

An example of calculations by formula (2) is given in table 2.

As a result, we get two types of zeros - the trivial and nontrivial. The first are located, as seen from the two tables on the left to the vertical 1 in each block. A nontrivial zeros are located within a two-column with 1, where the left column 1 is shifted by blocks with the increase in prime number. In table 1 the trivial zeros are shown empty cells.

Table 2. **A number of prime numbers (fragment) in decimal notation**

The order n of the prime number	Prime number $a(n)$	The category of the number i_2 of binary system of calculation											
		12	11	10	9	8	7	6	5	4	3	2	1
		The value of the part $a_{i_2}(n) = 2^{i_2-1}$ of the prime number											
		2048	1024	512	256	128	64	32	16	8	4	2	1
1	2	0	0	0	0	0	0	0	0	0	0	**2**	0
2	3	0	0	0	0	0	0	0	0	0	0	2	1
3	5	Trivial zeros			0	0	0	0	0	0	**4**	0	1
4	7				0	0	0	0	0	0	4	2	1
5	11	0	0	0	0	0	0	0	0	**8**	0	2	1
6	13	0	0	0	0	0	0	0	0	8	4	0	1
7	17	0	0	0	0	0	0	0	**16**	0	0	0	1
8	19	0	0	0	0	0	0	0	16	0	0	2	1
9	23	0	0	0	0	0	0	0	16	0	4	2	1
10	29	0	0	0	0	0	0	0	16	8	4	0	1
11	31	0	0	0	0	0	0	0	16	8	4	2	1
12	37	0	0	0	0	0	0	**32**	0	0	4	0	1

Note. The beginning (rapper) of each block of prime numbers shown in bold.

3. The number of non-trivial zeros tends to infinity, because a number of quantization levels also tend to infinity in the conditions of $n \to \infty$, $a(n) \to \infty$ and $i_2 = (1, \infty)$.

4. When the first digit $i_2 = 1$ of the binary number (table 1) for the conditions $n = 1$ and $a(n) = 2$ is the incidence of $\xi(i_2, n) = 0$, and for some non-critical primes $P = \{3,5,7,11,13,17,...\}$ incidence is equal to $\xi(i_2, n) = 1$, where throughout the $n = (2, \infty)$ and $a(n) = (3, \infty)$. Critical primes require a separate study.

5. For non-critical primes $n = (2, \infty)$ and $a(n) = (3, \infty)$ will be adequate findings obtained on a finite number of $a(n) = \{3,5,...,3571\}$ at capacity $n = \{2,3,...,500\}$.

Mathematical landscape. In a remarkable series of films «De Code» (19.07; 26.07 and 08.02.2011) leading Mark Dyusotoy shows a graphical picture three-dimensional "mathematical landscape" Riemann zeta function. All pay attention to the non-trivial zeros on the critical line. They are already counted several trillion.

But we are attracted to this in the landscape of another - steep slopes rising at the approach $n \to 0$. Alignment of the binary system are infinitely high "mountain" makes projections of equal height, equal to one. Figure 1 shows a three-dimensional graph, for clarity, built only in the part of one block of 20 primes.

In figure 1 appears a certain ceiling from units, except "floor" from the nontrivial zeros. Between them there is an unknown relationship. Then a super Riemann surface, due to the presentation of complex numbers, converted to a double-layer "cake".

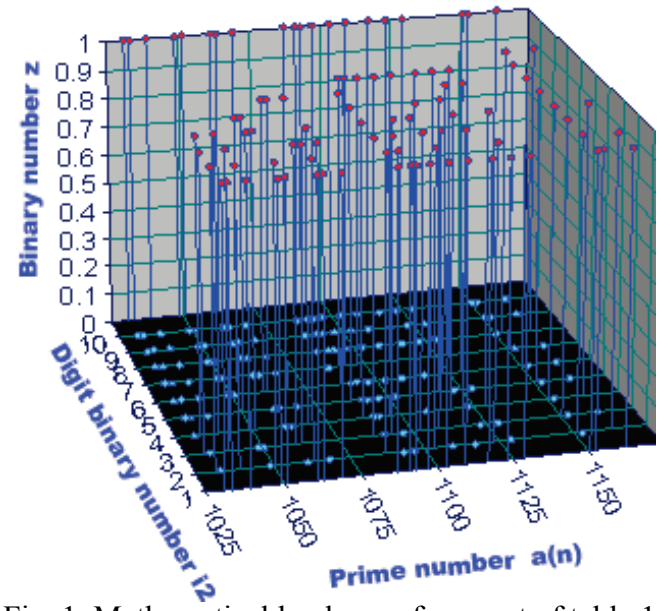

Fig. 1. Mathematical landscape fragment of table 1 of the 20 prime numbers from 1031 to 1163

Have to consider these two layers along (in the order of simple numbers) and across (per grade i_2). For the analysis we introduce a parameter - ***the binary number*** z_2 that takes real values.

Binary number along the row. For the analysis of the data in table 1 were taken only whole blocks of the incidence matrix, i.e. without trivial zeros. For the column $i_2 = 1$ will delete the first row and then we get $z_2 = 1$. This is the "mountain", from which

in the transverse direction there will be non-trivial zeros. The fact that $z_2 = 1$ the condition is unchanged for all infinite-length $a(n) = (3, \infty)$, let us consider in another article.

For $a(n) = (2,500)$ (except $i_2 = 1$) have average values (table 3).

Table 3

Effect of discharge

Digit number i_2	Fact $\bar{z}_{2\phi}$
1	1
2	0.51000
3	0.50402
4	0.50605
5	0.48988
6	0.4928
7	0.51452
8	0.03518
9	0.54036
10	0.51117
11	0.60366
12	1

Effect of discharge i_2. After the identification of stable laws for 500 lines (without $i_2 = 12$) was obtained (fig. 2) model

$$\bar{z}_2 = 7{,}38981\exp(-2{,}69622 i_2^{\,1{,}35327}) + 0{,}50080\exp(1{,}36513\cdot 10^{-5} i_2^{\,3{,}78640}) +$$
$$+ 0{,}00069615 i_2^{\,1{,}67395}\cos(\pi i_2/(5{,}77022 - 0{,}11402 i_2^{\,1{,}38683}) + 5{,}45805) +$$
$$+ 5{,}47011\cdot 10^{-5} i_2^{\,6{,}66405}\exp(-1{,}16267 i_2^{\,1{,}00235})\times$$
$$\times\cos(\pi i_2/(2{,}01814 - 0{,}054438 i_2^{\,1{,}00535}) - 0{,}26842). \qquad (3)$$

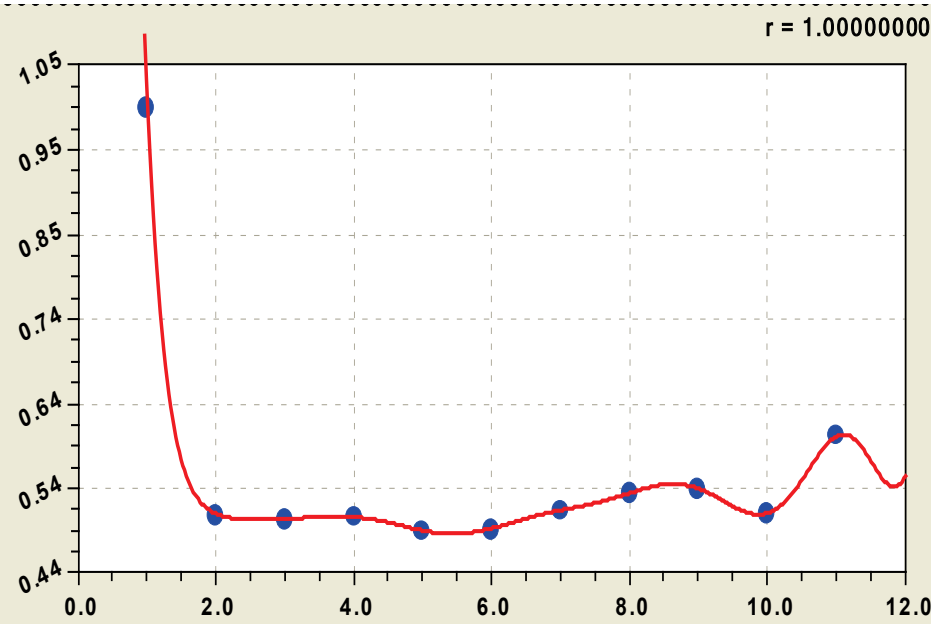

Fig. 2. The graph of the formula (3)

In a four-distribution model, of the distribution of the average value of the binary number of the first component is the law of exponential death (of the slope of the landscape), and the second - the law of exponential growth, starting from the third digit binary number system. Then, additional oscillatory disturbances produce two waves of adaptation. The first of these is the increasing amplitude, and shows that if $i_2 \geq 3$ half the amplitude of the binary number is increasing by the law of exponential growth.

The second wave through a discharge i_2 will be close to zero. The picture changes completely with further increase in number of primes.

The maximum relative error of formula (3) at $i_2 = 11$ is 100×2.47674e-005 / 0.60366 = 0,0041 %. At the same time schedule is very similar to the Riemann zeta-function.

Blocks of prime numbers. Computational experiments showed that the power series should be taken based on the completeness of the block incidence matrix. For example, take the block number 11 with a fragment that has parameters: $n = (173{,}309)$, $a(n) = (1031{,}2039)$, $i_2 = (1{,}11)$. Comparison showed a significant power series of prime numbers, whose serial number has only secondary importance. The indicator is average statistical (but not the arithmetic mean) binary number, and the explanatory variable - itself a prime number.

Calculations based on block number 11 (fig. 3) are given in table 4 and were performed according to the formula

$$z_2 = a_1 - a_2 \cos(\pi a(n)/(a_3 + a_4 a(n)^{a_5}) - a_6). \qquad (4)$$

Table 4. **Effect of the prime on the binary number of digits of the binary system**

Digit number i_2	Part $a_{i_2}(n) = 2^{i_2-1}$	Average statistical $\bar{z}_{2\phi}$	The parameters of statistical models (4) of the binary number						Correlation coefficient r
			a_1	a_2	a_3	a_4	a_5	a_6	
1	1	1	0.5	-0.5	0	0	0	0	1
2	2	0.51825	0.5	0.5	2	0	0	1.59217	1
3	4	0.51825	0.5	0.70711	4	0	0	1.57080	1
4	8	0.53285	0.50079	0.64897	8.00054	0	0	-4.72553	0.9251
5	16	0.48175	0.50339	-0.64642	15.99613	0	0	4.82479	0.9069
6	32	0.40876	0.50997	0.63517	32.02910	0	0	1.46990	0.8975
7	64	0.51825	0.52117	0.63090	66.31876	-0.00066974	1	0.090540	0.9066
8	128	0.51095	0.50345	0.61806	129.7168	8.62532e-5	1.11225	0.94630	0.9132
9	256	0.48175	0.49203	0.64200	266.3384	1.85033e-5	1.52406	0.73950	0.9147
10	512	0.48905	0.50536	0.61721	682.0366	-0.34387	0.64381	-0.35596	0.9291
11	1024	1	0.5	-0.5	0	0	0	0	1

If we ignore the first and last bits binary system, the closest to a rational number 1/2 on the real values of the formula (4) is the discharge $i_2 = 2$.

As can be seen from the graphs in figure 3, balances are close to zero only when the two digits 2 and 3. In other cases, they are all over the interval (-0.5, 0.5).

Critical zeros or ones? Equation (4) as we approach the second category is gradually reduced to the expression $\bar{z}_2 = a_1 - a_2 \cos(\pi a(n)/a_3 - a_6)$, obtaining a constant frequency oscillations with half-periods of 2 or 4. Become critical as zero and one. Critical become as zeros so and units.

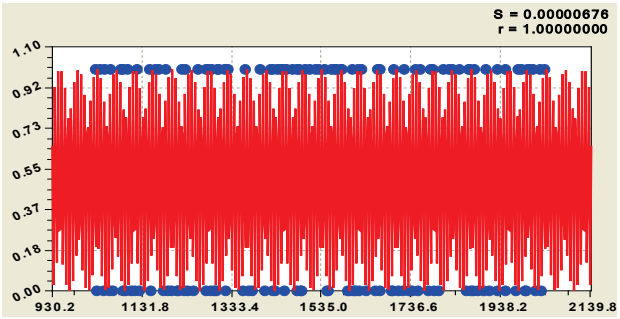

At discharge $i_2 = 2$ binary system

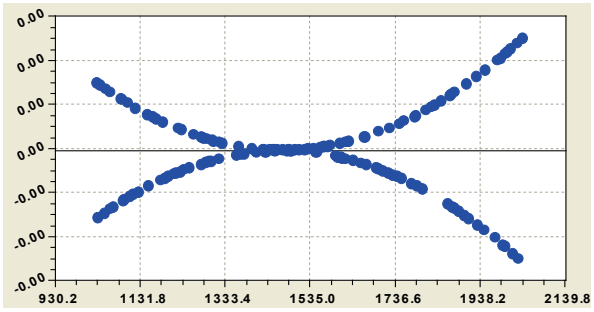

Remains after the model of a binary number

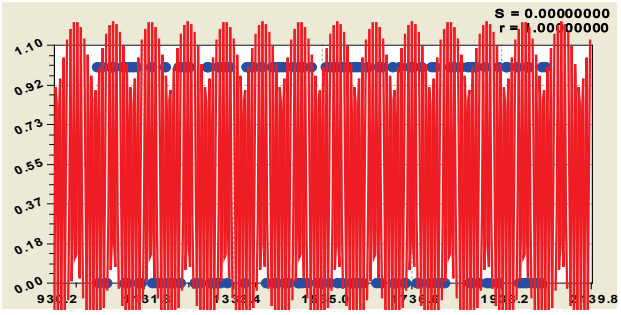

At discharge $i_2 = 3$ binary system

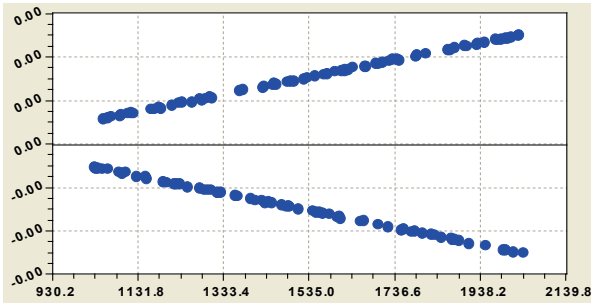

Remains after the model of a binary number

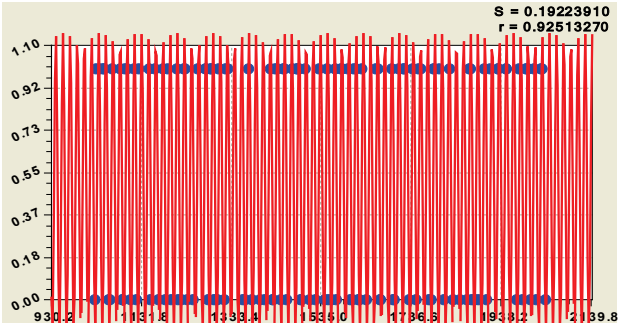

At discharge $i_2 = 4$ binary system

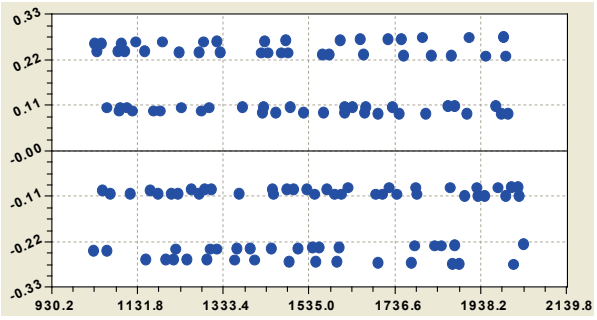

Remains after the model of a binary number

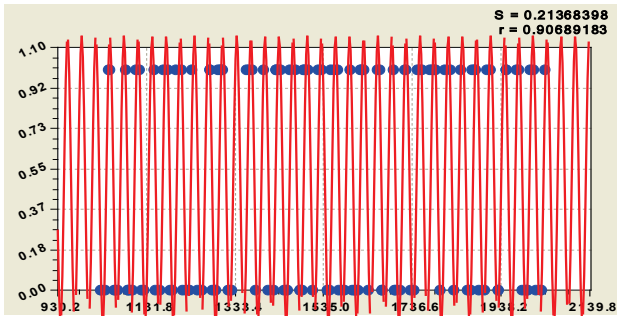

At discharge $i_2 = 5$ binary system

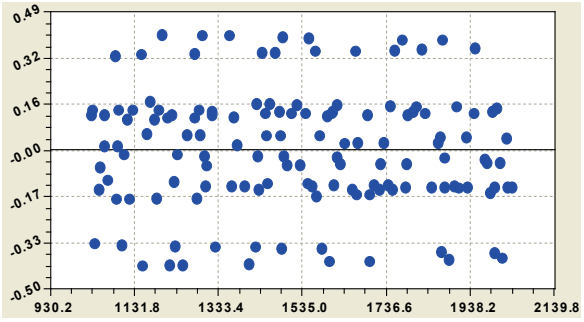

Remains after the model of a binary number

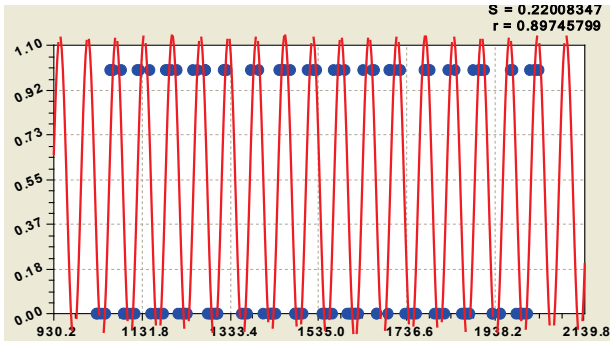

At discharge $i_2 = 6$ binary system

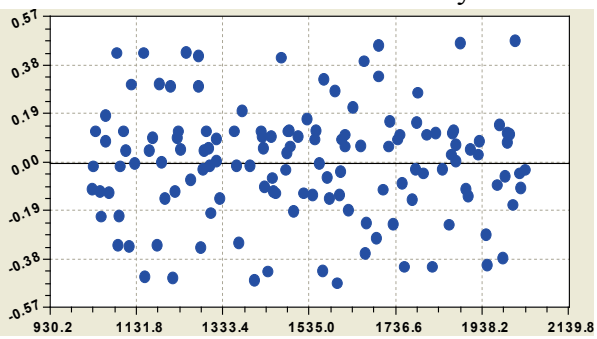

Remains after the model of a binary number

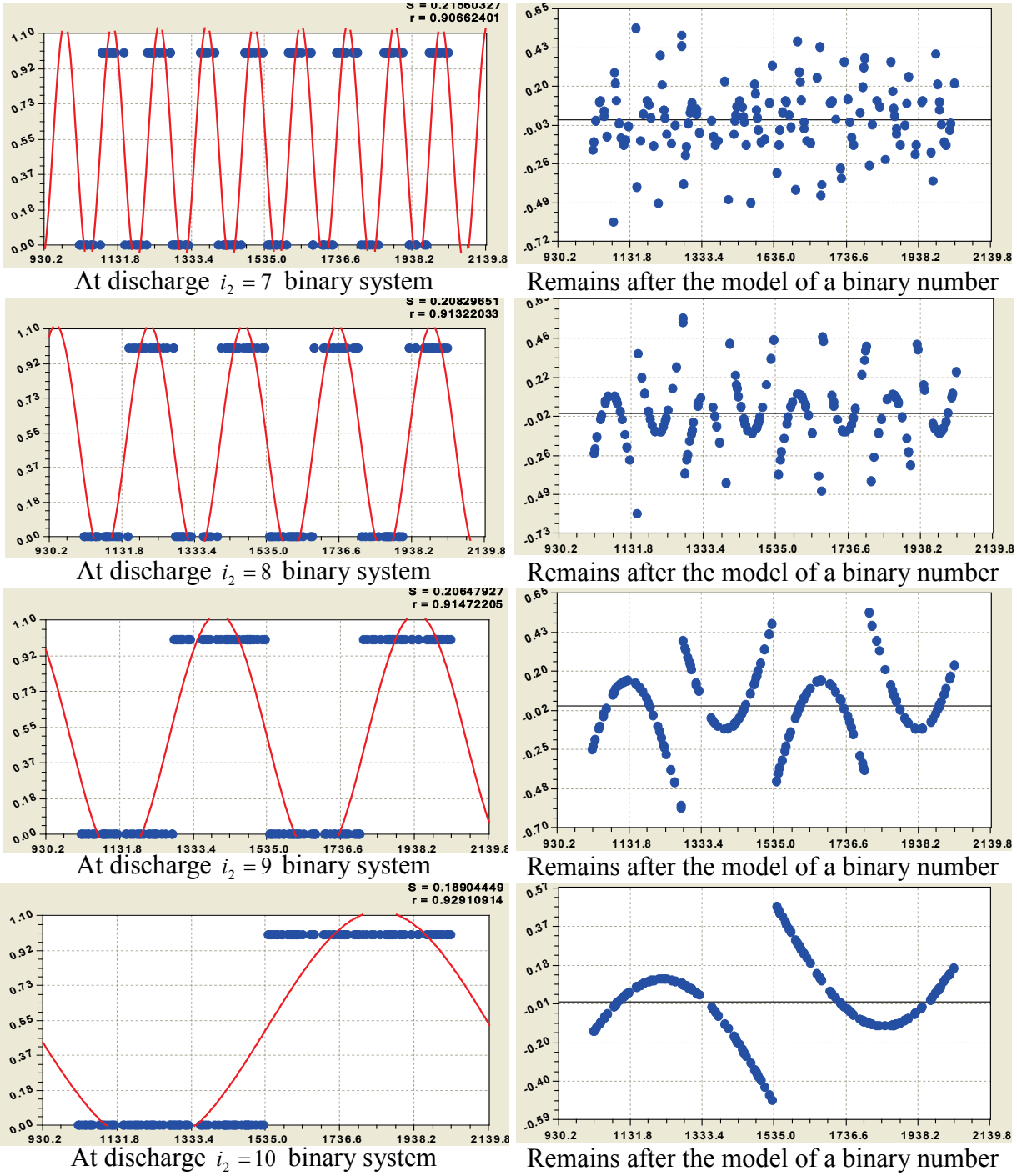

At discharge $i_2 = 7$ binary system — Remains after the model of a binary number

At discharge $i_2 = 8$ binary system — Remains after the model of a binary number

At discharge $i_2 = 9$ binary system — Remains after the model of a binary number

At discharge $i_2 = 10$ binary system — Remains after the model of a binary number

Fig. 3. Graphs of statistical models (4) of the binary number: S - dispersion; r - correlation coefficient

The real part 1/2. From the Internet we know: "Here is the famous Riemann hypothesis, that the real part of the root is always exactly equal to 1/2, has not yet been proved, though it would have to prove the theory of prime numbers is extremely important."

Equation (4) proves that not only the real part of the root is 1/2, but there are other interesting results. For example, in the formulas

$$\bar{z}_2(i_2 = 2) = 1/2 - 1/2\cos(\pi a(n)/2 - 1{,}59217) \text{ and}$$

$$\bar{z}_2(i_2 = 3) = 1/2 - 0{,}70711\cos(\pi a(n)/4 - 1{,}57080) \quad (5)$$

expression in front of the cosine function on critical line is exactly equal to 1/2. Options 1,59217 and 1,57080 showing the shift of a wave with constant amplitude, very close to the irrational number $\pi/2$, and the number 0,70711 is close to $\pi/4$. The emergence of a number of space π transforms equation (4) in a model of spatial signal. It is characterized by a symmetric wavelet with constant amplitude of $\pm 1/2$ and variable frequency (in the formula - half-period).

Riemann zeta-function has zeros at the negative, even, multiples of 2. But the data in table 3 show that the frequency of occurrence of the nontrivial zeros is 2^{i_2-1}. Then the Riemann obtained $2^{i_2-1} = 2$ only when $i_2 = 2$ that is exactly on the critical line.

Note also that the zeta-function in complex variables accepted function of sine, but cosine better for the real numbers, since it allows to ignore the signs in terms of a trigonometric function. Cosine works in both quadrants on a number of natural numbers. $(0,1,2,...,\infty)$ Therefore, it will be successful in a number of prime numbers.

The algorithm of predicting of a simple number. While we do not believe in the possibility of predicting the next term in the series of prime numbers. But, after their conversion to binary form, are clear boundaries between the blocks. Rules for translating decimal numbers to binary [1] is quite sufficient to explain the "jumps" in a series of prime numbers.

Asymptotic frames. Capacity of a number of prime numbers is quite possible to manage. To do this, from table 2 we write down the bold values N_R (table 4).

Table 4. **Asymptotic frames of number of prime numbers of 500 pcs.**

$a(n)$	2	5	11	17	37	67	131	257	521	1031	2053
N_R	2	4	8	16	32	64	128	256	512	1024	2048

Conclusions. To prove the famous Riemann hypothesis, that the real part of the root is always exactly equal to 1/2, the transformation was a series of prime numbers from decimal to binary number system. At the same time become visible and non-trivial zeros.

Literature

1. Gashkov S.B. Number systems and their applications. M. MCCME, 2004. 52.

2. Signal. URL:

http://ru.wikipedia.org/wiki/%D0%A1%D0%B8%D0%B3%D0%BD%D0%B0%D0%BB.

CID: J21210-925

Sukhotin A.M.

THE ALTERNATIVE ANALYSIS: THEORY AND APPLICATIONS

National Research Tomsk Polytechnic University

Abstract The principles of the alternative analysis have three main components: 1) there is the demonstrative refutation of the hypothesis about the existence of injective mappings $\varphi: A \to B$ *if* $B \subset A$*, 2) there is a proof of existence of such Cauchy sequences that does not limited with any finite number and 3) there is a proof of convergence independence of any alternative number series from permutation of this series terms.*

Keywords The criterion of bijectivity, C-exact pair, a potentially impracticable on all set N mapping, a convergence of number sequence, the e-divergent sequence w-convergent sequence, infinitely large number, a number series, the alternative series, the value of the sum Σ_n*, a permutation of the alternative series terms.*

1. Mappings of infinite sets

Following [1, Ch. 1.3.4] we shall consider that 'for arbitrary sets M_1, M_2 there is a set $(M_1 \to M_2)$ of all mappings from M_1 into M_2'. A mapping $\varphi: A \to B$ is named by [2, 1.6] the surjective one if $\varphi(A) = B$. Let some pair (q, A) be a variable. A mapping φ is said to be injective one if $(\varphi(a) = \varphi(q)) \Rightarrow (q=a)$. A different yet equivalent definition of the injective mapping named by [3, Ch. 1.2] an injection too has the following kind: $(a \neq q) \Rightarrow (\varphi(a) \neq \varphi(q))$. Injective mapping $\varphi: A \to B$, which is also surjective, is named a bijective one, or a bijection [3, Ch. 1.2]. In this case we

say the sets A and B are bijective and write $A \sim B$ [3, Ch. 1.3]. By virtue of these definitions we have (see also Theorem 1.6)

Theorem 1.1 Let $\boldsymbol{F}(A, B) \stackrel{\Delta}{=} \{\varphi : (\varphi : A \to B,\ \varphi(a) = \varphi(q) \Rightarrow a = q)\}$. If $\forall \varphi \in \boldsymbol{F}(A, B)$ $\varphi(A) \subset B$, then sets A and B aren't bijective ones, i. e., $\neg(A \sim B)$.

Theorem 1.2 Let the mapping φ be a arbitrary function $\varphi : A \to B$. And let for some partition of the set A into not crossed subsets A_i, i. e.,

$$A = \cup A_i,\ i \in I \subset \boldsymbol{N},\ A_i \cap A_j = \varnothing \text{ with } i \neq j, \tag{1.1}$$

the restriction $\varphi_{|A_i} \stackrel{\Delta}{=} \varphi_i$ of mapping φ on each subset A_i be mapping $\varphi_i : A_i \to B$. If

$$\text{for some } i \neq j \ \ B_i \cap B_j \neq \varnothing \text{ with } B_i \stackrel{\Delta}{=} \varphi_i(A_i), \tag{1.2}$$

then the mapping φ isn't an injective one.

Proof. If there exists such $i \in I$ that mapping $\varphi_i : A_i \to B$ isn't injective, then obviously the mapping $\varphi : A \to B$ isn't an injection. Let $\forall i \in I$ mapping $\varphi_i : A_i \to B$ be injective and (1.2) be valid. Then, $\exists b \in B_i \cap B_j$. Hence, there is a such subset $\{a, q\} \subset A$, $a \in A_i$, $q \in A_j$ that $\varphi(a) = \varphi(q) = b$ at $a \neq q$. ■

Theorem 1.3 (The criterion of bijectivity). A mapping $\varphi : A \to B$ is a bijection if and only if there is some partition (1.1) of set A into not crossed subsets A_i and the following two conditions are valid: 1) the restriction $\varphi_{|A_i} \stackrel{\Delta}{=} \varphi_i$ of mapping φ on each subset A_i is an injective mapping $\varphi_i : A_i \to B$, and 2) $\cup B_i = B$, where $B_i \stackrel{\Delta}{=} \varphi_i(A_i)$, and $i \in I$.

Proof Sufficienty Let for some partition (1.1) of set A there exist $\forall i \in I$ the injective mapping $\varphi_i : A_i \to B$ and, if $B_i \stackrel{\Delta}{=} \varphi_i(A_i)$, then $\cup B_i = B$. At first, as there

is $A_i \cap A_j = \varnothing$ with $i \neq j$ in (1.1) and $\forall i$ the mapping $\varphi_i : A_i \to B$ is an injection, then in view of Theorem 1.1 we have $B_i \cap B_j = \varnothing$. On the other hand, $\forall a \in A \ \exists i \in I : \ a \in A_i$ and $\varphi_i(a) \triangleq b \in B_i \subset B$, then the injective mapping $\varphi : A \to \cup B_i$ has been defined. And at last in view of $\cup B_i = B$, this mapping will be a surjection: $\varphi(A) = B$.

Necessity Let mapping $\varphi : A \to B$ be bijection, that is both $\varphi(A) = B$ and $\forall \{a, q\} \subset A \quad (\varphi(a) = \varphi(q)) \Rightarrow (a = q)$. Then for any partition (1.1) of the set A $\forall i$ the restriction $\varphi_i : A_i \to B$ of mapping φ into a subset A_i will be an injective mapping. It is necessary to show only that if $B_i \triangleq \varphi_i(A_i)$, then the equality $\cup B_i = B$ with $i \in I$ will be valid. We shall assume the contrary that $C \triangleq \cup B_i \subset B$. Then $\exists b \in B \setminus C$ and, by virtue of $\varphi(A) = B$ $\exists a = \varphi^{-1}(b) \in A$. Hence, $\exists i \in I : a \in A_i$, and $\exists \varphi_i : A_i \to B$ such that $b = \varphi_i(a) \in B_i \subset C$, *i.e.* $b \in C$. This contradicts $b \in B \setminus C$. ■

It is obvious, that validity of Theorems 1.2 and 1.3 will not be violated, if one of subsets A_i of set A and corresponding subsets B_i of set B is an empty set.

The following two theorems can be proved easily in view of Theorems 1.1–1.3.

Theorem 1.4 If there are both $A = C \cup D,\ C \cap D = \varnothing$, $B = E \cup F,\ E \cap F = \varnothing$ and $C \sim E$, $D \sim F$, then $A \sim B$.

Theorem 1.5 If there are both $A = C \cup D,\ C \cap D = \varnothing$ and $B = E \cup F,\ E \cap F = \varnothing$, then the bijectivity $D \sim F$ follows from both $C \sim E$ and $A \sim B$.

Theorem 1.6 If there are both $\varphi : A \to B$, $B \subset A$, and $\varphi(A) = B$, then there exists a subset $\{a,\ q\} \subset A$ with $a \neq q$ of such kind that $\varphi(a) = \varphi(q)$.

• On the contrary, we shall assume the function $\varphi : A \to B$ □is an injection and, hence, □□ $A \sim B$. □□ Let there be both $C \triangleq E \triangleq B$ and $F \triangleq \varnothing$ in the condition of

Theorem 1.5 Then there are both $A = D \cup B$, $D \cap B = \varnothing$ and $D \neq \varnothing$. As $B = B \cup F = B \cup \varnothing$, then in view of Theorem 1.5 and both $A \sim B$ and $B \sim B$, the condition $\varnothing \neq D$ ~$F=\varnothing$ is valid, i.e. $\varnothing \not\sim \varnothing$. Therefore, our assumption of the $A \sim B$ was false. As $\varphi(A) = B$ by the theorem condition then function $\varphi: A \to B$ is not injective, *i.e.* there exists, at least, one subset $\{q, q\} \subset A$ of such kinds that $a \neq q$ and $\varphi(a) = \varphi(q)$. ■

2. *C*-exact pairs and the mapping $\varphi: \boldsymbol{N} \to \boldsymbol{N}$ surjectivity

A variable is understood below as a triple (x, A, θ), where x is a symbol of the variable, A is set of values of the variable, and θ is some order in the set A. The infinity of set $\boldsymbol{N}$ of natural numbers is understood as an unlimited opportunity of transition from (n) to (n+1), and the phrase 'at limiting transition in F (n)' means the following:

$$\forall n \in \boldsymbol{N}\ F(n) \Rightarrow F(n+1). \tag{2.1}$$

Following both the principle of the limiting transition (2.1) and *equally ordered variables* of G.M.Fikhtengolts [4, item 759], we are introducing a novel concept of natural variables *C–pair*. Let sets $A \subset \boldsymbol{N}$ and $B \subset \boldsymbol{N}$ be infinite with $A \cap B \supseteq \varnothing$ and $E \triangleq A \cup B \subseteq \boldsymbol{N}$.

Definition 2.1 The pair (m, k) of natural variables $m \in A$ and $k \in B$ is said to be *C-exact pair* if there exists such a number C that for every neighboring in E elements $m \in A$ and $k \in B$ there is valid the inequality

$$|m-k| < C. \tag{2.2}$$

Condition (2.2) has the following equivalent form of record:

$$\exists \widetilde{C},\ \widetilde{C} \geq C, (\forall k \in B \ \forall m \in A): k = m + p(m)),\ p(m) \in \boldsymbol{Z},\ p(m)| < \widetilde{C}. \tag{2.2′}$$

In this item we will consider injective functions $\varphi \in \boldsymbol{F}(\boldsymbol{N}, \boldsymbol{N})$, on default. A sequence of natural numbers $\xi \triangleq \{1, n_1, n_2, \ldots, n_i, \ldots\} \subseteq \boldsymbol{N}$ is said to be a sequence with a limited step if there exists such number $C_\xi \in \boldsymbol{N}$ that $\forall i \in \boldsymbol{N}(\xi)$, where

$N(\xi)\triangleq\{i:\ \exists n_i\in\xi\}\subseteq N,\ 0<n_i-n_{i-1}<C_\xi$, and $n_0\triangleq 1$. Further, let $N_i\triangleq\{1, 2, \ldots, n_i\}$. The sequence ξ and a mapping φ: $N\to N$ define two sequences $\{\delta_i\}$ and $\{d_i\}$, $i\in N(\xi)$ of non-negative integers:

$$\delta_i\triangleq\max_{n\le n_i}\{\varphi(n)-n_i\}\ge 0 \text{ and } d_i\triangleq|D_i|\ge 0,\ D_i\triangleq N_i\setminus\varphi(N_i). \tag{2.3}$$

If $D_i^-\triangleq\varphi(N_i)\setminus N_i$ and $d_i^-\triangleq|D_i^-|\ge 0$, then it is obvious that $0\le d_i^-=d_i\le\delta_i$. Really, $d_i^-=\delta_i$ if $\{p:\ n_i<p<\delta_i,\ \forall n\le n_i\ \ p\ne\varphi(n)\}=\varnothing$. In other cases $d_i^-<\delta_i$. The mapping φ: $N\to N$ defines a sequence $\{\varphi_n\}_{n=1}^{\infty}$ of integers $\varphi_n\triangleq\varphi(n)-n$ as well, too.

If $\delta_\varphi\triangleq\sup_{n\in N}\{\varphi(n)-n\}$ and for some sequence ξ $\delta_\xi\triangleq\sup_{i\in N(\xi)}\{\delta_i\}$ then it is obvious, that $\delta_\xi\le\delta_\varphi$. It is easy to prove [5, Stat. 2.1] the following

Statement 2.1 For any injective mapping φ: $N\to N$ there exists a sequence ξ of such kind that

$$\delta_\xi=\delta_\varphi. \tag{2.4}$$

Now we formulate the direct and obvious corollary of the set D_i definition in (2.3) and the mapping φ: $N\to N$ surjectivity as follows:

Statement 2.2 The necessary condition of the mapping φ: $N\to N$ surjectivity has the following two equivalent forms:

$$\forall i\in N(\xi)\ \forall j\in N:\ D_i\cap D_{i+j}=\varnothing \text{ и } N_i\subset\varphi(N_{i+j}). \tag{2.5}$$

Below, for short we say ‘for almost all *i*’ instead of the phrase ‘except for a final set of indexes *i*’ and we write by definition «$\widetilde{\forall}\, i$».

Now we shall describe the attributes of the surjectivity and antisurjectivity of φ.

Statement 2.3 Sufficient conditions of the surjectivity (*a*) and antisurjectivity (*b*) of the mapping φ: $N\to N$ have, accordingly, the following form in terms of sequence $\{d_i\}$:

$$(a)\ \widetilde{\forall}\, i \in \boldsymbol{N}(\xi)\ d_i = 0, \quad (b)\ \forall C\, \exists\, i(C) \in \boldsymbol{N}(\xi)\ d_{i(C)} > C. \tag{2.6}$$

Proof Each number d_i determines a quantity of such elements n each of which belongs to a subset $\boldsymbol{N}_i$ and does not have a prototype $\varphi^{-1}(n)$ in $\boldsymbol{N}_i$. Therefore, an unboundedness of sequences $\{d_i\}$ in (*b*) contradicts the condition $\varphi(N) = N$ of a mapping φ surjectivity. The condition (*a*) in (2.6) guarantees an existence of such number i_0 that for the mapping φ the following circuit of implications is valid:

$$\forall j > i_0\ \ d_j = 0 \Rightarrow D_j = \varnothing \Rightarrow \varphi(N_j) = N_j \Rightarrow \varphi(\boldsymbol{N}) = \boldsymbol{N}. \blacksquare$$

We shall speak about an antisurjective injective mapping φ: $\boldsymbol{N} \to \boldsymbol{N}$ that it is *potentially impracticable on all set* $\boldsymbol{N}$.

As the examples show, the conditions (2.6) are not necessary for the surjectivity and antisurjectivity, accordingly, of function φ.

In view of conditions (2.4)–(2.6) there is easily proved [5, Th. 2.1]

Statement 2.4 Sequences $\{\delta_i\}$ and $\{d_i\}$, $i \in \boldsymbol{N}(\xi)$, defined by means of the pair (ξ, φ), satisfy one and only one of the following three conditions:

$$a)\ \widetilde{\exists}\, i \in \boldsymbol{N}(\xi):\ (\delta_i = 0) \oplus (d_i = 0), \tag{2.7}$$

$$(b)\ (\exists\, C_1, C_2,\ C_2 \le C_1 \in \boldsymbol{N}):\ (\widetilde{\exists}\, i \in \boldsymbol{N}(\xi)\ (0 < \delta_i < C_1) \oplus (0 < d_i < C_2)), \tag{2.8}$$

$$(c)\ i \in \boldsymbol{N}(\xi)\ \ (d_i \to \infty) \oplus (\delta_i \to \infty). \tag{2.9}$$

The corollary of Statements 2.1–2.4 will be written below [5, Th. 2.2].

Theorem 2.1 The boundedness of sequence $\{\varphi_n\}$ of integers $\varphi_n \triangleq \varphi(n) - n$ with $n \in \boldsymbol{N}$ is a necessary condition of the injective mapping φ: $\boldsymbol{N} \to \boldsymbol{N}$ surjectivity, i. e. $\varphi(\boldsymbol{N}) = \boldsymbol{N}$ holds

$$\lim_{n \in \boldsymbol{N}} (\varphi(n) : n) = 1. \tag{2.10}$$

Theorem 2.2 The injective mapping φ^*: $\boldsymbol{N} \to \boldsymbol{N}$, which defines some sequence $\xi^* = \{1, m_1, m_2, \ldots\}$ with an unlimited step at $m_{i+1} > m_i$, is antisurjective or, in other words, *it will be impracticable on all set* ***N***.

Proof Let ξ^* be sequence with an unlimited step, i. e., for the mapping φ^*: $\boldsymbol{N} \to \boldsymbol{N}$ defining ξ^*, there is valid the following condition:

$$\forall C > 0 \; \exists i(C) \in N(\xi) : \; m_{i(C)+1} - m_{i(C)} > C. \tag{2.11}$$

Now at ξ=***N*** and, hence, $\boldsymbol{N}(\xi) =$***N*** we have $n_i = i + 1$. Hence, $\forall i \in \boldsymbol{N} \setminus \{1\}$ $\varphi^*(i) = m_{i-1}$ and in this case (see (2.3)) $\delta_i^* \triangleq m_i - i$, $i \in \boldsymbol{N}$. Therefore, $\forall i \in \boldsymbol{N}$ $\delta_{i+1}^* - \delta_i^* =$ $(m_{i+1} - (i+1)) - (m_i - i) = m_{i+1} - m_i - 1$. Thus, by virtue of (2.11) the inequality $\delta_{i(C)+1}^* - \delta_{i(C)}^* > C - 1$ is valid for $i(C) \in \boldsymbol{N}$. Hence, $\delta_{i(C)+1}^* > \delta_{i(C)}^* - 1 + C$. The unboundedness of the sequence $\{\delta_i^*\}$, defined by means of pair(***N***, φ^*), follows from the last inequality by virtue of arbitrariness of number C in (2.11). Therefore, the mapping φ^*: $\boldsymbol{N} \to \boldsymbol{N}$, which defines the sequence ξ^* in this theorem, is an antisurjective one by virtue of (2.5)–(2.10). ■

Theorem 2.2 implies the following statement.

Theorem 2.3 Let $A \triangleq \{k\} \subseteq \boldsymbol{N}$ and $B \triangleq \{m\} \subseteq \boldsymbol{N}$ be infinite subsets of set ***N***. Then there exists such a number $C \in \boldsymbol{N}$ that the pair (k, m) of natural variables $k \in A$ and $m \in B$ is *C-exact* pair.

As the examples show, the necessary conditions (2.5) and (2.10) of surjectivity of injection φ: $\boldsymbol{N} \to \boldsymbol{N}$ are independent ones, hence, any of these conditions cannot be sufficient. However, the following statement below is valid.

Theorem 2.4 The joint satisfiability of conditions (2.5) and (2.10) is a sufficient attribute of an injection φ: $\boldsymbol{N} \to \boldsymbol{N}$ surjectivity.

The obvious corollary of both Theorem 1.6 and Theorem 2.4 is written down.

Theorem 2.5 *There isn't any bijection between set* ***N*** *and its own subset* $A \subset N$

.

3. Convergence of number sequences

Number sequence $(\boldsymbol{a}) \triangleq \{a_n\}_{n=1}^{\infty} \triangleq (a_1, a_2, \ldots, a_n, \cdots)$ is called fundamental one, or Cauchy sequence **(*CS*)** if

$$(\forall \varepsilon > 0 \; \exists n(\varepsilon) \in N): \; (\forall m, n \geq n(\varepsilon) \; |a_m - a_n| < \varepsilon). \tag{3.1}$$

The condition (3.1) is equivalent to the following limit equality:

$$\lim_{n,\, m \to \infty} (a_m - a_n) = 0. \tag{3.2}$$

The condition (3.2) has (see [6, p. 355]) a more concrete form of record

$$\lim_{\min(m,n) \to \infty} (a_m - a_n) = 0. \tag{3.3}$$

Statement 3.1 *The pair* (*m, n*) *of variables m and n on the conditions* (3.1) - (3.3), *each of which defines* Cauchy sequence, *is C-exact pair.*

● Let, for example, in a condition (3.1) $\boldsymbol{A}=\boldsymbol{B} = \boldsymbol{N} \,|\{1, 2, \ldots, n(\varepsilon)\}$, $\boldsymbol{A} \triangleq \{m\}$, and $\boldsymbol{B} \triangleq \{n\}$. For all finite values of the variables *m* and *n* condition (2.1) is valid obviously. Let in condition (3.1) the variables *m* and *n* be connected, for example, by equality $m = \psi(n)$. Then for practicability of this equality on all set ***B,*** which is postulated by Cauchy condition, it is necessary that mapping $\psi: \boldsymbol{B} \to \boldsymbol{A}$ should satisfy Theorem 2.3 and, in particular, condition (2.2′) should be valid. □■

The number sequence (***a***) is said to be converging to a finite number *A*, if $\lim(a_n) = A$. Otherwise, i. e., if $\lim(a_n)$ doesn't exist or it is equal $\pm\infty$, the sequence (***a***) is named divergent (***DS***) in the analysis. It is obvious, that $\{(\boldsymbol{a})\}=\{\boldsymbol{CS}\} \cup \{\boldsymbol{DS}\}$. As well, how it is accepted in the classical analysis, there is valid the following equality

$$\{\boldsymbol{CS}\} \cap \{\boldsymbol{DS}\} = \varnothing. \tag{3.4}$$

For a refutation of equality (3.4) we introduce a novel following concept.

Definition 3.1 The number sequence (***a***) is named *e-divergent* one (*e-**DS***) if there are such two infinite subsequences $\xi_1, \xi_2 \subset \boldsymbol{N}, \xi_1 \cap \xi_2 = \varnothing$, that there is fairly

a following condition:

$$\exists(\delta > 0,\ n^* \in \boldsymbol{N}) : \forall(m, k) \in (\xi_1, \xi_2)\ m, k > n^* \left|a_m - a_k\right| \geq \delta. \tag{3.5}$$

The direct comparison both of conditions (3.1)–(3.3) and (3.5) gives a proof of the following statement:

Theorem 3.1 Any number sequence is either a fundamental sequence, or an e-divergent one, *i. e.*

$$\forall(\boldsymbol{a})\ (\boldsymbol{a}) \in \{\boldsymbol{CS}\} \cup \{e\text{-}\boldsymbol{DS}\} \text{ и } \{\boldsymbol{CS}\} \cap \{e\text{-}\boldsymbol{DS}\} = \varnothing. \tag{3.6}$$

It is easy to show, that

$$\{e\text{-}\boldsymbol{DS}\} \subseteq \{\boldsymbol{DS}\} \tag{3.7}$$

The example of the sequence $(\boldsymbol{a}) \stackrel{\Delta}{=} \{n^{\alpha},\ 0 < \alpha < 1\}_{n=1}^{\infty}$ confirms the following inclusion:

$$\{e\text{-}\boldsymbol{DS}\} \subset \{\boldsymbol{DS}\}. \tag{3.8}$$

Proof The Sequence $(\boldsymbol{a})$ $0 < \alpha < 1$ holds $\lim n^{\alpha} = \infty$ is divergent one, as .

On the other hand, by virtue of the sequences $\xi_1, \xi_2 \subset \boldsymbol{N}$ infinity in (3.5) the pair (m, k) of variables $m \in \xi_1$ and $k \in \xi_2$ is (see the Theorem 2.3) a *C-exact* pair (2.2): $\exists(C > 0 \text{ и } q(k) \in \boldsymbol{Z},\ |q(k)| < C) :\ m = k + q(k)$. Now we examine the function $f :\ R_+ \to R_+$, which is determined by the formula $f(x) = (x + q(x))^{\alpha} - x^{\alpha}$. The value $f(k) = (k + q(k))^{\alpha} - k^{\alpha}$ of the function f at $x=k$ coincides with a difference $(m^{\alpha} - k^{\alpha})$ at $m = k + q(k)$. It is easy to show, that $x \to \infty$ holds $\lim f(x) = 0$. Hence, the condition (3.5) will be violated, at least, for any one pair $(m_0, k_0) \in (\xi_1, \xi_2)$ of values $m_0 > n^*$ and $n_0 > n^*$. Therefore, the sequence $(n^{\alpha}) \notin \{e\text{-}\boldsymbol{DS}\}$ at $0 < \alpha < 1$.■

Therefore, the strict inclusion (3.8) takes place instead of condition (3.7). And, hence, in view of (3.6), the following below inequality is valid instead of (3.4)

$$\{\boldsymbol{CS}\} \cap \{\boldsymbol{DS}\} \neq \varnothing. \tag{3.9}$$

Now we introduce a new concept, which is of fundamental importance in the proofs below.

Definition 3.2 *The number sequence* (***a***) *is said to be w-convergent* (*w*-***CS***) *if the following condition is satisfied*

$$(\forall \varepsilon > 0\ \exists\, n(\varepsilon) \in N):\ (\forall\ n \geq n(\varepsilon)\ \ |\, a_{n+1} - a_n \,| < \varepsilon), \tag{3.10}$$

or, in another limiting form of record

$$\lim(a_{n+1} - a_n) = 0. \tag{3.11}$$

Theorem 3.2 Any Cauchy sequence (***a***) is *w-convergent*, i. e., $\{\boldsymbol{CS}\} \subseteq \{w\text{-}\boldsymbol{CS}\}$.

Proof It is enough for the theorem proof to put $m = n + 1$ in the conditions (3.1)–(3.3), which are valid at all *m* and *n*. ■

Theorem 3.3 Any *w-convergent* sequence is the Cauchy one, *i. e.*, $\{w\text{-}\boldsymbol{CS}\} \subseteq \{\boldsymbol{CS}\}$.

Proof We shall assume the opposite that there is a number sequence (***a***) satisfying to condition (3.10), being fundamental one. Then by virtue of (3.6) it is *divergent*, i. e., it satisfies to condition (3.5), infinity of sequences ξ_1, ξ_2 in (3.5) a pair (*m, k*) of variables $(m, k) \in (\xi_1, \xi_2)$, is *an C-exact* pair (see (2.2) and (2.2)). Then, at least, for one $q \in \boldsymbol{N}$, $0 < q < \widetilde{C}$, there is the infinite set of such pairs $(m^*,\ k^*) \in (\xi_1, \xi_2)\ m^*,\ k^* > n^*$, that, for example, $m^* = k^* + q$ and, by virtue of (3.5)

$$|\, a_{m^*} - a_{k^*} \,| = |\, a_{k^*+q} - a_{k^*} \,| \geq \delta. \tag{3.12}$$

On the other hand, there exists for $\varepsilon \overset{\Delta}{=} \delta / q$ in (3.10) $n(\varepsilon) \in N$ such that $\forall\ n \geq n(\varepsilon)\ \ |\, a_{n+1} - a_n \,| < \varepsilon$. Hence, $\forall\ n \geq n(\varepsilon)$ we shall receive the following estimation:

$$|\, a_{n+q} - a_n \,| \leq |\, a_{n+q} - a_{n+q-1} \,| + |\, a_{n+q-1} - a_{n+q-2} \,| + \cdots + |\, a_{n+q} - a_n \,| < \varepsilon \cdot q = \delta \tag{3.13}$$

from the equality $a_{n+q} - a_n = (a_{n+q} - a_{n+q-1}) + (a_{n+q-1} - a_{n+q-2}) + \cdots + (a_{n+1} - a_n)$

.

Let $n^{**} = \sup\{n^*,\ n(\varepsilon)\}$. The inequality (3.13) is valid at all values $n > n^{**}$, including, $n = k^*$: $|a_{k^*+q} - a_{k^*}| < \delta.$ This inequality contradicts (3.12). ■

Theorems 3.2 and 3.3 compile the following statement:

Theorems 3.4 The set of Cauchy sequences coincides with the set of w-convergent sequences: {***CS***} = {***w-CS***}.

Corollary of Theorem 3.4 There exists a Cauchy sequence which is not limited by a some finite number.

For example, the sequence $(\boldsymbol{a}) \triangleq \{\ln n + C_e + \gamma_n\}$ of the sums of harmonious series (see [7, it. 388]) satisfies to condition (3.11), but its limiting value is more than any finite number. The corollary of Theorem 3.4 motivates an introduction of the following concept.

Definition 3.3 *The limit value of Cauchy sequence* (***a***), *which is not limited by any finite number, is said to be an infinitely large number* (***ILN***), *defined by this sequence* (***a***).

A symbol **Ω** denotes the set of all ***ILN,*** and the convergence of *Cauchy sequence* (***a***) to ***ILN*** is said to be *w*-convergence. In the non-standard analysis the ***ILN*** are named (see [8, Ch. 2.1]) as either non-standard, or impracticable, or actually infinite large, or inaccessible numbers.

4. Convergence of alternative number series

Let's designate by the symbol Σ_n the sum of n the first members a_i of the number sequence $(\boldsymbol{a}) \triangleq (a_n) \triangleq (a_1,\ a_2,\ \ldots,\ a_n, \ldots)$: $\Sigma_n \triangleq a_1 + a_2 + \cdots + a_n$, and the symbol S_n is called the value of the sum Σ_n. Thus

$$\Sigma_{n+1} = \Sigma_n + a_{n+1} \text{ and } S_{n+1} = S_n + a_{n+1},\ n \in \boldsymbol{N}. \qquad (4.1)$$

Definition 4.1 *The pair of sequences* (Σ_n) *and* (S_n), *defined by means of* (4.1), is said to be *a number series defined by sequence* (***a***), *and we shall write*

$$\Sigma_\infty(\boldsymbol{a}) \triangleq \sum_{n=1}^{\infty} a_n \triangleq \sum a_n = a_1 + a_2 + \cdots + a_n + \cdots \triangleq (\boldsymbol{A}). \qquad (4.2)$$

Here and below the summation at symbol Σ is supposed formally, by default, from 1 up to ∞, that means an unlimited opportunity of transition from the partial sum Σ_n to the partial sum Σ_{n+1}.

Definition 4.2 *The number series* (***A***) *is said to be convergent to the number A, if the number sequence* (S_n) *of the values* S_n *of partial sums* Σ_n *converges to this number A. In this case number A is named the sum of series* (***A***)*, and we write* $\lim S_n = A$.

Equality (4.2) can be written in the following way:

$$(\boldsymbol{A})=\sum a_n =(a_1 + a_2 + \cdots + a_n) + (\sum_{n+1}^{\infty} a_i) \triangleq \Sigma_n + \rho_n . \qquad (4.3)$$

The value of the infinite sum $\rho_n \triangleq \sum_{k=n+1}^{\infty} a_k$ in (4.3), which is called *n-th* rest of series (***A***), shall be denoted by the symbol r_n.

The number series $(\boldsymbol{A})=\sum_{i=1}^{\infty} a_i$ is said to be an alternative one, if its quantities of both positive and negative terms aren't limited. Such series is said to be convergent absolutely, if the series of its terms modules converges. Otherwise, one speaks about a 'conditional', or 'non-absolutely' convergence of alternative series.

Theorem 4.1 The number series (***B***), being any permutation of alternative series (***A***) which not absolutely converging to some number A, converges to the same number *A*.

Proof. Let a convergent to number *B* number series $B = \sum b_j \triangleq \widetilde{\Sigma}_n + \widetilde{\rho}_n$ be resulted by means of a mapping φ: $\boldsymbol{N} \to \boldsymbol{N}$, φ(*k*)=*j*, where $a_k \triangleq b_j$ from the series (***A***):

$$A = \Sigma_n + \rho_n = \sum_{1}^{n} a_j + \sum_{n+1}^{k(n)} a_i + \sum_{k(n)+1}^{\infty} a_i \triangleq \Sigma_n + \sigma(n) + \rho_{k(n)}, \qquad (4.4)$$

in (4.4) the $k(n)$ denotes a max{*k*: $a_k \triangleq b_j$, *j*≤*n*}. Step by step we shall carry out the mapping φ: $\boldsymbol{N} \to \boldsymbol{N}$ and simultaneously build both the sequence ($\widetilde{\Sigma}_n$) of the

partial sums $\widetilde{\Sigma}_n$ of series (***B***) and the sequence ($\widetilde{S}_n$) of these sums values $\widetilde{S}_n$. We shall receive the following bellow equality on *n-th* step from the identity $\sum a_i \equiv \sum a_i$ in view of (4.4):

$$\sum a_i = \Sigma_{k(n)} + \rho_{k(n)} = \Sigma_n + \sigma(n) + \rho_{k(n)} = \widetilde{\Sigma}_n + \widetilde{\sigma}(n) + \rho_{k(n)}, \qquad (4.5)$$

in (4.5) the sum $\widetilde{\sigma}(n) \overset{\Delta}{=} \sum_{i=n+1}^{k(n)} a_{n_i}$ with $n_i < k(n)$ contains those terms of the partial sum $\Sigma_{k(n)}$ of series (***A***), which don't belong to the partial sum $\widetilde{\Sigma}_n$ of series (***B***(*n*)), and $\sigma(n) = \sum_{i=n+1}^{k(n)} a_i$. Thus, in view of (4.5), we have the following equalities $\forall n \in \boldsymbol{N}$:

$$\rho_n - \sigma(n) = \widetilde{\rho}_n - \widetilde{\sigma}(n), \quad \Sigma_n + \sigma(n) = \widetilde{\Sigma}_n + \widetilde{\sigma}(n). \qquad (4.6)$$

If we denote by $\widetilde{s}(n)$ and $s(n)$ respectively the values of the sums $\widetilde{\sigma}(n)$ and $\sigma(n)$, then we will obtain the equivalent of (4.6) number equality:

$$S_n + s(n) = \widetilde{S}_n + \widetilde{s}(n), \quad r_n - s(n) = \widetilde{r}_n - \widetilde{s}(n). \qquad (4.7)$$

The $\lim a_n = 0$ holds $\lim s(n) = 0$ and $\lim r_{k(n)} = 0$ follows at $n \to \infty$ from the convergence of series (***A***), then we have $\lim \widetilde{r}_n = \lim \widetilde{s}(n)$ from the second equality in (4.7). Now from the first equality in (4.7) we receive the following result:

$$\lim S_n = \lim \widetilde{S}_n + \lim \widetilde{s}(n), \text{ } i.\ e. \text{ } \lim \widetilde{r}_n = A - B \text{ at } n \to \infty. \qquad (4.8)$$

Thus, in view of $\widetilde{S}_n \to B$, $S_n \to A$ at $n \to \infty$, there is the required implication:

$$(\widetilde{r}_n \to 0, \ r_n \to 0) \Rightarrow (B = A). \blacksquare$$

In the general case, at $S_n \to A$ and $r_n \to 0$ the biconditional ($\widetilde{S}_n \to B$) $\Leftrightarrow$ ($\widetilde{r}_n \to (A-B)$) follows from equality (4.7), *i. e.* it is valid (compare [9, Ch. I.XII.3])

Theorem 4.2 If the sequence (Σ_n^*) of the sum Σ_n^* was constructed arbitrarily from the members of convergent to number *A* alternative series (***A***) and the sequence

(S_n^*) of the sums Σ_n^* values S_n^* converges to number *B*, then the sequence (r_n^*) of the values of respective rests ρ_n^* converges to number *A*-*B*.

There are the examples in [10, it. 3] which illustrate these theorems.

There is a description in [11, Ch. 4.1] of 'some possible types of convergence of series $\sum_{i\in\omega} x_i$ of any linear vector space elements', which depends on the choice of the type of series terms summation. In particular, there have been noted following types of series convergence: the ordered convergence (**A**), permutable convergence (**B**), disorder convergence (**C**), and convergence on subsequences **(D)**. The permutable convergence has been named in [12, Ch. 1.1, Definition 1] by an unconditional one.

As it follows from Theorems 4.1 and 4.2, which are also valid for series $\sum_{i\in\omega} x_i$ of some linear vector space elements, the noted above types of convergence are equivalent.

References

1. Kolmogorov, A. N., Dragalin, A. G. Introduction in mathematical logic. – Moscow: Publishing house of the Moscow State University, 1982. (In Russian)

2. Dieudonne, J.Z. Foundations of modern analysis: Trans. from Eng.– Moscow: Mir, 1964. (In Russian)

3. Kolmogorov, A.N., Fomin, S.V. Elements of functions theory and functional analysis: 3rd edit.– Moscow: Science, 1981. (In Russian)

4. Fikhtengolts, G M. Course of differential and integral calculus.– Moscow: Science, 1969.–V. 3. (In Russian)

5. Sukhotin, A.M. The application of concept *C*- pair in the analysis // Modern problems of a science and education. 5, 2007, 101–107. (In Russian)

6. Weisstein, Eric W. CRC Concise Encyclopedia of Mathematics. – 2nd ed. – London–New York: Chapman&Hall/CRC, 2002.

7. Fikhtengolts, G M. Course of differential and integral calculus.– Moscow: Science, 1967.–V. 2. (In Russian)

8. Gordon, E.I., Kusraev, A., Kutateladze, S.S. The Infinitezimal analysis. P. 1.– Novosibirsk: Publishing house of Mathematics Institute, 2001. (In Russian)

9. Riemann, B. Works.– Leningrad: GosTexIzdat, 1948. (In Russian)

10. Sukhotin, A.M. About convergence of number series // Modern problems of a science and education. 6, 2007, II, 124–131. (In Russian)

11. Day, M.M. Normalized linear spaces. – Moscow: Mir, 1961. (In Russian)

12. Kashin, B. C, Saakyan, A.A. Ortohonal Series. – Moscow: AFTs, 1999. (In Russian)

CID: J21210-845

Mazurkin PM

GROWTH PRIMES

Mari State Technical University, Yoshkar-Ola

The growth of prime numbers was a clear indication. Increase - the number increases, the addition of something. If the number of prime numbers, figuratively called the "ladder of Gauss-Riemann", the increase may well be likened to the steps, separated from the ladder itself.

We prove that the law is obeyed $z_2(i_2 = 2) = 1/2 - 1/2\cos(\pi p(n)/2)$ *in the critical line* $i_2 = 2$ *of the second digit binary number system. This functional model was stable and in other quantities of prime numbers (3000 and 100 000).*

The critical line is the Riemann column $i_2 = 2$ *binary matrix of a prime rate. Not all non-trivial zeros lie on it. There is also a line of frames, the initial rate (yields patterns of symmetry) and left the envelope binary number 1.*

Cryptographers cannot worry: even on the critical line growth of prime numbers $z_{2j} = 1/2 - 1/2\cos(\pi p_j/2)$ *contain the irrational number* $\pi = 3{,}14159....$

Keywords: prime numbers, increase, the critical line, the root of 1/2

Introduction. Gauss, Riemann, and behind them and other mathematicians carried away by the relative power $x/\pi(x)$ of prime numbers with a truncated start,

represented in dotted decimal notation. In this case, apparently unconsciously, this figure has been expressed with the logarithm of the irrational basis $e = 2{,}71...$, and thus the transition from ten degrees to its natural logarithm of false identification has occurred. It is the main error of more than 150 years.

Application $\ln 10$ and false idea that future discharges of the decimal system the number of primes all the time increases to about 2.3, based on the assumption that $\pi(x) \sim |x / \ln x|$. And the reason for this turn in the study of prime numbers has been rather prosaic. As noted in [1]: "Gauss, the greatest of mathematicians discovered the law $\pi(x) \sim |x / \ln x|$ the age of fifteen, studying tables of primes contained in the gift to him a year before the table of logarithms."

We refused to logarithms, went to the binary system. It turned out that the very prime, $a(n) = \{2,3,5,7,11.13.17,...\}$, $n = \{1,2,3,...\}$ is not sufficiently effective measure. To avoid any claims to the proof, we adopt this traditional range.

The growth of prime numbers. This new figure was visible and at the same time is mathematically equivalent to a series of prime numbers. Growth - the number increases, the addition of something. If the number of primes $a(n) = \{2,3,5,7,11.13.17,...\}$ long figuratively called the "ladder of Gauss-Riemann", the increase may well be likened to the steps, separated from the carrier farm the base of the stairs. A long and tall ladder physically may well contain two parts - apart from the construction of stairs and a separate farm grounds.

Algorithm building a number of prime numbers. He is widely known, has the

$$a(n+1) = a(n) + p(n), \qquad (1)$$

where $p(n)$ - the growth of a prime number, n - the order of (number) of a prime number. The very number of primes is given initially, it is determined by the condition of the indivisibility of the other numbers, except on unit and itself (the latter condition, even excessive).

Therefore, growth is always calculated by subtracting

$$p(n) = a(n+1) - a(n). \qquad (2)$$

500 prime numbers. In table 1 shows fragments of the growth of a number of $a(n) = \{2,3,5,...,3571\}$. Among the 500 prime numbers was a maximum increase $p(217) = 34$ for a prime $a(217) = 1327$ with code 100010 in binary.

The fundamental difference of a number of growth of the number of primes is that in the growth (the same number - an abstract measure of the amount), only one column $i_2 = 2$ bit binary numbers is completely filled and critical, and the first class has only zeros for the set $a(n) > 2$.

Table 1. **A number of primes increase in 10th and binary number systems**

Order n prime	Prime $a(n)$	The growth $p(n)$ of a prime	The category of number i_2 of binary system					
			6	5	4	3	2	1
			Part of the increase $p_{i_2}(n) = 2^{i_2-1}$					
			32	16	8	4	2	1
1	2	1						1
2	3	2	trivial zeros				1	0
3	5	2					1	0
4	7	4				1	0	0
5	11	2					1	0
6	13	4				1	0	0
7	17	2					1	0
8	19	4				1	0	0
9	23	6				1	1	0
10	29	2					1	0
11	31	6				1	1	0
12	37	4				1	0	0
13	41	2					1	0
14	43	4				1	0	0
15	47	6				1	1	0
16	53	6				1	1	0
17	59	2					1	0
18	61	6				1	1	0
19	67	4				1	0	0
20	71	2					1	0
21	73	6				1	1	0
22	79	4				1	0	0
23	83	6				1	1	0
24	89	8			1	0	0	0
25	97	4				1	0	0
26	101	2					1	0
27	103	4				1	0	0
28	107	2					1	0
29	109	4				1	0	0
30	113	14			1	1	1	0
...	...	...	...	...	...	...	...	...
495	3539	2					1	0

496	3541	6				1	1	0
497	3547	10			1	0	1	0
498	3557	2					1	0
499	3559	12			1	1	0	0

Full filling will continue to infinity, therefore, can be considered a proven fact the appearance of the $p(n) = 2$ at any power $a(n)$.

Mathematical landscape. To construct (fig. 1) we take the example $i_2 = 1,2,3,4,5$ and delete those rows in which the five columns contains at least one trivial zero.

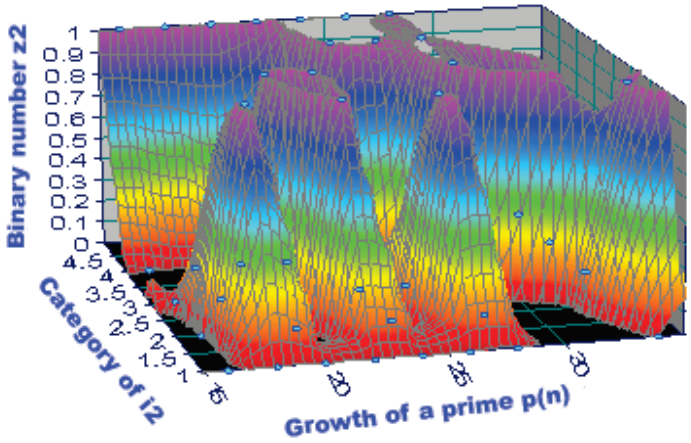

Fig. 1. The landscape of growth in the number of 500 prime numbers

An indicator is a binary number z_2 in the field of real numbers (0, 1).

Critical line. The first line in table 1 will automatically fall out of the set. After that, at any length series of prime numbers the first column $i_2 = 1$ is zero. Then each value increment from right to left starting from zero and ends with the unit. And for the unit as a wave broken lines are only trivial zeros.

All non-trivial zeros are arranged in any row between 1 (left) and 0 (first column on the right). Then ***Riemann's critical line*** in a vertical column $i_2 = 2$. But it is clear that not all non-trivial zeros lie on the critical line. They are available in other binary digits, interspersed with trivial zeros.

Critical start of the series. In table 2 shows the three critical primes.

Table 2. **Gain critical primes at the beginning of a series**

Order n	Prime $a(n)$	Growth $p(n)$	Digit number i_2					
			6	5	4	3	2	1
			part of the increase					
			32	16	8	4	2	1
-1	0	1						0
0	1	1	trivial zeros					1
1	2	1						1

Together with table 1 critical prime numbers give a full range of prime numbers, which this article is not considered. To accept it, you must: a) to recognize as simple that number which shares only on unit (zero/zero

indefinite); b) change the order in a number $N = \{0,1,2,3,4,...\}$; c) gain 1 is a border in the uncritical range includes non-critical prime $P = \{3,5,7,...\}$.

Further detailed analysis of the growth will fulfill a number of non-critical primes.

Effect of discharge i_2. In the software environment of Excel sum over the columns in table 1 (excluding the first line) and get the number of units $\sum z_2$ in the ranks of the binary system.

Table 3. **Influence of discharge binary system (498 lines)**

i_2	p_{i_2}	$\sum z_2$	Share 1	$\sum(z_2 = 0)$	Share 0	$2^{i_2-1}\sum z_2$	$\sum z_2 / \sum\sum z_2$
1	1	0	0	498	1	0	0
2	2	298	0.5984	200	0.4016	596	0.3855
3	4	285	0.5723	213	0.4277	1140	0.3687
	8	153	0.3072	345	0.6928	1224	0□1979
5	16	36	0.0723	462	0.9277	576	0.0466
6	32	1	0.0020	497	0.9980	32	0.0013
All		773	-	2215	-	3568	-

Model should give the relative values that allow comparison between different series of growth of prime numbers. After the identification of bio-law [2] was to teach the following conclusions:

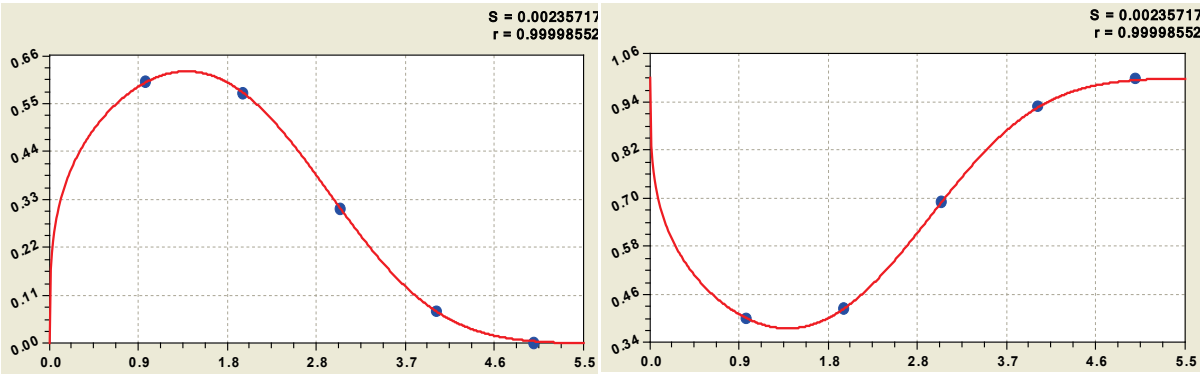

Fig. 2. Share units (left) and zero (right) in the rows of the matrix:
S - dispersion; r - correlation coefficient

- the share of units (fig. 2) lines of the binary matrix of growth of prime numbers

$$\nu(1) = \sum z_2 / 498 = 0{,}61623(i_2 - 1)^{0{,}28783} \exp(-0{,}029314(i_2 - 1)^{3{,}22295}); \quad (3)$$

- the proportion of zeros in (fig. 2) lines of the binary matrix of growth of prime numbers

$$\nu(0) = (498 - \sum z_2) / 498 = 1 - 0{,}61623(i_2 - 1)^{0{,}28783} \exp(-0{,}029314(i_2 - 1)^{3{,}22295})$$

.(3a)

In favor of computing the number of units, there are two distinctive features:

1) the number of zeros (trivial and nontrivial) is almost three times as many units (table 3);

2) the design of the formula (2) is easier compared with the expression (3).

Apparently, the option is 0,61623 with increasing number of $n \to \infty$ will approach to the golden ratio 0,618 .... Then, on the critical line are $\varphi^{-1} = 0{,}618...$ ones and 0,6182 zeros. Contribution amounts for units of columns (fig. 3) to the total (table 3 773) will be equal

$$\sum z_2 / \sum\sum z_2 = 0{,}39902(i_2 - 1)^{0.32247} \exp(-0{,}034914(i_2 - 1)^{3{,}09819}). \quad (4)$$

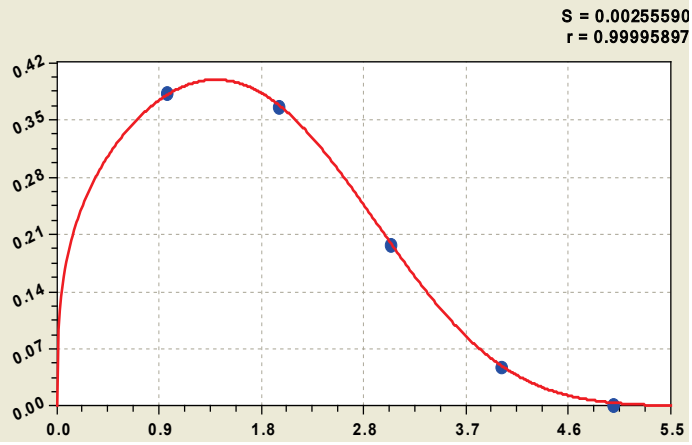

Fig. 3. Schedule the amount of the contribution of units in the columns of table 1

On the critical line $i_2 = 2$ contribution approaching to the square of the golden section.

Influence of growth. The explanatory variable we take the increase of a prime number. Then on the different digits of the binary number system formed their statistical model (table. 4)

$$z_2 = a_1 - a_2 \cos(\pi p(n)/(a_3 + a_4 p(n)^{a_5}) - a_6), \quad (5)$$

where $a_1 ... a_6$ - the parameters of the model (5).

If we ignore the first and last bits binary system, the closest to a rational number 1/2 on real values is the discharge $i_2 = 2$. For the critical line $i_2 = 2$ (5) is reduced (fig. 4) to the form

$$z_2(i_2 = 2) = 1/2 - 1/2 \cos(\pi p(n)/2). \quad (6)$$

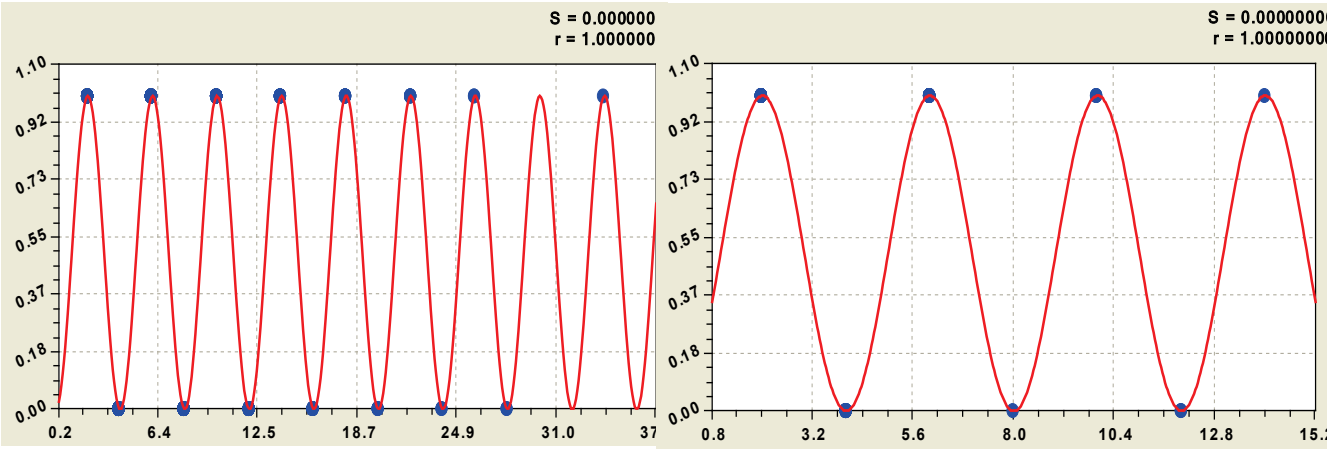

A number of prime numbers 500 A number of prime numbers A000040

Fig. 4. Graphics (6) to prove the Riemann Hypothesis: S - dispersion; r - correlation coefficient

Thus completes the proof of the Riemann hypothesis and remove the message from the Internet: "Here the famous Riemann hypothesis, that the real part of the root is always exactly equal to 1/2, no one has yet proven, although the proof of it would have been for the theory of prime numbers in the highest degree the importance. At the present time, the hypothesis is verified for seven million of the roots".

With increasing power of prime numbers equation (6) for the critical line continues, but the graphs such as figure 4 will be more frequent fluctuations due to higher growth. The growth is growing much more slowly than simple numbers. This will increase the power of the series.

The binary number for non-emergency lines. Table 4 shows the parameters of equation (5).

Table 4. **The influence of the growth of a simple number to a binary number of digits of the binary system**

Digit number i_2	Part $p_{i_2}(n)$	The parameters of the statistical model of a binary number						Correlation coefficient. r
		a_1	a_2	a_3	a_4	a_5	a_6	
1	1	0	0	0	0	0	0	1
2	2	1/2	½	2	0	0	0	1
3	4	1/2	0,70711	4	0	0	0,78540	1
4	8	0,45433	0,62621	155,4496	-128,0887	0,038904	-0,99258	0,9367
5	16	0,50303	0,50302	708,9489	-17,94895	1,02956	-2,82289	0,9997

To model the formula (5) patterns $z_2(p(n)) = f(p(n))$ of table 1 excludes those lines that are in the column trivial zeros (empty cells). Then there is an array of ones and non-trivial zeros. With the increase in the discharge of a binary number of lines in the array $z_2(p(n))$ will be reduced. Graphs are shown in figure 5.

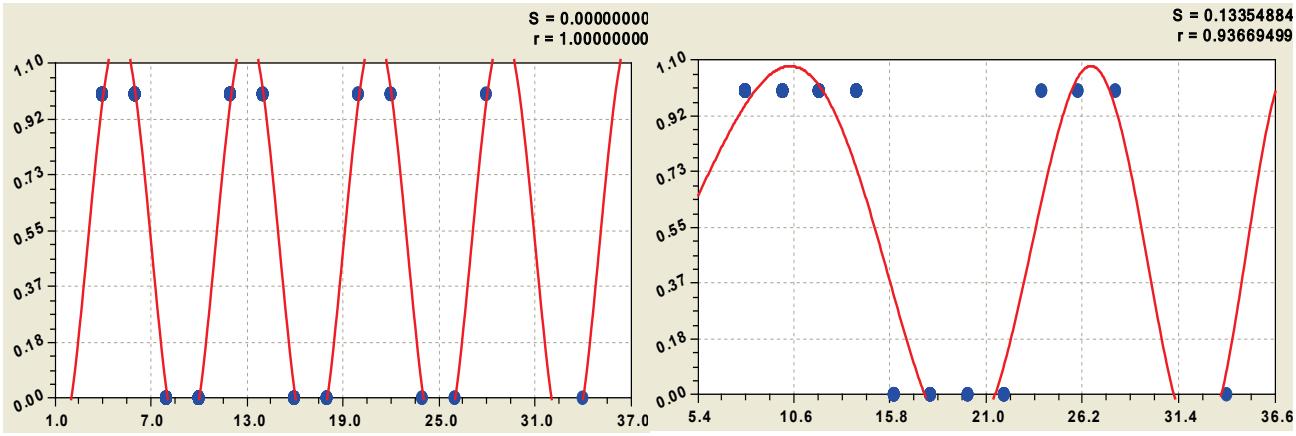

Digit $i_2 = 3$ binary number system Digit $i_2 = 4$ binary number system

Fig. 5. Graphics (5) changes in the binary number: S - dispersion; r - correlation coefficient

Zeros and ones are grouped together. Because of the small number of primes in an array 500 in column $i_2 = 4$ table 1, as seen from the right graph in figure 5, formed only two complete groups of four elements. Therefore formula (5) gets a full design.

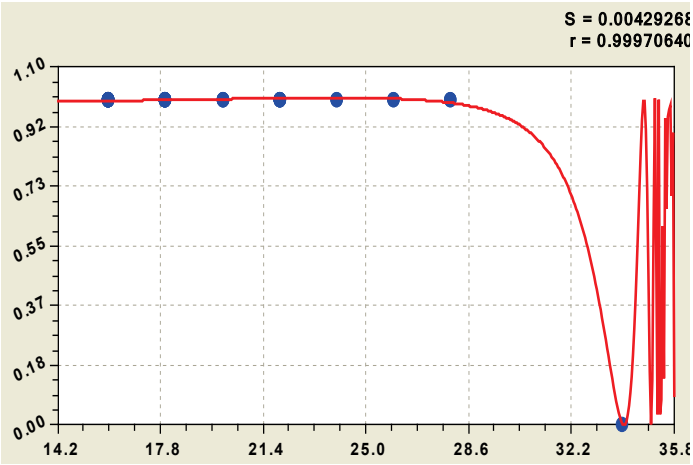

Fig. 6. Schedule (5) for the fifth digit

To discharge $i_2 = 5$ the number of groups of ones and zeros (fig. 6) is clearly insufficient.

At the top there was formed the group of seven units, but at the bottom of the group of zeros is only being formed. Therefore we can define a rational power series of prime numbers, providing all the bits. The data in table 4 shows that for $i_2 = 5$ the required 710 prime numbers (more than 708,9489).

It is noticed that while reducing the data set at $i_2 = 5$ to 36 lines of the character of the formulas in columns $i_2 = 2$ and $i_2 = 3$ is not changed. This indicates the saturation of these bits are the number of groups of ones and zeros. They are sufficient to identify patterns (5) with parameters from table 4.

Then the third category with an increase in power $p(n)$ gets the physical meaning

$$z_2(i_2 = 3) \to 1/2 - 0{,}70711\cos(\pi p(n)/4 - \pi/4), \qquad (7)$$

as shear waves 0,78539815 almost coincides with the value of the angle of $\pi/4$ = 0,7853975… .

Check the law $z_2(i_2 = 2) = 1/2 - 1/2\cos(\pi p(n)/2)$**.** On the critical line $i_2 = 2$ indicated this model is stable and the other quantities of prime numbers (fig. 7).

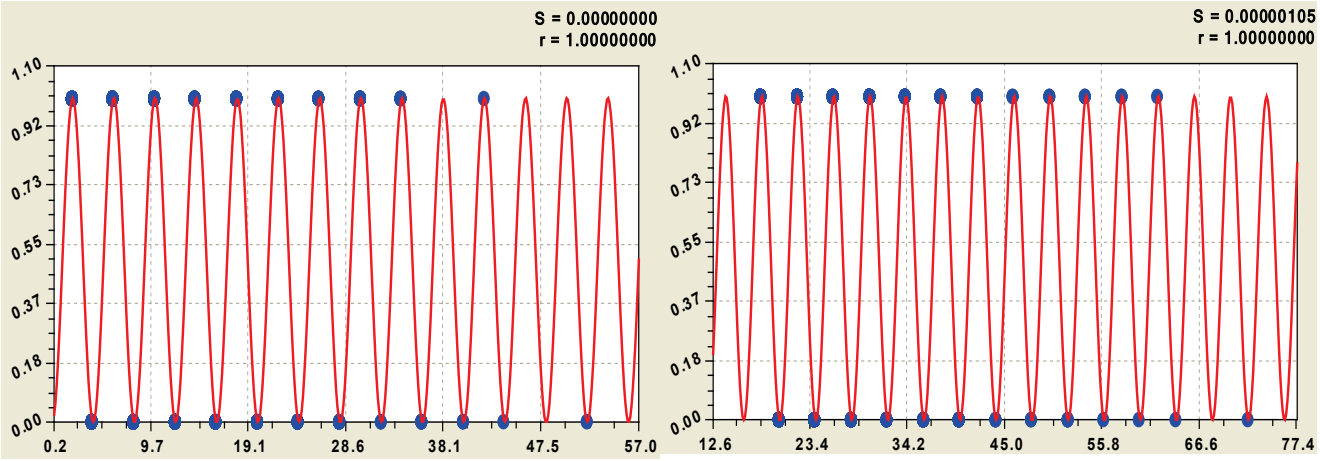

Increase in the number of prime numbers from 3000 members

Increase of more than 16 in a number of 100 000 members

Fig. 7. Graphs of law the distribution of the binary digits 0 and 1:
S - dispersion; r - correlation coefficient

With the increase in power series to 3000 increases the number of points in the graph (fig. 7). To test the subset was taken (1704 lines) increments $p(n) \geq 18$ from 100 000 prime numbers. It follows that in any sample observed our law (6) of the critical line.

The minimum sample of prime numbers. The method of cutting off the bottom of table 1 (table 5) determine the minimum sample, where the law still in effect sustained the critical line.

Table 5. **The minimum number of prime numbers**

Order n	Prime number $a(n)$	Growth $p(n)$	Discharge i_2 number					
			6	5	4	3	2	1
			Part of the increase					
			32	16	8	4	2	1
2	3	2	trivial zeros				1	0
3	5	2					1	0
4	7	4				1	0	0

The minimum number of non-critical primes form only three members, which was obtained by equation (5) with rational parameters given in table 6.

Approximation error of $0.5 \to 1/2$ is negligible. Schedule a simple in construction of equation (6) is shown in figure 6.

In other discharges $i_2 > 2$ should be increasing the number of (power) of primes.

Between growth and its component there is a pattern of transition of the numbers from the decimal system of notation to binary.

Benchmarks. The first unit of the left formed the asymptotic line to the left of which there are only trivial zeros. Consider the benchmarks in the 500 prime numbers.

Table 6. **The influence of the growth of a prime number to a binary number by the second digits of the binary system**

Prime number $a(n)$	Growth $p(n)$	Parameters (5)			Correlation coefficient r	Error ε
		a_1	a_2	a_3		
3	2	$\frac{1}{2}$	$\frac{1}{2}$	2	1	-9.989e-10
5	2					-9.989e-10
7	4					9.989e-10

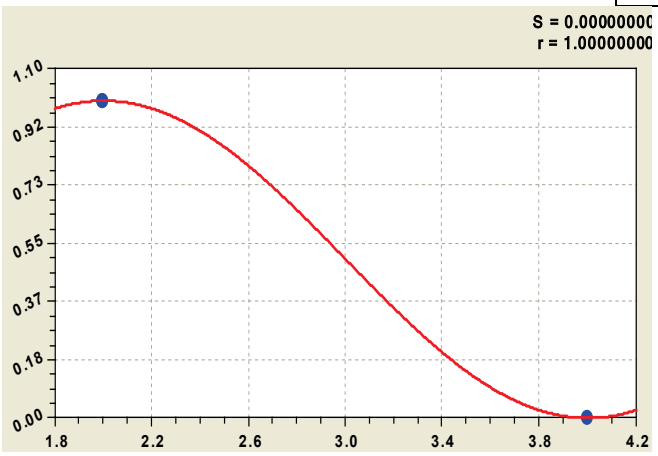

Fig. 6. Schedule of the formula (6) for the three prime numbers

Benchmarks form a block. In an array of 500 points are few (table 7), only five.

Proceeding from the condition that in the beginning of the series (table. 2) the gain is equal to the unit, was obtained (fig. 7) the formula

$$p_R(n) = \exp(0{,}80738 a_R(n)^{0{,}20489}), \quad (8)$$

where the index R denotes a fixed points a prime number.

Table 7. **Benchmark rate 500 prime numbers**

Order n	Prime number $a(n)$	Growth $p(n)$	Binary digit i_2					
			6	5	4	3	2	1
			Part of the increase					
			32	16	8	4	2	1
2	3	2					1	0
4	7	4				1	0	0
24	89	8			1	0	0	0
99	523	18		1	0	0	1	0
217	1327	34	1	0	0	0	1	0

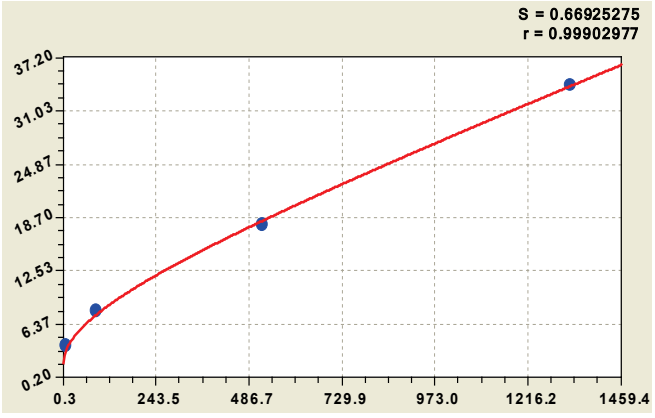

Fig. 7. Schedule of benchmark of growth

The use of benchmarks is much more compact than a relationship $x/\pi(x)$.

Primary growth. This - the third parameter (the first - a critical line 1/2), giving a picture of the growth rate of prime numbers. Parameter $p_P(n)$ for a number of 100 000 prime numbers are shown in table 8, and he compiled the first appearance of the

subsequent term. Primary growth is irregular, for example, an increase of 14 comes after 8 and earlier values of 10 and 12.

Various font allocated triangles (patterns of geometry) with sides (with $i_2 = 1$ - non-trivial zeros). Then the harmonious geometrical structures define the algorithm capacity growth, and even prime number (table 8).

Table 8. **The primary increase in the number of 100 000**

Prime number $a(n)$	Growth $p(n)$	Binary digit i_2					
		6	5	4	3	2	1
		Part of increase					
		32	16	8	4	2	1
3	2					1	0
7	4				1	0	0
23	6				1	1	0
89	8			1	0	0	0
113	14			1	1	1	***0***
139	10			1	0	***1***	**0**
199	12			1	***1***	**0**	0
523	18		1	***0***	**0**	1	0
887	20		1	**0**	***1***	0	0
1129	22		**1**	0	1	***1***	0
1327	34	**1**	0	**0**	0	1	***0***
1669	24		**1**	1	**0**	***0***	0
1831	16		1	**0**	***0***	**0**	0
2477	26		1	***1***	**0**	1	**0**
2971	28		***1***	1	1	**0**	**0**
4297	30		1	***1***	1	**1**	**0**
5591	32	1	0	0	***0***	0	0
9551	36	1	0	**0**	1	***0***	0
15683	44	1	**0**	1	1	0	***0***
16141	42	**1**	0	1	0	1	0
19333	40	1	**0**	1	0	0	0
19609	52	1	1	**0**	1	0	0
28229	48	1	1	0	**0**	0	0
30593	38	1	0	0	1	**1**	0
34061	62	1	1	1	1	1	**0**
35617	54	1	1	0	1	1	0
45893	50	1	1	0	0	1	0
58831	58	1	1	1	0	1	0
81463	46	1	0	1	1	1	0
82073	56	1	1	1	0	0	0

Line growth varies with the initial constant "deuce", and there will be fluctuations, the trend

$$p_P(n) = 2 + 2{,}09287\, p(n)^{2{,}09287} \exp(-0{,}31341 p(n)^{1{,}06442}) \quad (9)$$

For conditions $n \to \infty$ will always be $p_{\min}(n) = 2$.

The envelope of the line. Increments to the left of the asymptotic lines have trivial zeros. Therefore, taken into account the wave envelope line, which in different places concerns a critical line $i_2 = 2$.

This - the fourth parameter of the series.

Divide the increase in two parts $p(n) = p'(n) + p''(n)$. On the envelope line by line in the table (fig. 8) are located $p'(n) = 2^{i_{2\max}-1}$. And in the blocks $0 \le p''(n) = 2^{i_{2\max}-1} - 1$.

The trend with unit from the formula with three fluctuations looks like

$$p'(n) = 1 + 0{,}59470\, p(n)^{1{,}06436} + \ldots . \quad (10)$$

At $n \to \infty$ in the formula (10) always will be in the beginning 1.

Conclusions. The critical line Riemann is located in a vertical column $i_2 = 2$ binary matrix of growth of number of simple. Not all non-trivial zeros lie on it. There is also a line of benchmarks, the initial rate (giving patterns of symmetry) and the bending around.

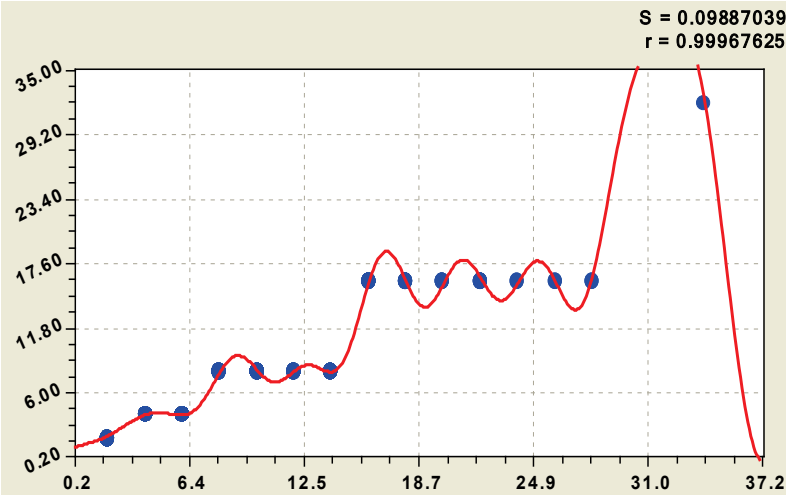

Fig. 8. The graph of the envelope line growth numbers 500

Literature

1. Don Zagier. The first 50 million prime numbers. URL: http://www.ega-math.narod.ru/Liv/Zagier.htm.

2. Mazurkin P.M. Biotechnical principle and stable distribution laws // Successes of modern natural sciences. 2009. № 9, 93-97. URL: www.rae.ru/use/?section= content&op= show article&article_id=7784060.

CID: J21210-076

UDC 511.216

Matyukhina A.G.

DIVISIBILITY OF RECURSIVE SEQUENCES ELEMENTS

Donetsk National University

For the recursive sequences of second order studied the divisibility of elements defined by arithmetic expressions from the root of a number of D-discriminate of the characteristic equation, on the primes number p. Depending on whether D-quadratic residue in the field of residues modulo p, we derive two theorems that allow knowing the recursive sequence, its first element and its characteristic equation, you can specify the elements of this sequence, which are divided without remainder by giving us a prime number.

Keywords: *divisibility, sequence, residue, field, Fibonacci, Binet formula.*

In this report explored a variety of tasks on the divisibility of numbers given by the arithmetic expressions from the root of an integer D- discriminate of the characteristic equation of recursive sequences of the second degree. Depending on whether the D quadratic residue is a residue of prime modulo p, apply one of two methods. If D is quadratic residue modulo p, this expression is itself an element of the field of residues modulo p. Otherwise, it is part of the extension of the field of second order, which was built by using the $\sqrt{D}$. In the first case using Fermat's little theorem for study of the divisibility, the second - its analogue for finite fields.

The results are applied to study the divisibility of Fibonacci sequence elements, and then arbitrary recursive sequences elements, by the prime number p. In this case the answer is very different, depending on whether, the discriminate of the characteristic equation of a sequence is quadratic residue of modulo p.

Additional designation

Z_p -field of residues prime modulo p. The order of Z_p is equal to p.
Z_p^*- multiplicative group of a finite field Z_p. The order of Z_p^* is p-1.
$Z_p[\xi]$ - the set, which came out extension of Z_p, by dint of root ξ irreducible equation of the second degree, just ξ^2-D=0.

The set $Z_p[\xi]$ is a field, so to do all the field properties. The order of the field $Z_p[\xi]$ is equal to p^2.

$a + b\ \xi$; $a + d\ \xi$; $e + f\ \xi$ - elements of the field $Z_p[\xi]$ ($a, b, a, d, e, f \in Z_p$).
So, ξ^2= D - quadratic non-residue of modulo p, in Z_p.
$Z_p\ [\xi]$ *- multiplicative group of a finite field $Z_p\ [\xi]$. The order of $Z_p\ [\xi]$ * is equal to p^2-1.

The case, when the discriminant of the characteristic equation is a quadratic residue in the field of residues a prime modulo p

$a_i = \frac{1}{\sqrt{5}}\left(\left(\frac{1+\sqrt{5}}{2}\right)^i - \left(\frac{1-\sqrt{5}}{2}\right)^i\right)$ — Binet formula for calculate the i-th member of the Fibonacci sequence.

When i=n(p-1), n∈Z, p— prime number, Binet formula looks like:

$$a_{n(p-1)} = \frac{1}{\sqrt{5}}\left(\left(\frac{1+\sqrt{5}}{2}\right)^{n(p-1)} - \left(\frac{1-\sqrt{5}}{2}\right)^{n(p-1)}\right).$$

If 5— quadratic residue modulo p (в поле Z_p), then

$\frac{1+\sqrt{5}}{2} \equiv x \pmod p$ and $\frac{1-\sqrt{5}}{2} \equiv y \pmod p$, Binet formula looks like:

$$a_{n(p-1)} = \frac{1}{\sqrt{5}}(x^{n(p-1)} - y^{n(p-1)}), \quad x,y \in Z_p ,$$

(p≠2 and p≠5— as the Binet formula in Z_2 and в Z_5 has division by zero).

By Fermat's little theorem, for p prime and m, which is not divisible by p, we have:

$m^{p-1} \equiv 1 \pmod p$

If $m=x^n$ и x≠0(mod p), then $x^{n(p-1)} \equiv 1 \pmod p$

If $m=y^n$ и y≠0(mod p), then $y^{n(p-1)} \equiv 1 \pmod p$

As a result, we obtain: $a_{n(p-1)} \equiv \frac{1}{\sqrt{5}}(1-1) \pmod p$, so $a_{n(p-1)} \equiv 0 \pmod p$

Theorem 1. " Divisibility of the Fibonacci sequence elements ": *"If 5 - quadratic residue in the field of residues modulo p, in Z_p, p≠2 and p≠5, then $a_{n(p-1)}$ member of the Fibonacci sequence $\{a_i\}$ which divided without remainder by p, $a_{n(p-1)} \equiv 0 \pmod p$ n∈Z, p, p -prime. "*

Summing up the conclusion of the divisibility of the Fibonacci sequence elements $\{a_i\}$ to any recursive sequence $\{u_i\}$, we have:

Let $u_0=0$— holds for any recursive sequence $\{u_i\}$, then the expression for the calculation of n(p-1) member of the sequence $\{u_i\}$ looks like:

$$u_{n(p-1)} = \frac{\gamma}{\sqrt{D}}\left(\left(\frac{a_0+\sqrt{D}}{2}\right)^{n(p-1)} - \left(\frac{a_0-\sqrt{D}}{2}\right)^{n(p-1)}\right) \quad \gamma \in R$$

(1)

D- discriminate of the characteristic equation $q^2=a_0q+b_0$ of the recursive sequence $u_{i+2} = a_0 u_{i+1} + b_0 u_i$ ($a_0 , b_0 \in Z$);

$\frac{a_0+\sqrt{D}}{2}$ та $\frac{a_0-\sqrt{D}}{2}$ - the roots of the characteristic equation

Considering the D, as a quadratic residue in Z_p and using to the expression (1) Fermat's little theorem, we have: $u_{n(p-1)} \equiv 0 (\mathrm{mod}\ p)$

$p \neq 2$ that $D \not\equiv 0 \pmod p$ - as in (1) is the division of these numbers;

$b_0 \not\equiv 0 \pmod p$ - as one of the roots of the characteristic equation for $b_0 \equiv 0 \pmod p$ is zero.

So:

Theorem 2. "Divisibility of the recursive sequence elements of the second degree":

"If the discriminant of the characteristic equation of the second degree is a quadratic residue a prime modulo p, then $u_{n(p-1)}$ a member of any recursive sequence $\{u_i\}$ is divided without remainder, so $u_{n(p-1)} \equiv 0 \pmod p$ $n \in Z$, p — prime"

The case, when the discriminant of the characteristic equation is a quadratic non-residue in the field of residues a prime modulo p

As the order of elements - the degree you have to raise an element to get one. [3,p.412]

The order of element is equal to the order of the cyclic subgroup containing this element (because the sub-group is limited) [3,p.412]

For any finite group G, the order (number of elements) of every subgroup H of G divides the order of G. (Lagrange's theorem).

So, every element of a group finite field, which raise to the order of this group is equal

to 1.

Applying this theorem to the groups $Z_p[\xi]^*$ and Z_p^*, we have:

any element of $Z_p[\xi]^*$ raising to the order p^2-1 is equal to 1. So, $(a + b\xi)^{p^2-1} = 1$;

any element of Z_p^* raising to the order p-1 is equal to 1. So, $c^{p-1}=1$, $c \in Z_p^*$

In the set $Z_p[\xi]^*$ equation $c^{p-1}=1$ has more than p-1 roots. So, elements in the set

Z_p^* p-1,and each of them are the root of this equation, so the other roots of this equation in the $Z_p[\xi]^*$ does not exist.

And as $(a + b\xi)^{p^2-1} = ((a + b\xi)^{p+1})^{p-1}=1$, so $(a + b\xi)^{p+1}=c$.

So, during we raise any element of $Z_p[\xi]^*$ the degree p +1 in the end we always get a definite element, included in the Z_p^*. $(a+b\xi)^{p+1}=a_1$, $a_1 \in Z_p^*$

Using mathematical induction we prove:

If conjugates of $Z_p[\xi]^*$ raised to the n power, then we also get conjugates belonging to $Z_p[\xi]^*$, i.e.

$(a+b\xi)^n= a_1+b_1\xi$

(2) $(a-b\xi)^n= a_1-b_1\xi$

When n = p +1 and using the fact that $(a+b\xi)^{p+1}=a_1$, $a_1 \in Z_p^*$, we have:

$(a+b\xi)^{p+1}=a_1$, $a_1 \in Z_p^*$

$(a-b\xi)^{p+1}=a_1$, $a_1 \in Z_p^*$

So, $(a+b\xi)^{p+1}=(a-b\xi)^{p+1}$

If you raise both sides of equations (2) the degree p +1, we obtain

$((a+b\xi)^n)^{p+1}= (a_1+b_1\xi)^{p+1}=a_2$

$((a-b\xi)^n)^{p+1}= (a_1-b_1\xi)^{p+1}=a_2$

So, $(a+b\xi)^{n(p+1)}=(a-b\xi)^{n(p+1)}$

Therefore, in general:

Conjugates of Z_p^*-a+b ξ and a-b ξ is to raise to the n (p +1) power, where n $\in$ Z, p-prime, are equal to each other, i.e . $(a+b\ \xi)^{n(p+1)}=(a-b\ \xi)^{n(p+1)}$.

We apply this evidence to the Binet formula of Fibonacci sequence$\{a_i\}$:

$a_i=\frac{1}{\sqrt{5}}\left(\left(\frac{1}{2}+\frac{1}{2}\sqrt{5}\right)^i-\left(\frac{1}{2}-\frac{1}{2}\sqrt{5}\right)^i\right)$

If $\frac{1}{2}$= a; $\frac{1}{2}$=b; $\sqrt{5}$= ξ, i.e. 5- quadratic non-residue in Z_p

i=n(p+1)

So $a_{n(p+1)}=\frac{1}{\sqrt{5}}\left((a+b\ \xi)^{n(p+1)}-(a-b\ \xi)^{n(p+1)}\right)$

We have proved early $(a+b\xi)^{n(p+1)}=(a-b\xi)^{n(p+1)}$, so

$a_{n(p+1)}\equiv 0 (\mathrm{mod}\ p)$

Theorem 3 " Divisibility of the Fibonacci sequence elements ": ***"If 5 - quadratic non-residue in the field of residues modulo p, in Z_p, p≠2 and p≠5, then $a_{n(p+1)}$ member of the Fibonacci sequence $\{a_i\}$ which divided without remainder by p, $a_{n(p+1)}\equiv 0(\mathrm{mod}\ p)$ $n\in Z$, p, p -prime. "***

Summing up the conclusion of the divisibility of the Fibonacci sequence elements $\{a_i\}$ to any recursive sequence $\{u_i\}$, we have:

$u_{n(p+1)}=\frac{\gamma}{\sqrt{D}}\left(\left(\frac{a_0}{2}+\frac{1}{2}\sqrt{D}\right)^{n(p+1)}-\left(\frac{a_0}{2}-\frac{1}{2}\sqrt{D}\right)^{n(p+1)}\right)$ $\gamma \in R$

If $a=\frac{a_0}{2}$; $b=\frac{1}{2}$; $\xi=\sqrt{D}$, D- quadratic non-residue in Z_p,

So $u_{n(p+1)}=\frac{\gamma}{\xi}\left((a+b\xi)^{n(p+1)}-(a-b\xi)^{n(p+1)}\right)$

We have proved early $(a+b\xi)^{n(p+1)}=(a-b\xi)^{n(p+1)}$, so

$u_{n(p+1)}\equiv 0(\mathrm{mod}\ p)$

So,

Theorem 4. " Divisibility of the recursive sequence elements of the second degree":

"If the discriminant of the characteristic equation of the second degree is a quadratic non-residue a prime modulo p, then $u_{n(p+1)}$ a member of any recursive sequence $\{u_i\}$ is divided without remainder, so $u_{n(p+1)}\equiv 0(\mathrm{mod}\ p)$ $n\in Z$, p — prime"

Literature:

1. *A.I. Markushevich.* Recursive sequences.-1950.-p.3-47.
2. *I.M. Vinogradov.* Fundamentals of theory of numbers.-1981.- p.17-21,38-82.
3. *A.G. Kurosh A.* Course in higher algebra.-1975.-p.110-123, 266-305,392-417.
4. *A.I. Kostrikin.* An introduction to algebra.-2000.-p.8-493.
5. *N.N. Vorob'ev.* Fibonacci numbers.-1978.-p.3-115.

CID: J21210-726

G.M. Trunov

ANOTHER FORM OF THE RECORDS OF NEWTON'S EQUATION OF GRAVITATION.

Perm National Research Polytechnic University

It is known, for example [1], that gravitational interaction of two spherical bodies in vacuum, can be written as (for the absolute value of forth):

$$Fгр = G\frac{\rho_1 V_1 \cdot \rho_2 V_2}{r^2}, \quad (1)$$

where G = 6,67·10–11 N·m2/kg2 – is the gravitational constant;

ρ1 and ρ2 – densities of bodies with volumes V1 and V2.

It is generally accepted that Newton's law of gravitation (1) does not depend on properties of medium in which interacting bodies are placed, although the classic experiments determining the gravitational constant were carried out by Cavendish only in air.

Let's consider interaction of spherical bodies, with densities ρ1 and ρ2 and volumes V1 and V2 placed in a medium with density ρ0 (see Figure 1).

Given the symmetry principle and the correspondence principle, it is possible to assume that the gravitational interaction of these bodies is described by the equation:

$$F12 = -G\frac{(\rho_1 - \rho_0)V_1 \cdot (\rho_2 - \rho_0)V_2}{r^2} r0, \quad (2)$$

where F12 – is the force of gravity acting on first body induced by second body;

r0 – the unit vector directed from the second body to the first body.

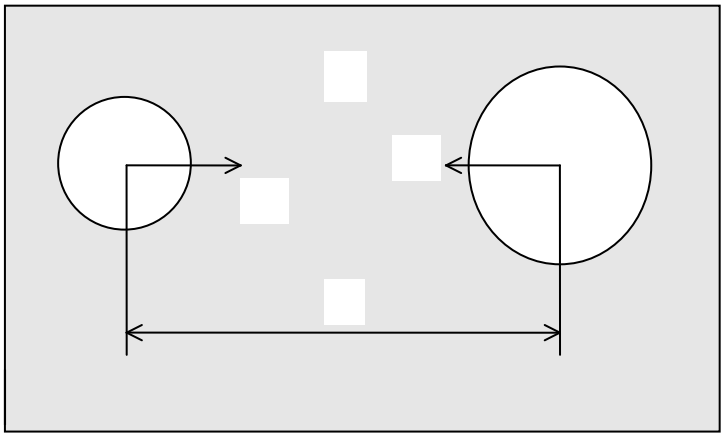

Fig. 1. Illustration of the formula (2).

The validity of equation (2) is confirmed in the two extreme cases. 1. Consider the interaction of the Earth (volume V2, density ρ2 = 5,5·103 kg/m3) and an iron ball (volume V1, density ρ1 = 7,9·103 kg/m3) in air near the Earth's surface (r – radius of the Earth), under normal conditions (ρ0 = 1.29 kg/m3). In this case, equation (2) becomes (taking ρ1 >> ρ0 and ρ2 >> ρ0,) the Newton's law of gravitation (1):

$$F12 = -G\frac{\rho_1 V_1 \cdot \rho_2 V_2}{r^2} r0, \qquad (3)$$

i.e. interaction between the Earth and an iron ball appears as force of attraction (the direction of the force F12 is opposite to r0).

2) Consider the interaction between the Earth and a rubber ball with infinitely thin walls (neglecting the thickness and weight of the shell), with a volume V1 and filled with hydrogen (ρ1 = 0.09 kg/m3). In this case, equation (2) becomes (considering ρ2 >> ρ0, ρ1 < ρ0 and r – radius of the Earth) equation

$$F12 = -G\frac{\rho_2 V_2 \cdot (\rho_1 - \rho_0) V_1}{r^2} r0 = g(\rho 0 - \rho 1)V1\ r0\ , \qquad (4)$$

where $g = G\frac{\rho_2 V_2}{r^2}$ = 9, 81 m/s2 – is the gravitational constant.

Equation (4) represents a positive difference between the two forces - Archimedes force FArch = ρ0gV and gravity m1g:

In this case, interaction of the Earth and a ball filled with hydrogen appears as a repulsive force (direction of force F12 coincides with direction of r0).

Note that equation (2) does not contradict to two fundamental principles:

1) The principle of symmetry, since the subscripts 1 and 2 in the equation can be interchanged

2) The principle of conformity, since in the limiting case (ρ1 >> ρ0 and ρ2 >> ρ0) equation becomes the Newton's law of gravitation..

Thus, equation (2) can be considered as another form of Newton's equation of gravitation.

References

1. A.N. Matveev, "Mechanics and relativity". Moscow: Higher School, 1976 (in Russian).

CID: J21210-609

Malashenko V.V., Malashenko T.I.

MOTION OF EDGE DISLOCATIONS IN HYDROSTATICALLY COMPRESSED METALS AND ALKALI-HALIDE CRYSTALS

Donetsk Physicotechnical Institute, National Academy of Sciences of Ukraine
Donetsk National Technical University

Analytical expressions are obtained for the force of dynamic drag of mobile dislocation pairs by pinned dislocations and for the drag force of isolated dislocations by dislocation dipoles in hydrostatically compressed crystals.

***Keywords**: dislocation, hydroextrusion, deformation.*

Processing with a high hydrostatic pressure (hydroextrusion) is one of the promising methods for creating materials with given properties, in particular, metals and alloys combining a high strength and plasticity [1-4]. The authors of [5] showed that a high hydrostatic pressure does not create a force on a dislocation; however, it changes the dislocation–dislocation interaction and, thus, affects the law of dispersion of dislocation vibrations. As shown in [6–11], the spectrum of dislocation vibrations substantially determines the character of dislocation retardation by other structural defects in a dynamic velocity range, i.e., in the range of over_barrier dislocation slip. This slip mode usually occurs at sufficiently high velocities ($v \geq 10–2c$ s, where c is the transverse sound wave velocity); however, dislocations in most metals move at higher velocities even at a relatively low level of applied stresses. In this work, we analyze the effect of a high hydrostatic pressure on the force of dynamic drag of mobile dislocation pairs pinned by dislocations and the force of retardation of isolated dislocations by dislocation dipoles. The presence of small dislocation groups and dislocation walls is characteristic of the structure that forms during easy slip, especially at high strains or during a local action of bending momenta.

The dynamic retardation of a pair of edge dislocations by pinned dislocations that are parallel to them was studied in [9], and the retardation of isolated dislocations by dislocation dipoles was analyzed in [10]. In [9], a dislocation pair was taken to be a linear harmonic oscillator whose vibrations can be excited by its interaction with immobile dislocations. The dissipation mechanism consisted in an irreversible transformation of the kinetic energy of moving dislocations into the energy of their vibrations with respect to the center of gravity of the dislocation pair. A linear oscillator can also be represented by a dislocation dipole whose vibrations are excited by dislocations moving in a crystal [10]. A hydrostatic pressure increases the dislocation interaction force and, thus, can substantially affect the dislocation dynamics; however, it was not taken into account in the works noted above. The purpose of this work is to take into account the effect of hydrostatic compression on the dynamic retardation of mobile dislocation pairs by immobile dislocations and of isolated dislocations by dislocation dipoles.

We consider two infinite edge dislocations moving under constant applied stress in a crystal subjected to hydrostatic compression. Dislocation lines are parallel to axis *z*, their Burgers vectors are parallel to axis *z*, and dislocation slip occurs along axis *x*. Dislocations move at constant velocity v in one plane normal to slip planes. This configuration of edge dislocations, which is equilibrium and stable, becomes more stable in the case of hydrostatic compression [5]. The distance between slip planes is *a*. The lines of immobile edge dislocations are taken to be rigid and parallel to axis *z*; for simplicity, their Burgers vectors are considered to be identical to those of glide dislocations. As a result of the interaction of mobile and immobile dislocations, the mobile dislocations begin to vibrate in their slip panes with respect to the plane *x* = v*t*, which is perpendicular to these planes. We now write an equation of dislocation motion in the *x*0*z* plane.

$$F_{dis}^0 = b^2 M \frac{x(x^2 - y^2)}{r^4} \approx -\frac{b^2 M w}{a^2}, \qquad M = \frac{\mu}{2\pi(1-\gamma)}, \tag{1}$$

where γ is the Poisson ratio and μ is the shear modulus. When writing this formula, we also took into account that dislocations vibrate slightly about the center of gravity of a dislocation pair. Under hydrostatic compression, the dislocation–dislocation attracting force increases and additional force Δ*F*dis(*p*) proportional to the hydrostatic pressure appears [5]

$$F(p) = F_{dis}^0 + \Delta F_{dis}(p) = F_{dis}^0 (1 + \beta p) \tag{2}$$

$$\beta = \frac{1}{\mu}\left(K_2 + \left(2K_1 - \frac{K_2 \lambda}{\mu} \right) \frac{(1-2\gamma)^2}{2(1-\gamma)} \right) \geq 0, \tag{3}$$

$$K_1 = -\frac{\frac{1}{2}\lambda - \mu + 3l - m + \frac{1}{2}n + p}{3\lambda + 2\mu + p}; \quad K_2 = -\frac{3\lambda + 6\mu + 3m - \frac{1}{2}n - 2p}{3\lambda + 2\mu + p} \tag{4}$$

In [9], we showed that two edge dislocations located one above the other in parallel slip planes represent a linear harmonic oscillator. In the absence of hydrostatic compression, it has vibration frequency ω_0

$$\omega_0 = \frac{b}{a}\sqrt{\frac{M}{m}} = \frac{c}{a}\sqrt{\frac{2}{\ln(D/L)}} \approx \frac{c}{a}, \tag{5}$$

For a hydrostatically compressed crystal, an increase in the dislocation–dislocation interaction force leads to an increase in the oscillator eigenfrequency.

$$\omega(p) = \omega_0\sqrt{1+\beta p} \tag{6}$$

Thus, the force of dynamic retardation of a moving dislocation pair by immobile dislocations under conditions of a high hydrostatic pressure changes according to the following two factors: first, an increase in the interaction inside the dislocation pair results in an increase in the dislocation oscillator eigenfrequency; second, the interaction of immobile dislocations with the moving pair dislocations increases. We perform computations and find the form of the desired force

$$F(p) = F(0)(1+\beta p)^{\frac{3}{2}}; \quad F(0) = \frac{nb^4\mu^2}{16m\omega_0(1-\gamma)^2 v} \approx n_0\mu a\frac{c}{v} \tag{7}$$

We now consider the case of retardation of an isolated edge dislocation by dislocation dipoles. The distance between dipole dislocations is *a*. In the absence of hydrostatic pressure, this type of dynamic retardation was studied in [10]; it was also shown that a dislocation dipole is a harmonic oscillator. When repeating the calculations performed above for this case, we found that dislocation dipole eigenfrequency also increases during hydrostatic compression of a crystal according to Eq. (6) and that the increase in the force of dynamic retardation of an isolated dislocation by dislocation dipoles can be described by Eqs. (7). To estimate the effect of a hydrostatic pressure on the quantities under study, we use the numerical estimates from [5]. At a pressure of 10^9 Pa, the dislocation–dislocation interaction force in potassium iodide crystals was found to increase by 65%. Then, according to the formulas obtained in this work, the force of dynamic retardation of dislocations by dislocation dipoles increases by 112%, the dipole eigenfrequency increases by 28%, and the minimum value of steady state velocity increases by 46%. According to the data in [5], the dislocation interaction induced by hydrostatic compression at the same pressure (10^9 Pa) in sodium chloride crystals increases by 30%. When performing the required computations, we find that the force of dislocation retardation by dislocation dipoles in these crystals increases by 48%, the dipole

eigenfrequency increases by 14%, and the minimum steady_state velocity increases by 22%. These estimates demonstrate that a high hydrostatic pressure can substantially affect the dynamics of dislocations, especially in alkali–halide crystals.

The results obtained in this work can be useful for an analysis of plastic deformation in hydrostatically compressed crystals, in particular, for the study of dislocation network motion.

REFERENCES

1. J.P. Hirth and J. Lothe, *Theory of Dislocations* (McGraw_Hill, New York, 1967; Atomizdat, Moscow, 1972).

2. V.A. Beloshenko, V.N. Varyukhin, and V.Z. Spuskanyuk, *Theory and Practice of Hydroextrusion* (Naukova Dumka, Kiev, 2007) [in Russian].

3. R.Z. Valiev, N.A. Enikeev, and M.Yu. Murashkin, Scr. Mater. **63**, 949 (2010).

4. R. Z. Valiev and I. V. Alexandrov, *Nanostructured Materials Produced by Severe Plastic Deformation* (Logos, Moscow, 2000) [in Russian].

5. V.V. Tokii and V.I. Zaitsev, Fiz. Tekh. Poluprovodn. (Leningrad) **15**, 2460 (1973) [Sov. Phys. Solid State **15**, 1634 (1973)].

6. V.V. Malashenko, Physica B **404**, 3890 (2009).

7. V.V. Malashenko, Mod. Phys. Lett. B B **23**, 2041 (2009).

8. V.V. Malashenko, Fiz. Tverd. Tela (St. Petersburg) **51**, 703 (2009) [Phys. Solid State **51**, 744 (2009)].

9. V.V. Malashenko, Zh Tekh. Fiz. **79** (4), 146 (2009) [Tech. Phys. **54**, 590 (2009)].

10. V.V. Malashenko, Kristallografiya **54**, 312 (2009) [Crystallogr. Rep. **54**, 288 (2009)]

11. V.V. Malashenko, Zh Tekh. Fiz. **76** (6), 127 (2006) [Tech. Phys. **51**, 806 (2006)].

CID: J21210-775

UDK 621.47

Borodzich EV

INSTITUTE OF GLOBAL PROBLEMS OF ENERGY EFFECTIVENESS AND ECOLOGY.

ENDOGENOUS PERTURBATIONS

ABSTRACT:

Article is based on the book published by Fund1 LOCAL ENDOGENOUS PERTURBATIONS. It is known, how modern geodynamics local vertical pulsations, essentially influence all geospheres, mentioning superconductivity many aspects of power. Possibility of use of high temperature is considered at sense of smell, and also other

A phenomenon origin

As experimental basis of the forecast of earthquakes significantly observable variations of various parameters served: a time course of deformations of a surface, electric resistance of breeds, concentration of chemical components and many other things[1]. It was found out, that the over whelming majority of variations of all without an exception of parameters do not reflect process of a ripening seismic centre, i.e. Are not harbingers of the last. It has appeared, the specified variations are caused by the local vertical pulsations lasting from ten of minutes to tens of years and covering territories with diameters from units to thousand of kilometers with amplitudes of vertical moving of both signs, multimeter sizes reaching sometimes.

The found out geodynamic phenomenon has received the short half life undercrust local perturbations – SULP[2]. SULP arise on a surface of a firm kernel of the Earth because of proceeding differentiation of its substance, cover not only liquid substance and a cloak, but also in many respects define a condition lithoD, hydro , atmo , ionospheres[3]. SULP have allowed to explain existence of ring structures and

morphostructures of the central type (MCT [4], and the polymodality of a sartorial component of the last has led to revealing in a liquid kernel of a planet of They are formed by the self ordered system convection Bernard's cells, adjoining to each other [5],

Because of distinction mass transfer convection cells on their general borders under the Earth core there are the contour currents provoking transmantle breaks. The easy component of differentiated substance getting into them provides buoyancy of a cloak in a liquid phase (Archimedes law). As a first approximation depth Z of a waterline of a cloak from a surface is defined as

$$Z=R_0\{1-[\rho_\mu/\rho_k](1-R^3_k/R^3_0)^3+R^3_k/R^3_0]^{1/3}$$

where R_0 and R_k radiuses of the Earth and the cloak arch, and ρ_μ, ρ_k average values of density of a mantle and components of contour flows.

$$R_в = R_0\{\rho_\mu/\rho_k(1-R^3_k/R^3_0)^3+R^3_k/R^3_0\}^{1/3}$$

Waterline position is conditional, since density continuously vary with depth, and the component places leaves on a surface ($Z=0$).

The mass transfers breaks have generated planetary lineament system which orderliness attributes by symmetry of Platon's rectilinear polygons[5]. The magnetic field topology will quite be coordinated with topology of contour currents, and variability of which, possibly, is responsible not only for strange behaviour of compasses in abnormal zones, but also for a planetary magnetic field. Same mass transfers rift zones where they lift lithosphere plates and bark[6] spread in asthenosphere. Creeping away from a raising, plates and bark plunge into where «waterline» is rather deep.

Fluctuation of mass transfers through degenerated transmantle breaks – mantle[7] form channels MCT[5] and a characteristic field of deformations. Inphase surfaces of this field settle down on conic coaxial surfaces with the general pole on the arch of a cloak and secondary poles on borders of sections of environments and phase transitions. Polymodal zone component MCT forms on a surface concentric system of shafts and hollows with amplitude decreasing to periphery. On surfaces of

the maximum tangents of pressure zones of the raised permeability for deep fluids are stretched. Fluidcomponent compulsorily arriving in a network (because of relative mutual moving of cones) sometimes forms the mineral deposits dated for a network. Deposits of hydrocarbons concern the last also.

SULP in lithosphere

Fluctuations of mass transfers in the bases of transmantle formations (breaks, channels) make active over them a network of cortical breaks. The crawl substances are lifted the surface, opening breaks, substance outflow lowers it, compressing boards of breaks. Earthquakes occur, as a rule, on a lifting phase since rocks (a crystal substratum) hold compression deformations. At considerable vertical movement relative horizontal deformations are insignificant. So, at diameter L~10m domeshaped swelling in height h~1m, relative horizontal deformation $\varepsilon = \Delta L/L \cdot 0{,}1h^2/L^2 \cdot 10^9$ that is accessible to measurement by laser deformograph. Close characteristics possessed swelling in the San Andreas (USA) and Gazly (USSR). In the first lifting and dome lowering has ended safely, in the second it was accompanied by earthquakes.

As the network of cortical breaks on a surface traces zones of the maximum tangents of pressure boards of breaks test relative vertical motions (as keys). The last loosen in a sedimentary cover over these breaks [8], being the reason of origin and growth of ravines, and also landslips, including on a ^{9}sea bottom. The specified motions are especially dangerous to lengthy constructions: the monolithic foundations, tunnels, bridges, highspeed railways, various delivery ducts. The last possess considerable flexural resilience, but are vulnerable because of rigidity at torsion. The last arises when the site departing perpendicularly from a highway (to compressor station) settles down in a zone of relative vertimoments constitutive at relative vertical throws.

Considerably bigger SULP[9] can expect geothermal power of the future. Overflows on conic zones of the raised permeability arise on depths $\Delta H \sim 10^5$ m. An

example of such overflows are simultaneous eruptions of the volcanoes carried on the Smoked Kamchatka arch observed sometimes, having the general (secondary?) pole.

Overflows of fluids (and SULP) occur not only under modern volcanic zones since are connected with reorganization of planetary contour currents. Traces testify to it powerful water sandy emissions in Central Asia, modern mud volcanism and emissions of hydrocarbons at some earthquakes. (For example, as in 1927 when on water area of Sevastopol «the sea» burnt). If SULP with H>>10^3 m will arise in a rich deposit of hydrocarbons moreover with the high maintenance of sulphurous and fluoric connections emission consequences small would not seem both to mammoths, and dinosaurs.

At last, fluctuations of mass transfers to the bases of transmantle formations, changing in them substance density, lead to occurrence of not tidal variations of acceleration of a gravity. Crawl substances weight, outflow increases it reduces. The geometry of variations, basically, repeats geometry of a field of deformations and the changes of density of substance of a cloak caused by them and in formations. Features of variations is their sharp recession at a deviation of a direction from an axis of the channel and slow recession of size of a variation with removal from a surface of the Earth. Measurements of size of a variation by land gravimeters do not reflect its true size since distributions of density under gravimeter unknown, caused by fluctuations of mass transfers. Nevertheless, variations of acceleration of a gravity are responsible substantially for conditions of mobile geospheres.

SULP in hydrosphere

In open hydrosphere of fluctuation mass transfers at SULP cause curvatures of equipotential with deviations from sphere (geod) on size $h \approx 2\Delta g/g \cdot R_0$, where $\Delta g/g$ relative change of acceleration of a gravity, R_0 radius of the Earth. Such curvatures at oceans were observed by cosmonaut Kovalyonok, and in atmosphere – «lenses» over Baikal and in the South East of Caspian sea. Crawl substances at SULP (+ Δg) are created by a convex dome on equipotential where water from not indignant periphery directs. At diameters of dome D~10^5 m and h~10 m (a deviation accessible to visual

supervision) overflows cover tens km^3 of waters. Under the influence of Kariolis force overflows twist in a whirlwind counter clockwise in Northern hemisphere. Outflows at SULP (Δg) create on hollows, whence waters direct to periphery, and their swirl changes a sign. An example of such whirlwind is the whirlwind in North East of Japan. It has diameter $D \approx 10^5 m$, changes a rotation sign about time in hundred days and covers all oceanic thickness $H \approx 5 \cdot 10^3 m$. Whirlwinds have received the unsuccessful name «synoptic» since it was supposed, that they are caused by cyclones and anticyclones. The last, however, revolt only surface waters ($H \leq 10^2 m$), and directions of overflows of real water and air weights are opposite, see SULP energy and mass exchange in atmosphere». Overflows of oceanic waters intensify with atmosphere, cause motions of ice fields in high widths, form z (Δg) and hummoching($+\Delta g$).

Causing overflows in all sea thickness, SULP make active breaks, decompressing soils, generating suspension streams and landslips on a sea bottom, an exit of the aggressive components dangerous to benthonic inhabitants and designs introgizationntroe by the general fluctuations of mass transfers systems located close to Bernard's cells paralel transmantle breaks creates interfering field of waves with abrupt fronts and amplitudes ~ 30 m . The amplitude of these «waves murderers» does not decrease with depth that represents danger not only to underwater constructions, but also for submarines. The listed features of display SULP in hydrosphere are necessary for considering at operation of deposits of hydrocarbons on a shelf, including deepwater.

At last, found out in subequatorial to a strip of world ocean system of cells the Ale Nin'o, quite concordant with, directly specifies in communication the Ale Nin'o with modern geodynamics. Most likely, the system the Ale Nin'o covers not only a strip

In underground hydrosphere overflows of waters occur on zones of breaks since filtrational streams are insignificant. The liftings of a bark noted earlier open breaks, lowering underground level of waters. Allocated in breaks ignite spontaneously gases

(«witch» fires on bogs) lead to burning of peatbogs. Drainage of the risen site strengthens the anticyclone formed over it (see « SULP in atmosphere»). On a lowering phase SULP water is squeezed out of breaks, and the cyclone over a site strengthens it irrigation. So, for example, in communication of flooding in St. Petersburg with SULP specifies appeared at flooding on island a spring. With SHL variations in the field piesometric levels in underground hydrosphere (opening 273) are connected. Amplitude of these variations $h \approx H \cdot \Delta l/(d + \Delta l)$, where H depth of a break, d it having opened on a surface, Δl change aperture at a surface pulsation. It is necessary to avoid categorically at a burial place of a dangerous waste, including radioactive, in zones of breaks since at SULP there is a demothballing of burial places. Curvatures equipotential at SULP lead to changes of coastal lines of the seas and the rivers and even to their current «back» at small difference of heights of their not indignant relief riverbeds.

SULP in atmosphere

The analysis has shown, that atmosphere reacts to variations ±Δg which effectively redistribute in it an aerosol on an influence height of a quantitative estimation it is necessary to consider in Boltsmanovsky distribution two more real forces: electric $E \cdot e$ and aerodynamic $0{,}5 \cdot \rho \cdot v^2 \cdot S_A$. Here E intensity of electric field of the Earth, e a charge on an aerosol particle, ρ and v density and speed of a stream of air which is flowing round a particle with section S_A. This stream is created by a particle, transferring to it warmly, received from the Sun. Therefore in its beams in gorges rises in the morning a fog. The same stream is created by heavy particles in a stream of the smoke rising from a cigarette.With the account told distribution Boltsman's registers :

$$n(\mu,H) = n_0 \cdot exp\ [\_(\text{«}\mu\text{»} \cdot m_0 \cdot g \_ E \cdot e \_ 0{,}5 \cdot \rho\, v^2 \cdot S_A) \cdot H/kT],$$

Where n_0 number of particles in volume unit at H=0, «μ» D molar particle weight, m_0 a nuclear mass unit. At a particle diameter $\sim 10^{D7} m$ its «μ» $\sim 10^9$, but it appears «weighed» if it is charged negatively (as in Miliken's experiment) Positively

charged particles quickly will settle on a surface. Not charged particles with relatives «μ» will be weighed by aerodynamic forces at suitable heights and at the clear sky. Thus, heavy particles which without instructions of electric and aerodynamic forces would be in a half meter from ground layer, appear participants equal in rights in Boltsmanovsky distribution along with air molecules (μ~30). But the number of particles of an aerosol in volume unit appears extremely sensitively to gravity variations:

$lg[n(g + \Delta g)/n(g)] = \mu \cdot m_0 \cdot \Delta g \cdot H \cdot lg\, e/kT$, where e Euler's number.

At H~10^3 m, μ~10^9, Δg~10^{D6} m/s^2 concentration of an aerosol changes in one thousand times!

These changes also define an atmosphere condition at SHLSP. ($+\Delta m$) in the basis, for example, the channel condenses its substance ($+\Delta\rho$) and generates a variation $+\Delta g$. If in atmosphere over the channel at height H there is a layer where intensity of evaporation and condensation are approximately equal the variation will repeatedly reduce concentration of an aerosol (Δn). Intensity of evaporation and heat loss will increase (ΔQ), will go down layer temperature (ΔT), the layer becomes more dense ($+\Delta d$) and will start to fall ($\partial H/\partial t$).

Under a layer as under the piston, will increase pressure ($+\Delta p$) and from area over the channel air will direct on periphery. If this area over ocean at $+\Delta g$ waters will direct to its centre from periphery. Outflow of substance from the channel will change all signs:$(\Delta m)\rightarrow(\Delta\rho)\rightarrow(\Delta g)\rightarrow(+\Delta n)\rightarrow(+\Delta Q)\rightarrow(+\Delta T)\rightarrow(\Delta d)\rightarrow(+dH/dt)\rightarrow(\Delta p)$. Thus the wind will be from periphery to the area centre, and waters at (Δg) go on periphery. As it was already marked, directions of streams and swirl air and water – are opposite. Unfortunately, only at cyclone formation (Δg) thanking condensation it is possible to see and photograph an emerging layer – the piston. Over it $\Delta p_i^i > 0$ at fast emersion in a layer the funnel is formed, and at constitutive Δg tornado formation is possible[10]. Corresponding member of the USSR Academy of sciences Mr. Kurbatkin on a symposium in Obninsk has noticed, that introduction of more and

more full data about an atmosphere condition practically do not improve weather forecast for the third day. The reason of it is absence of data about a place, time and intensity SULP, i.e. about layers – the pistons forming cyclonees and anticyclones. Without the account of it defining weather of the factor, its forecast can not be justified even next day. By present time the technique short term (some days) forecast SULP, checked up retrospective developed. There is a hope of success more, than one hundred days forecast of the meteoanomalis caused SULP in the State of Colorado (USA).

SULP are responsible for formation of ozone gaps, air blows, «jet streams», for fluorescences of the sky and even for the phenomena accepted for UFO. Really, ozone destruction on usages is accelerated on a surface of the firm phase (aerosol) which distribution corresponds to spatial position of fluctuations of mass transfers planimetric currents. Therefore geometrical similarity of Benar's cell and an ozone gap over Antarctica unequivocally shows interrelation of the last with SULP.

The mechanism of a luminescence of the sky speaks a deflection of positively charged layer and electric field increase between a deflection and a surface of the Earth. If the amplitude $+\Delta g$ is sufficient and there is a shock ionization of molecules at heights $\sim 5 \cdot 10^4 m$, and consequent they recombination are caused by a luminescence. currents at a layer deflection ($+\Delta g$) causes Elm's fires that reduces.

The sharp increase in atmospheric penetrative pressure of high

voltage insulators. Running off of charges from a deflection carries away neutral gas, creating descending streams and air holes that has been established as a result of the hundred analysis of the accelerogramm flights Внукovo Magnitogorsk. At considerable sizes $+\Delta g$ descending streams reach speeds of hundred meters per second and, surpassing speeds of a sound, cause thunder peals «dry thunder storms» thunder storms among the clear sky [11]. It is obvious, that air blows can destroy planes, that time and again was found out at the analysis of records of black boxes. The technique of a choice of more safe air routes and a technique of remote definition of places of occurrence of these descending streams from the plane board is developed, allowing in due time to change its course. Short term local descending

streams cause ring whirlwinds (as in experiments of R. Wood), steady against external influences with vertically focused axis, which observers accept for UFO. At last, «jet streams». These quasi horizontal κair streams at height H~$10^4 m$ with speeds v~$10^2 m/s$ with and kilometer diameters most likely are caused by the self coordinated fluctuations of the mass transfers in planimetric currents. These fluctuations can quite create «a running field» variations of a gravity like iphase of stator the heavy particles which are carrying away a stream of air will be which «rotor».

In an ionosphere at SULP there is a redistribution in space of the identical charges having different weight. Division of monovalent ions and electrons, since m_i/m_e~10^3 is greatest. Such division is caused by the vertical radiant structures [12] adhered to certain places observed by cosmonauts, but not found satisfactory explanations. Deformation of layers of an ionosphere and redistribution charges quite explain an observable radio emission.

The conclusion

Arguments in favour of existence SULP have been stated in 1980. This phenomenon has helped to explain quantitatively the known phenomena, including variations in the field piezometric levels of underground hydrosphere (opening search out acknowledgement assumptions following from a phenomenon (Benar's cell, «air holes», *et al*) . Nevertheless. It is necessary to recognize, as by present time of direct tool measurements on extensive regions still is not present. It is connected with fantastic cost of necessary data though the need in them has ripened for a long time. The most accessible and systems of measurement of heights of a surface of the Earth by means of laser range finders on enough dense network of angular reflectors would be effective. By comparative comparison of the measured heights it would be possible to reveal swelling and deflections on continents as visually marked Kovalyonok on an ocean surface. The matter is that trajectories of the companions forming «a geodetic space network», are deformed the same as and equipotential at SULP, because of weak dependence of anomalies on height. Despite recognition SULP leading scientists (I.L.Nersesov, A.L.Janshin, M.A.Sadovsky, S.L.Nightingale,

V.N.Strahov, V.J.Hain, *et. al*) It was not possible to organize monitoring SULP by an original technique by means of the Ministry of Emergency Measures. Monitoring would allow to keep lives not one ten miners and to prevent serious technogenic accidents. At last, without Besprozvannogo's titanic work on creation of original programs and models so not trivial results would be hardly received. The

5 6

[2] Rise in temperature in system slimereceptor on an input is caused sduvaniem «hot» molecules of steam from slime and Thomson's effect (when the dog sniffs, it narrows nostrils on a breath.) it is curious, that climbers in mountains мерзнут «from within». Inhaling drier, and exhaling damp air, they with each gramme of lost water give the 500 cal. The clothes do not rescue!.... And here ravens (as, possibly, and other birds) not merznut «from within» since possess effective dehumidifiers recuperators (on a frost at breath at them are not present steam from a beak). Here a problem for the heating engineers who are engaged energosberegeniem!

Author is grateful to Fund for support, and to the grand daughter, a daughter, the son in law and the wife for manuscript preparation for printing.

Sense of smell uses high temperature superconductivity?

Following features of sense of smell allow to make such judgement. First, extremely low threshold of sensitivity sometimes only one molecule in sm^3. Secondly, sharp dependence of this threshold on temperature – we feel smells on a breath when the temperature goes down all on some gradusov.2 On an exhalation and at rise in temperature of a body because of illness (too on some degrees) sense of smell temporarily disappears. Slime presence in a nose which, possibly, allows to transfer receptor structure (as water transfers quartz structure in B.V.Derjagina's capillaries) is essential and to clear a receptor of odorous substances. Slime participates and in cooling of a receptor and itself. As a sign of a healthy animal knowingly consider a wet and cold nose. Dryness of a nose sharply worsens sense of smell.

Since experimental detection of a superconductor in system slime receptor business of any future, we will try to show, that the parity of capacities of a signal to noise is not enough for maintenance of so low threshold of sensitivity. As a principle of work of a receptor of sense of smell we will choose a principle of work of a coded lock with n buttons. If $n \geq \mu \sim 10_i^3$, where μ молярный weight of a molecule of odorous substance, the number of combinations is great enough to provide detection of a necessary set of smells. We consider, that the molecule of odorous substance at interaction with a receptor exchanges with it all μ charges. Certainly, models of sense of smell can be chosen different, but the exchange of electric charges is obligatory. By definition capacity of signal $S=I^2R$, where $I=Q/\Delta t \approx \mu \cdot ev^*/l$. Here e – an elementary charge, l – a thickness of slime on a receptor, and $v^* = v \cdot \mu^{-1/2}$ – srednya thermal speed of a molecule of odorous substance. Considering told, we will receive $S=\mu \cdot e^2 \cdot v^2 \cdot R/l^2$, where R – entrance resistance of system slime receptor, *S*capacity of a signal.

According to theorem Найквиста $E^2 = N \cdot R = 4k \cdot T \cdot R \cdot v^*/l$, where E^2 – a square электродвижушей forces, and N – capacity of noise. As super conducting resistance, i.e. $R \neq 0$ it is possible to reduce to it is supposed usual, instead of. We will receive $N = 4kTv\mu^{-1/2}$, $v=300m/s$ with, $j \approx 10^{D4} m$ (as in experiences B.V.Derjagina). The smaller thickness of slime l on a receptor would complicate compulsory and natural clarification of a receptor from slime. At $k=1,4 \cdot dzh/hailstones.$, $T=300\ K°$ we will receive $S/N = R \cdot 1,5 \cdot 10^7$.Для confident definition of a smell, it is necessary $S/N \geq 1$, i.e. $R \geq 10^7\ Ohm$.

It is improbable, since slime has saltish taste, i.e. has appreciable conductivity. Hence, made assumption $R \neq 0$ is improbable and with the help нанотехнологии, probably, the organic structure of a hightemperature superconductor will be received.

5 8

REFERENCES

1. Borodzich E.V. «Revealing of a harbinger of seismic activity from experimental data». The express train the information. VIEMS regional, prospecting and trade geophysics, 1982, 22, pp. 1-9.

2. Borodzich E.V. «About variations of various parametres in seismic areas». VIEMS, regional, prospecting and trade geophysics, 1982, 22, pp. 1016.

3. Borodzich E.V. «Influence short halflif undercrust local perturbations on litho , hydro , and atmosphere», Gagarinsky readings on astronautics and aircraft, 1989,. Moscow, Nauka, 1999, pp. 130-141.

4. Borodzich E.V., *et. al* «About an origin of ring structures». 131, pp. 1081-1085 is given the USSR, 1990.

5. Besprozvanny, *et. al* «about revealing of orderliness of a planetary network lineament by results of the numerical analysis». Fizica zemli. 1994, 2., pp 57-66.

6. Atlantic Ocean FLOOR for National Geographic magazine, june, 1968.

7. Artjushkov E.V. «Geodynamics», «Nauka», M, 1979, p. 118.

8. Grigorev A.T., *et. al* «Dependence between characteristics of vertical movings of a surface and an intense condition of a cover in super break zones», Fields of pressure and deformations, M, «Nauka», 1979, p. 97-125.

9. The copyright certificate № 1266322 from 11.02.85

10. The Priroda № 6 1976, p. 53,.

11. «A Terra incognito and short half life undercrust local perturbations». Fund of Institute of global *problems of* energy effectiveness and ecology. M, 2002

12. Konjushaja J.P. «the Phenomenon vertically radiant structures of day radiation of the Earth». Opening of the Soviet scientists. M, Moskovsky rabochiy

13. Gohberg M. B, *et. al* «Electromagnetic harbingers of earthquakes». The Earth and the Universe. 1987, p. 16-20.

5 9

CID: J21210-716

UDK 678.7:678.4

R.I.Ableev *, A.R.Valiev *, Z.A.Perestoronina **,

S.K.Kurljand, A.S.Ramsh,

I.V.Baranets **, R.N.Gimaev*

RESEARCH IN STRUCTURE AND PROPERTIES OF OLEFINIC THERMOPLASTIC ELASTOMERS THROUGH THE METHOD OF DIELECTRIC SPECTROSCOPY

**The Bashkir state university,*

*** Research institute of synthetic rubber n.a. academician S. V.Lebedev*

The article deals with the experimental data on the application of the method of dielectric relaxation spectroscopy which studies the morphology and properties of dynamically vulcanized intermixtures of polypropylene with ethylene-propylene-diene rubber.

Key words: thermoplastic elastomers, dynamic vulcanized thermoelastoplastics, dielectric relaxation spectroscopy.

Today a wide spectrum of thermoplastic elastomeric materials or thermoelastoplastics (TPE), which have diverse important performance properties [1] is released in the world. Thus "dynamic" vulcanized stocks (TPV) based on intermixtures of polyolefins and various rubbers [2] are of great interest. Homo- or copolymers of ethylene-propylene are used as thermoplastics; natural, isoprene, butadiene, styrene-butadiene, acrylonitrile-butadiene, butyl rubber, ethylene-propylene, and other elastomers are used to create the elastomeric phase. By means of full or partial vulcanization of the elastomeric phase, using various vulcanizing systems (sulfur, peroxide, pitch), appears the possibility to carry out the modification of the physicochemical and performance characteristics of materials [3]. Unique properties of TPV are defined by the features of structure and determined by formation when combining the elastomer and thermoplastic of a specific transitive (boundary) layer. Therefore for working out new highly effective compositions and

materials on their basis, the knowledge of mechanisms of structural change and properties of TPV in the course of processing and long-term operation is necessary. The key role in the balance of technological and performance properties of TPV belongs to morphology [2].

The purpose of the article is the study of interrelation between structure and properties of olefinic thermoelastoplastics, carried out by means of the dielectric relaxation spectroscopy (DRS) and the estimation of possibility of the yielded method application for studying the relaxation properties of the mixed polymeric compound-elastomeric systems gained by the method of dynamic vulcanization.

To study the dynamics of the relaxation transitions related to heterogeneous structure of TPV, the method of the dielectric relaxation spectroscopy (DRS) (dielectrical loss tangent change tgδ), which proved itself in researches of mixed polymeric systems [4], has been chosen. Maximums in the form of absorption peaks of various intensity and breadth, which are related to various mechanisms of mobility of base units in a polymetric compound, are observed on temperature (or frequency) dependences tgδ; that allows to precisely fixate the transition temperature. The reflexion of the mechanism of losses on quantity tgδ in a corresponding maximum depends directly on the electrical dipole moment of the base unit, whose mobility is displayed in a spectrum. Such selectivity, combined with a wide dynamic range, allows to effectively explore temperature transitions and to record phase alterations in polymeric intermixtures [5,6]. So, it seems interesting to esteem possibilities of application of the yielded method for morphology study of dynamically vulcanized intermixtures of polypropylene with rubbers (TPV).

Spectrums of the dielectric relaxation spectroscopy were gained with use of the dielectric bridge Orion TR9701, connected to the exterior sinusoidal generator, providing a frequency range from 30 Hz to 300 кHz. A selective millivoltmeter with the double T-shaped bridge, rated for the same frequency range, was used as a null indicator. Measuring was carried out in a three-electrode pocket at 110 Hz, in the range of temperatures $-150^{o} \div +150^{o}$C, at constant speed of a heating of ~1 ^{o}C/minute. The temperature of the sample was controlled by the thermocouple

through a hole in a guarded electrode. For quantity tgδ of 100 • 10^{-3} order and at frequency of 110 Hz the percentage error did not exceed 2 %.

Morphology of the samples of TPE gained was difined through the method of numeral microscopy, using the image analyzer by Leica on the basis of exploratory microscope DM-2500, color camera DFC-420S for recording images, and Leica Las software for capture, storage, and quantitative analysis of structural units of objects of examination. The information on the shape, size, arrangement, and character of boundaries of the dispersed phase is obtained in the mode of a light field. Identification of a crystalline phase in intermixtures and TPV is carried out in the mode of crossed nicols. A wide set of object lenses helps to detect the hierarchy of structural units in the diapason from 180 nanometers to 1000 microns.

Research targets:

A) Commercial samples of polymeric materials of domestic and foreign production - TPV «Santoprene 261-87» (ExxonMobile Chemical), TPV «Tompolen PP 305K-M» (JSC “"NPK" Polymer-Compound”), isotactic polypropylene «Balen 01030» (PP), ethylene-propylene-diene elastomer EPDM-50 (JSC «Ufaorgsintez»);

B) Laboratory samples of TPV on the basis of intermixtures of polypropylene with EPDM, obtained on the mixer-plasticorder “Brabender PLV-151” at the temperature of (195±5) ^{0}C and rotating speeds of a rotor of ~50 rpm. Standard samples for physical-mechanical and dielectric tests were made through the pressure molding method, and in accordance with the requirements of ASTM D 412; to measure the spectrums of DRS, 0,3 mm films were pressed at temperature of (190±5) ^{0}C.

Initially, changes of quantity of dielectrical loss tangent in the given interval of temperatures for dynamic vulcanizers and individual elements of TPE. Fig. 1 shows the area of glass transition (α-transition), related to the appearance of dipole-segmental losses of the initial EPDM, and, accordingly, a flexible phase of olefinic TPV. The maximum of the initial rubber α-transition is observed at -35 ^{0}C. Adding polypropylene to elastomer (#3 curve - laboratory sample of TPV) has led to the shift of α-transition field towards the positive temperatures by ~8 ^{o}C, thus coinciding with a corresponding maximum of Santopren (#2 curve). Adding transformer oil of

adequate quantity (#4 curve), compatible with elastomer, has provided coincidence of low-temperature shoulders of α-transition for initial rubber, domestic Tompolen and imported Santopren (##1,2 and 4 curves). The maximum of α-transition of the sample #4 moved in comparison with the sample #3 towards the negative temperatures, and its high-temperature shoulder appeared to be measurably expanded and indistinct. The later means the formation of a great number of the intermediate structures with a different level of compatibility in the triple system of PP/EPDM/oil extender. The data obtained allow to conclude on the identity of phase structure and, hence, affinity of physical-mechanical properties of olefinic thermoelastoplastics of Russian (Tompolen brand) and imported production (Santopren). It is proven by the results of comparative tests of given samples of TPV on major technological and performance characteristics (tab. 1). Fig. 2 shows spectrums of DRS for the sample of an industrial homopolymer of propylene with isotactic structure (PP). There are 3 characteristic transition areas: a) at -75 ^{0}C, related to dipole-group losses of PP; b) wide transition from -10^o to +60 ^{0}C - the complex area related to dipole mobility of chain sections in PP, that are placed in a defective (not crystallized) parts of PP; c) a transition area with the range of temperatures from +70^0 to +120 ^{0}C, driven by premelting of the crystallized part of PP.

The mixture of PP/EPDM (in the ratio 36/64 wt%) (fig. 2, #2 curve) represents unvulcanized thermoplastic polyolefin. In the low-temperature area its spectrum repeats both the low-temperature transition of PP and characteristic details of an amorphous layer of its crystalline phase (transitions at -18^0 and at +12 ^{0}C). Glass transition (α-transition) of EPDM is observed at the temperature about -30 ^{0}C - practically at the same place as in individual rubber. Observed at above +75 ^{0}C, exponential growth of dielectric losses, obviously, is caused by ionic conductivity processes. Spectrum of TPV on the basis of intermixture of PP/EPDM (#3 curve) is characterized by the low-temperature transition of PP, and it is observed at the temperature even lower than for previous samples. Possibly, it has to do with the presence of a plasticizer – oil extender (insulating oil) in the intermixture. α-Transition of EPDM is clearly visible (in the position not shifted), but in comparison

with the unvulcanized sample (#2 curve) the amorphous layer of PP can hardly be observed, and its fine structure is practically not visible. The later proves that dynamic vulcanization of rubber element essentially influences the processes of crystallization of PP, when cooling a composite, and the structure of the polypropylene phase itself.

Morphology of the intermixture of PP and EPDM (in the ratio 36/64 wt%), determined through the method of numeral microscopy, is characterized by the even arrangement of elements through the volume, contains a net of rubber consisting of thin amorphous lines, up to 250 nanometers thick, penetrating polypropylene areas, without essential segmental interactions of elements on phase boundaries (fig. 3a). At the same time, in the crossed nicols mode there is a measurable variation of sizes and intensity of luminescence of areas with the intermixture enriched with polypropylene. The lines of rubber, intercrossing fields of PP, have high contrast and do not influence PP crystallinity (fig. 3b). In spectrums of DRS it is seen in the stability of temperature position during polypropylene transitions, when it is added to EPDM.

Morphology of TPV on the basis of an intermixture of PP and EPDM is characterized by even distribution of ingredients in a polyolefin matrix. The thickness of areas of the crosslinked rubber varies from 150 to 300 nanometers. At the same time, morphology of EPDM differs from morphology of an intermixture reduction by a difference of optical densities of neighboring areas and the diffusion of interphase boundaries (fig. 4a). The later proves the segmental interactions between elements in the formation process of TPV. The study of EPDM in the crossed nicols has detected abrupt reduction of a diapason and the intensity of luminescence, characterizing the arrangement of a crystalline phase, and the reduction of the size and the degree of perfection of the areas that have long-range order; this indicates the modification of the shape of existence of PP in TPV (fig. 4b). Spectrums of DRS reflect these phenomena by the changes in the shape of a curve in the area of the response of an amorphous layer of a crystalline phase of PP in TPV (fig. 2, #3 curve).

Conclusion

Thus, the phase changes occurring in the structure of TPV, are reflected in the spectrums of DRS. The method allows to divide relaxation transitions of individual elements of thermoelastoplastics and is a convenient tool to study the features of morphology and dynamics of heterophase polymeric systems. It helps to purposefully model physical-mechanical properties of new materials.

References

1. Ableev R.I, Gimaev R.N. Innovations in the field of polymer materials for cable industry. // Vestnik of the Bashkir State University.- 2008.- №1. - volume 13.- P.214.

2. Coran A.Y., Patel R.P. Thermoplastic Elastomers based on dynamically vulcanized elastomer-thermoplastic blends. // Thermoplastic Elastomers.- New York: Hanser/Gardner.- 1996.- 540 p.

3. Wolfson S.I. Dynamic vulcanized thermoplastics: obtaining, processing, properties. M.: Nauka, 2004. – 173 p.

4. Kremer F., Arndt M. Broadband Dielectric Measurement Techniques. // Dielectric Spectroscopy of Polymeric Materials (Runt J.P., Fitzgerald J.J. (Editors). - American Chemical Society. – Washington. - 1997.

5. Kortaberria G., Arruti P., Gabilondo N., Mondragon I. // Eur. Polym. J. – 2004.- №40. – C.129-136,

6. Sengers W.G.F. Distribution of Oil in Olefinic Thermoplastic Elastomer Blends. / / Polymer.- 2005.- №46. – C.6391-6401.

7. Ellus M., Patel J., Tinker A. Grosslink denstites and phase morphologies in dynamically vulcanized TPEs // Rubber Chem. and Technol. 1995. Vol. 68, № 4. C. 573-584.

Table №1

Comparative characteristics of olefinic TPE of Russian and foreign production.

№	Characteristic	Specifications	Santoprene 261-87	Tompolen PP 305K-M
1.	Density, kg/m^3	ASTM D792	940	920
2.	Melt flow index (230^{o}C, 2,16 kg), g\10 min	ASTM D1238	0, 5	0,3
3.	Shore hardness, A	ASTM D2240	87	85
4.	Tensile strength, MPa	ASTM D 412	11,0	8,0
5.	Elongation at break, %		600	300
6.	Brittleness temperature, ^{o}C	DIN 53546	-55	-55
7.	Thermooxidative stability of elongation at break maintenance after 14 days at 150 ^{0}C, %.	UL 746B	95	90
8.	Cross-linking degree in elastomer phase, %	/7/	> 90	65-70

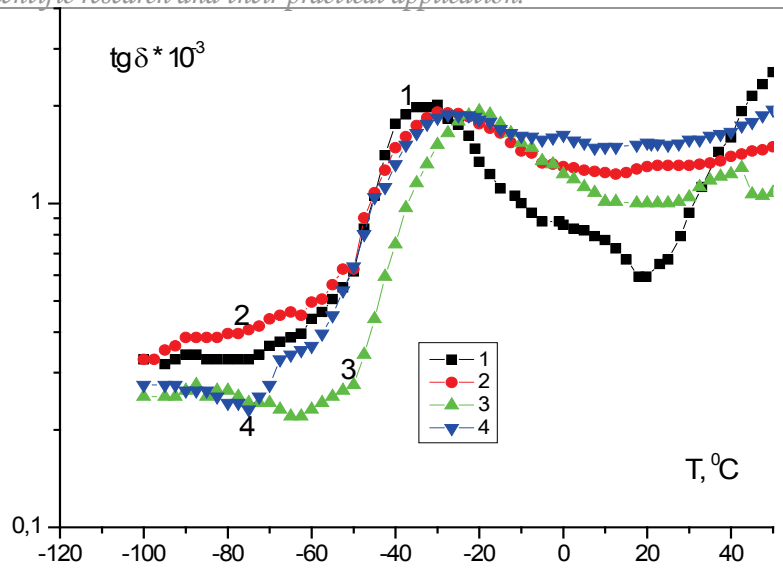

Fig. 1. Temperature dependence of dielectrical loss tangent for initial rubber EPDM and dynamic vulcanizers on the basis of its intermixtures with PP: 1 - EPDM; 2 - Santopren 261-87; 3 - laboratory samples of TPV without oil extender; 4 - Tompolen PP 305K-M.

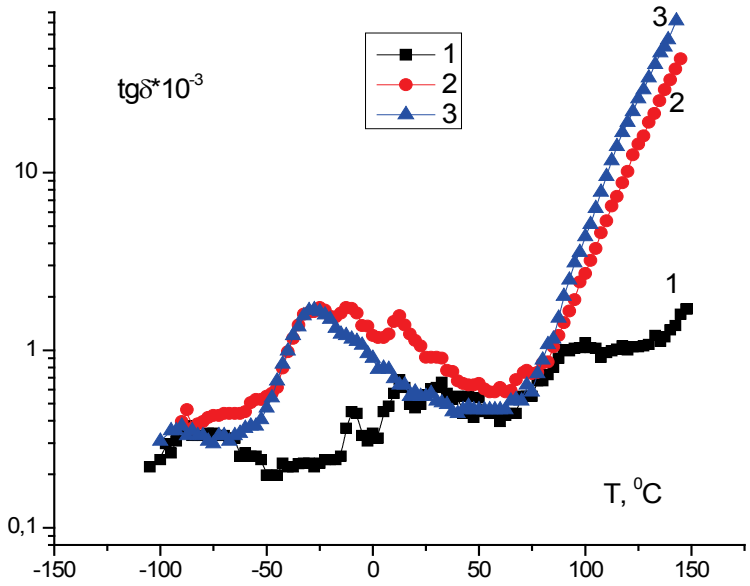

Fig. 2. The dielectric spectrums of isotactic PP 01030 (1), its intermixtures with EPDM rubber (2) and dynamically vulcanized TPE (PP+EPDM+peroxide+oil) (3).

a)

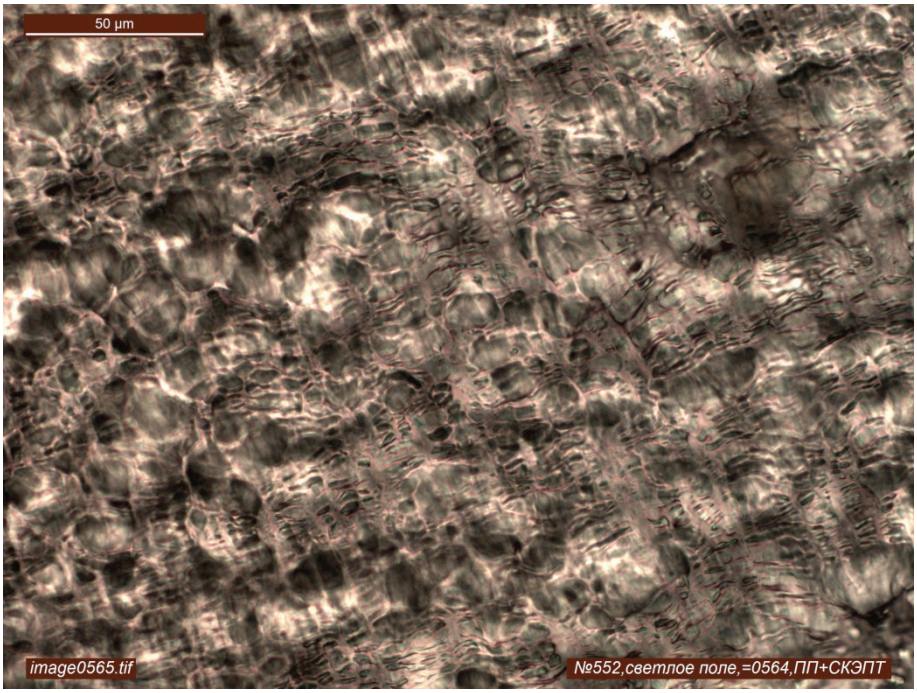

b)

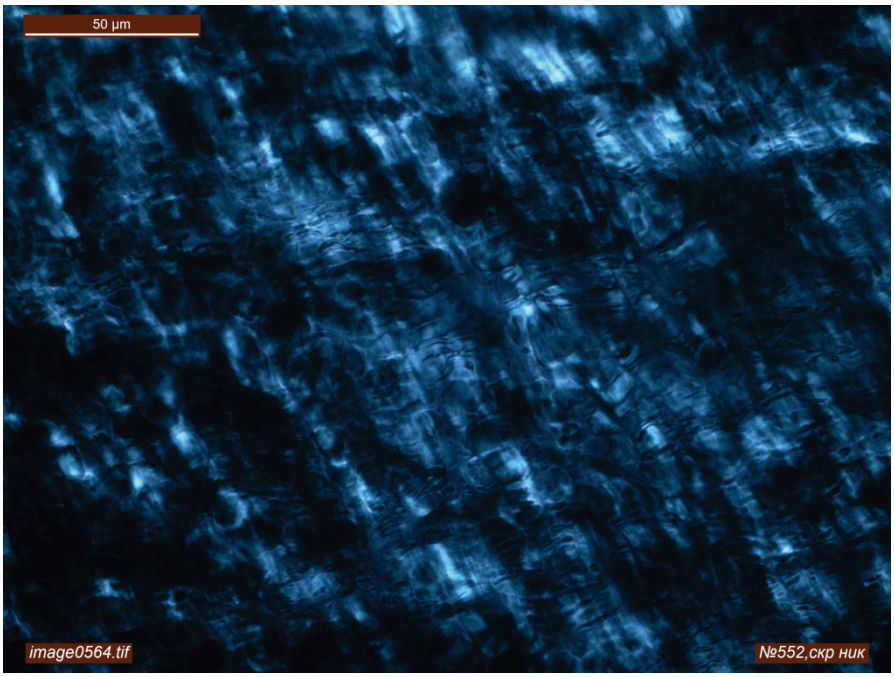

Fig. 3. Microphotographs of unvulcanized intermixture of PP+EPDM (36/64 wt%) in modes of a light field (a) and crossed nicols (b).

a)

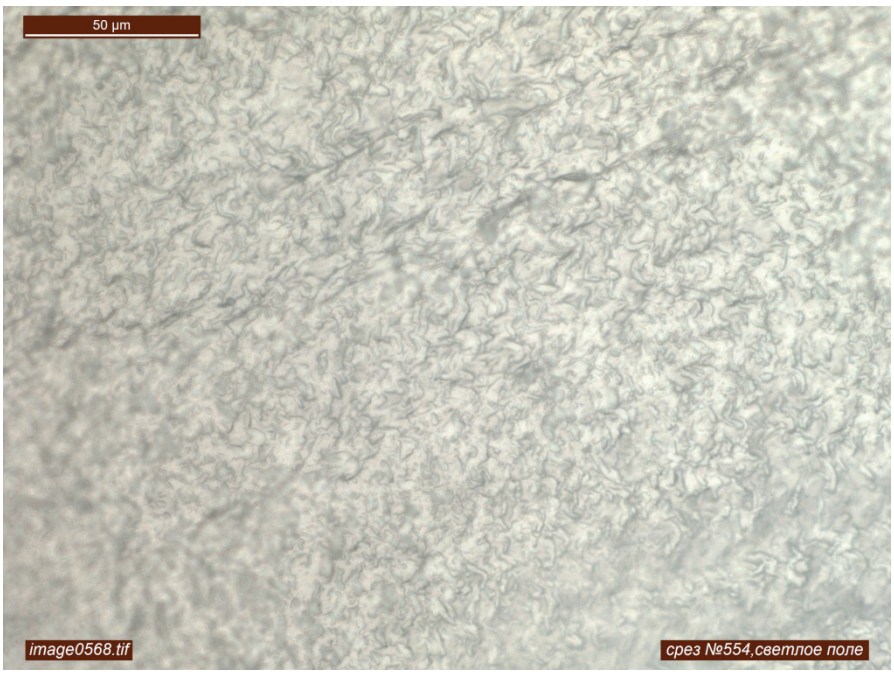

b)

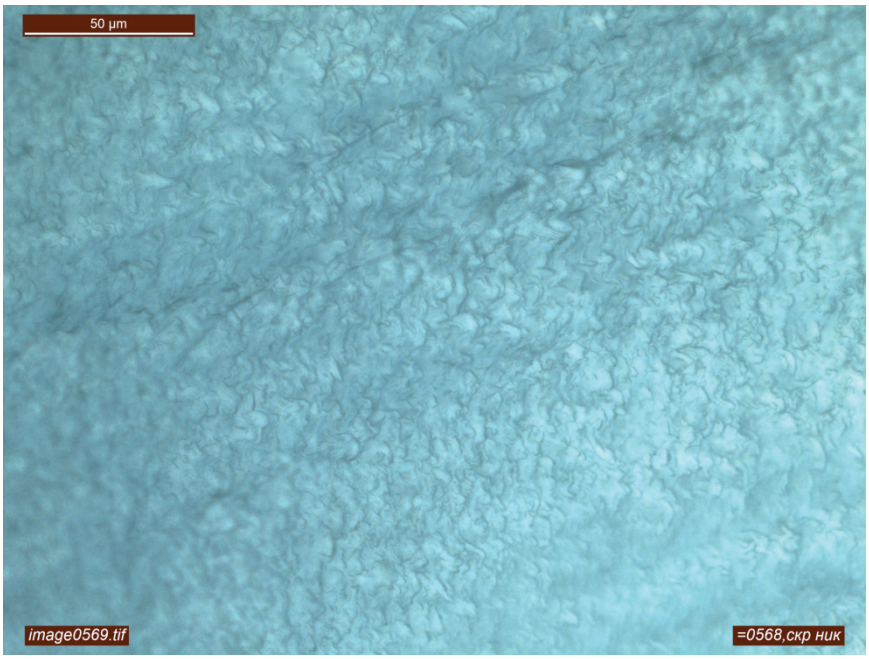

Fig. 4. Microphotographs of the intermixture of PP+EPDM (36/64 wt%), dynamically vulcanized by peroxide in modes of a light field (a) and crossed nicols (b).

Signatures to pictures.

Fig. 1. Temperature dependence of dielectrical loss tangent for initial rubber EPDM and dynamic vulcanizers on the basis of its intermixtures with PP: 1 - EPDM; 2 - Santopren 261-87; 3 - laboratory samples of TPV without oil extender; 4 - Tompolen PP 305K-M.

Fig. 2. The dielectric spectrums of isotactic PP 01030 (1), its intermixtures with EPDM rubber (2) and dynamically vulcanized TPE (PP+EPDM+peroxide+oil) (3).

Fig. 3. Microphotographs of unvulcanized intermixture of PP+EPDM (36/64 wt%) in modes of a light field (a) and crossed nicols (b).

Fig. 4. Microphotographs of the intermixture of PP+EPDM (36/64 wt%), dynamically vulcanized by peroxide in modes of a light field (a) and crossed nicols (b).

CID: J21210-701

L.F. Sayfulina
E.A Buluchevskii,
A.V. Lavrenov

Ethylene Oligomerization on PdO/SO_4^{2-}-ZrO_2

Institute of Hydrocarbons Processing SB RAS, Omsk, Russia, Institute of Hydrocarbons Processing SB RAS, Omsk, Russia; Omsk State University, Omsk, Russia; Institute of Hydrocarbons Processing SB RAS, Omsk, Russia

Introduction

Ethylene production by oxidative pyrolysis of methane at present time is considered as a perspective stage of GTL-technologies. Thus, the development of the processes for environmentally friendly fuels production from ethylene is of great importance. One of such processes is ethylene oligomerization to isoalkenes.

Conventional catalysts for ethylene oligomerization are nickel and palladium cations supported on acidic materials. This work is devoted to investigation of PdO/SO_4^{2-}-ZrO_2 system as a perspective catalyst of ethylene oligomerization in mild conditions (60-100˚C).

Experimental

Sulfated zirconia (SZ) was prepared as described previously [1]. Palladium was added to calcined SZ by incipient wetness technique using the appropriate amount of aqueous solution of H_2PdCl_4 or $[Pd(NH_3)_4]Cl_2$. The obtained solids were then dried at 120˚C and calcined in an air stream at 500˚C for 2 h. The samples were characterized by FTIRS of adsorbed CO and UV–Vis DRS**.** Ethylene oligomerization was performed in a fixed bed flow reactor at temperatures of 60, 100 and 200°C, 1.0 MPa total pressure and weight hourly space velocity of ethylene 0.5 h^{-1}.

Results and discussion

According to FTIRS of adsorbed CO palladium in the studied samples is presented mostly in cationic forms with minor part of Pd^0. IR spectra of adsorbed CO for PdO/SZ samples obtained with two different palladium precursors show bands at 1905, 1990 and 2131 cm^{-1} which can be attributed, respectively, to bridged CO complexes with Pd^0 and Pd^+ and linear CO complex with Pd^+ [2]. For the samples obtained with H_2PdCl_4 and $[Pd(NH_3)_4]Cl_2$ as palladium precursors CO complexes with Pd^{2+} were characterized by a.b. 2167 and 2180 cm^{-1} respectively. The presence of cationic forms of Pd on SZ surface was confirmed by UV–Vis diffuse reflectance spectroscopy. The band at 480 nm in the spectra of the PdO/SZ samples (obtained with two different palladium precursors) is attributed to d–d transition of either isolated Pd^{2+} ions linked to surface oxygen atoms of the support, or small $Pd(O)n^{2+}$ entities [3].

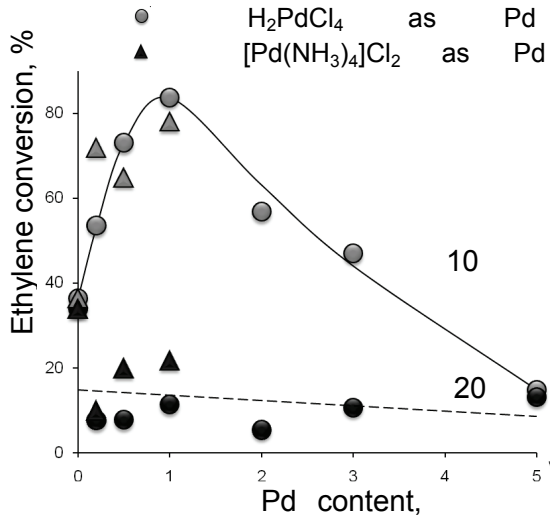

Fig. Ethylene conversion vs. palladium content in PdO/SZ samples.

Palladium loading significantly effects on the activity and selectivity of the catalysts (Fig.). It was found that for ethylene oligomerization optimal Pd content in PdO/SZ is 1 wt.% irrespective of the palladium precursor. These catalysts (with 1 wt.% of Pd) provide high ethylene

conversion (83 ± 5%) at 100°C with selectivities to C_{4+} hydrocarbons up to 90% (Table). At higher temperature (200°C) drastic decrease in activity occurs (ethylene conversion drops by a factor of 3.5-4 during 1 hour) probably due to the palladium reduction by ethylene. For the both PdO/SZ samples with 1 wt.% of palladium at studied conditions molecular weight distribution of the oligomerization products corresponds to Schulz-Flory distribution with α = 0.04-0.19.

Table. Influence of the palladium precursor on the catalytic properties of PdO/SZ samples in ethylene oligomerization (palladium content 1 wt.%). X – conversion; Y – yield; S – selectivity.

t, °C	Precursors					
	H_2PdCl_4			$[Pd(NH_3)_4]Cl_2$		
	X $C_{2=}$, %	Y C_{4+},%	S C_{4+},%	X $C_{2=}$, %	Y C_{4+},%	S C_{4+},%
60	71,3	64,7	90,7	69,3	56,3	81,3
100	83,6	72,2	86,4	78,0	62,7	80,4
200	11,3	2,5	22,4	21,6	16,3	75,2

References

[1] Belskaya O.B. Danilova I.G. Kazakov M.O. et al. *Appl. Catal. A,* **2010**, 387, 5.

[2] Hadjiivanov K.I., Vayssilov G.N. *Adv. Catal.,* **2002**, 47, 307.

[3] Kantcheva M., Cayirtepe I. *J.. Mol.. Catal. A,* **2006**, 247, 88.

CID: J21210-148

UDK: 544.72

Maschenko S., Cherny A., Dogadajlo R., Goncharov V.

INFLUENCE OF IMPLANTATION OF CHROME AND TITAN IONS ON SUPERFICIAL PROPERTIES OF STEEL Cr18Ni10Ti

Institute of Chemical Technology, V.Dal' East-Ukrainian National University

(Rubezhnoe)

On the modern stage of development of technologies ionic implantation (corpuscular alloying) becomes more attractive by virtue of application in many industries. By means of ionic implantation it is possible to process the surfaces of metals, changing their mechanical, physical and chemical properties, that in turn allows to recommend this technology as methodology of synthesis of catalytic compositions [1-3].

Number of researches was carried out showing perspective of application of this ionic technology in the production of catalysts [4, 5]. In this paper we studied the effect of low temperature ion implantation of titan and chrome on superficial properties of foil (thick 100 μm) from steel of Cr18Ni10Ti (SS). The mode of process provided the dose of introduction $2,5 \cdot 10^{17}$ ion/cm^2 and $5 \cdot 10^{17}$ ion/cm^2.

The microstructure of surface of initial and treated standards was analyzed through a microscope MIM-7, provided with the camera of «Kodak EasyShare C1013», and treatment of parameters was produced by means of the program «Gwyddion» [6].

The obtained values of the parameters of surface texture, the most significant of which - it is Wa (waviness) and Ra (average roughness) show that the change in the microgeometry of the surface depends on the nature of the implant dose and doping (table 1).

In particular, the ion implantation of chromium significantly increases the average surface roughness (from 152 to 189 nm, respectively, at a dose of doping $2,5 \cdot 10^{17}$ cm^{-2}). Titanium ions at the same dose of doping practically does not change the Ra. Not significantly change the surface roughness and an increase in implantation dose. At the same time, waviness at a dose of doping $2,5 \cdot 10^{17}$ cm^{-2} significantly increased in both samples, although with increasing doses of doping is greatly reduced. For the chromium ions Wa varies from 510 to 716 nm and 332 nm for titanium from 510 to 638 nm and 516 nm, respectively.

For clarity, in Figures 1 and 2 the three-dimensional images of surfaces of samples are presented.

Table 1 – Parameters of texture of standards surface

Standard	Dose of doping, cm^{-2}	Parameter	
		Waviness Wa, нм	Average roughness Ra, нм
Untilled steel (SS)	-	510	152
Ti/SS	$2,5 \cdot 10^{17}$	638	153
	$5 \cdot 10^{17}$	516	163
Cr/SS	$2,5 \cdot 10^{17}$	716	189
	$5 \cdot 10^{17}$	332	166

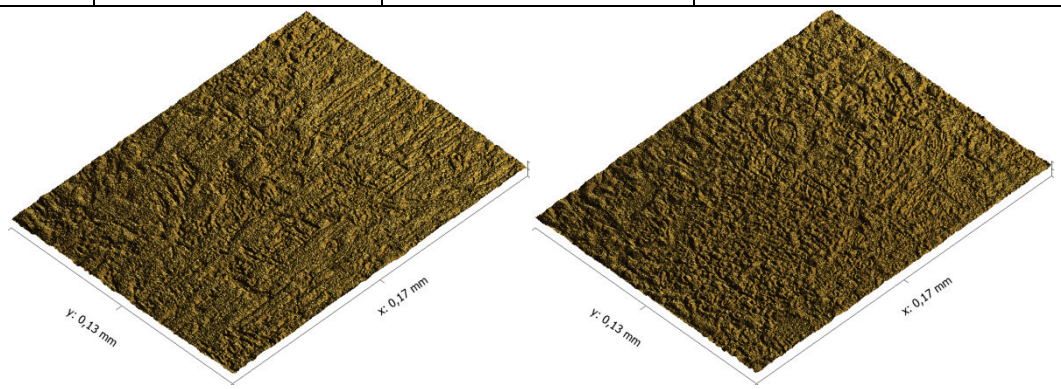

a) b)

Figure 1 – The three-dimensional images of surfaces of standards (Ti/SS - a, Cr/SS - b), got by means of the program «Gwyddion». Increase 300, dose of doping is a $2,5 \cdot 10^{17}$ cm^{-2}

These data (Table 1) show that the titanium ions deformed whole sections of the surface at low doses without changing the average roughness. Increasing the dose of doping to the value of $5 \cdot 10^{17}$ cm^{-2} levels the terrain, slightly increasing the average surface roughness.

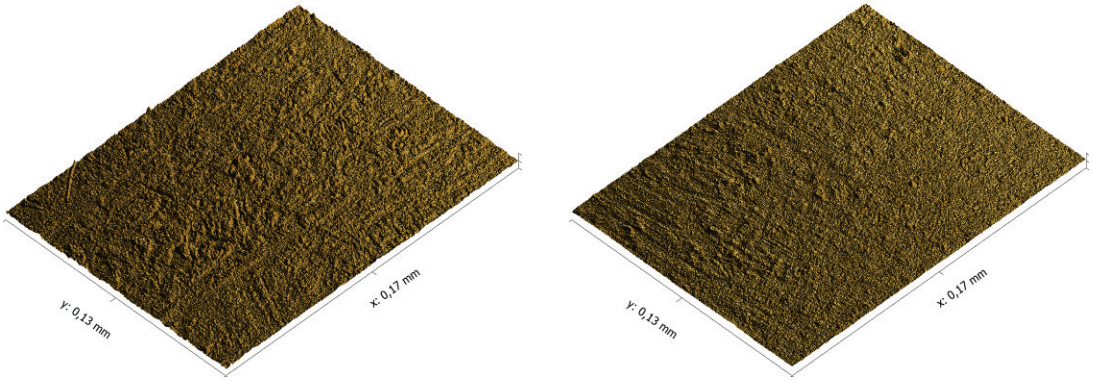

a) b)

Figure 2 – The three-dimensional images of surfaces of standards (Ti/SS - and, Cr/SS - b), got by means of the program «Gwyddion». Increase 300, dose of doping is a $5 \cdot 10^{17}$ cm^{-2}

The most interesting is the effect of the impact of chromium ions. At a dose of doping $2{,}5 \cdot 10^{17}$ cm^{-2} chromium ions significantly "loosen" the surface, increasing the waviness and roughness. However, the continuation of implantation leads to a leveling of forms of relief and a reduction in the height of local roughness.

Thus, we can confidently say that the ion implantation changes the surface geometry, in particular, such parameters as Ra and Wa, which in turn shows a promising development in this direction in terms of synthesis and modification of the composites with the aim of their application in materials science, catalysis , thermal physics, etc.

References:

1. Поут Дж. М. Модифицирование и легирование поверхности лазерными, ионными и электронными пучками / Поут Дж. М., Фоти Г., Джекобсон Д. К. – М. : Машиностроение, 1987. – 424 с.

2. Абдрашитов В. Г. Оптимальные режимы активации поверхности методом ионной имплантации / В. Г. Абдрашитов, В. В. Рыжов // Поверхность. Физика, химия, механика. – 1989. – №7 – С. 148 – 149.

3. Беграмбеков Л. Б. Модификация поверхности твердых тел при ионном и плазменном воздействии / Л. Б. Беграмбеков. – М. : МИФИ, 2001. – 34 с. – (Учебное пособие).

4. Potential of use of ion implantation as a means of catalyst manufacturing / V. N. Zlobin, M. G. Bannikov, I. P. Vasilev [та ін.] // Automobile Engineering**.** – 2002. – vol. 216, №D5 – C. 385-390.

5. Low temperature implantation method for preparation of the catalysts supported on stainless steel foil / V. Goncharov, V.Zazhigalov, R.Socha [та ін.] //

10th International Symposium on the Scientific Bases for the Preparation of Heterogeneous Catalysts. – Louvain-la-Neuve (Belgium), – 2010. – P62.

6. Gwyddion [Электронный ресурс] // Free SPM (AFM, SNOM/NSOM, STM, MFM, …) data analysis software.

- Режим доступа: **http://gwyddion.net/** Дата обращения: 13.12.2011.

AUTHOR INDEX

Bozhenyuk A.V.	professor	Doctor of Technical Sciences	Taganrog Rostov Region, 347900
Okhorzin V. A., Ryzhikov I. S.	professor	Doctor of Technical Sciences	Krasnoyarsk 660025
Sabirova F.M.	lecturer	Candidate of Physical and Mathematical Sciences	Elabuga The Republic of Tatarstan 423606
Mazurkin PM	professor	Doctor of Technical Sciences	Yoshkar-Ola, The Republic of Mari El 424036
Sukhotin A.M.		Candidate of Physical and Mathematical Sciences	Tomsk 634061
Matyukhina A.G.		student	Donetsk 83117
G.M. Trunov	lecturer	Candidate of Technical Sciences	Perm Perm Region 614068
Malashenko V.V., Malashenko T.I.	lecturer	Doctor of Physical Sciences	Donetsk 83114
Borodzich EV			Moskow, 117415,
R.I.Ableev *, A.R.Valiev *, Z.A.Perestoronina **, S.K.Kurljand, A.S.Ramsh, I.V.Baranets **, R.N.Gimaev*	professor	Doctor of chemical sciences	Ufa, 450074
L.F. Sayfulina E.A Buluchevskii, A.V. Lavrenov	lecturer	Candidate of Chemical Sciences	Omsk, Omsk region. 644050
Maschenko S., Cherny A., Dogadajlo R., Goncharov V.		student	Rubizhne Lugansk region. 93012